

5

MICROSCOPY

PATRICIA A. MOSS*

The University of Manchester Institute of Science and Technology
Manchester, England

LES GROOM

Southern Research Station
U.S. Forest Service
Pineville, Louisiana

I. Introduction	150
II. A Brief History of the Microscopy of Wood and Paper	151
III. Microscopical Techniques for Pulp and Paper Research	152
A. Optical Microscopes	152
B. Electron Microscopes	159
C. Scanning Probe Microscopes	167
IV. The Confocal Laser Scanning Microscope	168
A. Basic Principles of the CLSM	168
B. Imaging Modes	174
C. Specimen Preparation Techniques	175
D. Fluorescence Quantification	178
E. Image Acquisition and Processing	178
F. Artifacts of CLSM Imaging	180
G. Applications of the CLSM to Pulp and Paper Research	185
V. The Low Temperature Scanning Electron Microscope	203
A. The Cryosystem	204
B. Specimen Preparation	206
C. Comparative Evaluation of Preparation Techniques for LTSEM	208
D. Advantages and Disadvantages of Cryopreparation Techniques	208
E. Artifacts of Cryopreparation	209
F. Applications of the LTSEM to Pulp and Paper Research	211

**Current affiliation:* Oy Keskuslaboratorio—Centrallaboratorium Ab (KCL), Espoo, Finland.

VI. The Atomic Force Microscope	216
A. Principles and Operation of Atomic Force Microscopy	217
B. Operating Modes	220
C. Environmental Conditions	223
D. Applications of the AFM to Pulp and Paper Research	224
VII. Conclusions	247
Abbreviations	247
References	248

I. INTRODUCTION

Microscopy is the study and interpretation of images produced by a microscope. "Interpretation" is the key word, because the microscope enables one to see structures that are too small, or too close together, to be resolved by the unaided eye. (The human eye cannot separate two points or lines that are closer together than 0.1 mm.) It is important to remember that microscopy is not simply a matter of magnification and making objects larger, but of resolving features that may not have been seen before. Much microscopical analysis is subjective. Images cannot be interpreted intuitively on the basis of nonmicroscopical experience but require highly skilled microscopists with knowledge and practical experience of the materials they are examining and an "eye" for their subject. Correct interpretation can be achieved only when one has a thorough understanding of all the factors that influence the final image. These factors include instrumental effects, specimen preparation techniques, and microscope-specimen interactions. Three-dimensional objects projected onto a two-dimensional image, such as is the case with scanning electronmicrographs, can be particularly confusing and difficult to interpret. Images of surface features can be illusory, and the observation, recorded by the seventeenth century microscopist Robert Hooke [128], that "it is exceedingly difficult in some objects to distinguish between a prominence and a depression, between a shadow and a black stain, or a reflection and a whiteness in a color" still holds true today.

The aim of microscopy is to study material in a condition as near as possible to its natural state. This, therefore, means a minimum of specimen processing because each treatment that is applied runs the risk of introducing artifacts. As Stone and Scallan [309] pointed out, "The structural studies of water-swollen fibers should always be performed, if possible, while the fibers are still saturated with water."

This chapter discusses the applications of microscopy to pulp and paper research. Conventional optical and electron microscopical techniques are covered only briefly, because these are well documented elsewhere. Novel forms of microscopy—confocal laser scanning microscopy (CLSM), low temperature scanning electron microscopy (LTSEM), and atomic force microscopy (AFM)—are presented in detail. As yet, there are no official or standard methods pertaining to their use.

II. A BRIEF HISTORY OF THE MICROSCOPY OF WOOD AND PAPER

Robert Hooke was one of the first people to use a microscope to examine the structure of wood cells. He published his drawings in *Micrographia* in 1665 [128]. His observations raised many questions concerning the ultrastructure and functions of wood cells, but little advance was made until the second half of the nineteenth century, when the polarizing microscope was developed. This made possible the examination of crystalline structures and bundles of parallel filaments, and Carl von Nägeli laid the foundations of the physical chemistry of colloidal matter, which must also include the cell walls of wood.

Other advances included the development of ultraviolet and fluorescence microscopical techniques. Köhler developed the first ultraviolet microscope in 1904, and Reichert and Heimstadt demonstrated the first practical fluorescence microscope in 1911. Both instruments have proved to be very useful tools for studying plant material, which generally exhibits relatively intense primary fluorescence in the ultraviolet (UV) and blue spectra.

The discovery early in the twentieth century of electrons and an understanding of their behavior led to the development of electron microscopes and the opening up of a whole new field. High energy particles, which have wavelike properties analogous to those of light waves could be generated, so the wavelength of light was no longer a limiting factor to the resolution that could be achieved with a microscope. Ernst Ruska [280] produced the first electron micrographs of surfaces.

The development of the transmission electron microscope presented enormous scope for ultrastructural research because of its very high resolution. The microfibrillar structure of cell walls could be clearly seen, and measurements could be made of the fibrillar units. The scanning electron microscope, on the other hand, allowed larger specimens to be examined, but its main advantage was its enormous depth of field, enabling three-dimensional viewing of specimens. In 1959 the first SEM to be used specifically for solving problems associated with papermaking was installed at the Pulp and Paper Research Institute of Canada in Montreal [301]. Nowadays the SEM is widely used in paper science research and is a standard piece of equipment in most research centers.

The flying spot microscope, described by Young and Roberts in 1951 [371], was the first example of a sequential imaging system. The confocal scanning microscope was invented by Minsky [211], who filed a patent for it in 1957, but further development took a long time. Forerunners of the modern confocal laser scanning microscope (CLSM) used UV or white light, but the later development of the laser, giving a powerful source of monochromatic radiation that could be concentrated into one spot, provided greater versatility. Commercial production of the CLSM in the late 1980s led to a renaissance in optical microscopy, particularly in fluorescence microscopy. Its use quickly became a widely established technique in cell biology and medical research and is now indispensable for studying the three-dimensional structure of cells as well as dynamic processes in living cells. Nanko and Ohsawa [224] were the first to report on the use of a scanning laser microscope (SLM) for examination of paper, using it to observe changes that occurred in wet paper webs as they dried. The CLSM has become a recognized part of paper science research, with more and more centers acquiring their own microscope or gaining access to one.

A new family of scanning probe microscopes was developed in the 1980s that offered the possibility of atomic resolution. These include the scanning tunneling microscope (STM) invented by Binnig and Rohrer in 1982 [21, 22] and the atomic force microscope (AFM) subsequently developed by Binnig and coworkers in 1985 [20].

III. MICROSCOPICAL TECHNIQUES FOR PULP AND PAPER RESEARCH

Microscopes are powerful research tools, and both optical and electron microscopes have played an important role in elucidating mechanisms of papermaking processes. Direct observations are very important to gaining an understanding of the structure of fibers—both of their behavior in aqueous solutions and of their properties in the resultant paper. Direct visual methods need to be complemented with carefully planned measurements of physical properties carried out simultaneously so that causal relationships can be established. Microscopy needs to be applied systematically, with quantitative analysis of images undertaken. To this end most microscopes can be linked directly to an image analysis system and images can be processed and measured interactively. Image quality for all microscopy depends on optimizing the setup and adjustment of the microscope and on good specimen preparation. Good image quality results in high contrast, high resolution images that are free of artifacts. Finally, calibration of magnification is essential for interpretation. Diffraction gratings and latex spheres are commonly used for calibration purposes, but Watts and Emerton [346] recommend imaging the periodic structure of a diatom skeleton. This is particularly suitable for electron microscopy, because, being silica, the diatom skeleton is not subject to shrinkage.

So, what do these different methods of microscopy have to offer?

A. Optical Microscopes

Optical microscopy has always been, and will continue to be, an important part of paper science research. It has been much used for qualitative analysis but also has a large range of quantitative applications. However, the resolution of optical microscopes (around 0.2 μm) is poor compared to that of electron microscopes (down to a few nanometers). There are a plethora of books on optical microscopy, but a good overview of the different types of optical microscopes is given by Rollins and deGruy [277] in a book that was written primarily for analysis of cotton cellulose but also makes reference to papermaking fibers.

Much of the important work in the elucidation of fiber structure was done using optical microscopes, a great deal of it pioneered by plant anatomists. Many phenomena relating to the structure of wood and fibers were reported early on by skillful microscopists but did not receive recognition until much later. One such phenomenon was fibrillation. Strachan [310] was the first to observe fibrils on the surfaces of beaten fibers, but his observations could not be confirmed until Clark [45] produced micrographs of disintegrated fibers that had been silvered.

Optical microscopes can be used with incident or transmitted light or a combination of these depending on the specimen. Specimens may be living or dead, wet or dry. Optical microscopy using transmitted light requires samples to be relatively transparent and thin, and if they are not thin enough, then sections need to be

embedded and cut with a microtome. Embedding procedures normally entail dehydration, involving the use of a solvent, followed by infiltration and polymerization of the embedding medium, usually a resin.

The Stereoscopic Microscope Stereoscopic microscopy allows specimens to be viewed in three dimensions. Using incident light with a stereomicroscope at low power gives good depth of field, making it possible to obtain a great deal of information about surface structures of fairly large specimens. The stereomicroscope is often used for preliminary examination of specimens.

Compound Microscope The compound microscope is the “conventional” light microscope, a standard piece of equipment in paper technology laboratories and the classical tool for fiber and pulp analysis. Isenberg [136] gives a comprehensive account of the optical system of the compound microscope and lists its common uses in pulp and paper mill laboratories where routine standardized methods are employed for quality control. It is used for identification of wood [323,324] and nonwood [41,322] fibers. Photographic atlases have been compiled for identification of papermaking fibers [54,250], although for purposes of basic wood fiber identification it would be hard to better the fine light micrographs in Ilvessalo-Pfäffli’s *Fiber Atlas* [134]. The compound microscope is also used for fiber analysis of paper and board, determination of fiber coarseness and weight factor, analysis of fillers and coating particles, and analysis of foreign particulate matter in pulp, all according to the appropriate standards [320,321,325,326].

Jordan and Page [155] discuss the application of image analysis for measurement of fiber length, width, and coarseness and the determination of weighted average fiber length using automated and manual procedures. They also describe ways of defining and measuring fiber curl. Weidner [348] designed a special cell with through-flow of air from a constant humidity apparatus that fitted onto the microscope stage. The top of the cell was covered with a glass cover slip so that changes in fiber length and width with varying relative humidity could be measured.

Giertz [101] characterized fiber and fines fractions of various mechanical and chemimechanical pulps and showed some interesting features in his light micrographs. Pelton et al. [254] and Luukko et al. [194] measured the size distribution of fines particles in mechanical pulps. Samples of fines material were dyed and mounted on glass slides, and their images were captured by video camera for image analysis. McCool and Taylor [206] describe the techniques for quantitative analysis of ink particles and stickies that they used to determine the efficiency of deinking processes in waste paper recycling.

Measurement of contact ratio, the area of fibers bonded to a glass slide (measured under incident light) as a ratio of the total area of fibers (measured in transmitted light), was first proposed by Clarke [47] as a method for obtaining an indication of the wet plasticity of fibers. Sloane [300] used this method to study the effect of recycling on the bonding potential of softwood kraft pulps and provided details of slide preparation and image analysis procedure. Kallmes and Eckbert [157] felt that relative bonded area (RBA) was the parameter that best defined the structure of paper and applied it to pulp and paper evaluation. They found that direct measurements of RBA using optical microscopy did not correlate well with indirect methods such as N_2 adsorption, which measures uncollapsed lumen area in addition

to external fiber surface, so they used a lumen-corrected adsorption technique to take into account the contribution made by uncollapsed lumina.

Investigations into wet fiber flexibility have also been undertaken with the light microscope. Various workers have developed techniques for measuring wet fiber flexibility and conformability. Tam Doo and Kerekes [318] derived an index of flexibility by measuring the deflection of selected fibers in a flow of water. Their experimental setup included a microscope for measuring the diameter of each fiber before it was deflected. Mohlin [213] showed that the conformability of a wet fiber draped over a glass fiber on a microscope slide could be assessed by measuring the length of the fiber that was not in contact with the glass, and Steadman [305,306] formed a thin fiber network over a series of very fine steel wires laid parallel across glass slides. This allowed flexibility measurements to be made of a larger number of fibers.

Bucher [35] examined the structural organization of wood fibers. Fibers were macerated, and the use of a differential metachromatic stain enabled the primary and tertiary walls to be distinguished from the secondary wall. Helix angles in the tertiary walls were measured for several conifer species. Many workers have studied the effects of beating on the development of fibrillation. McIntosh [207] dried down well-beaten fibers onto microscope slides and then shadow-coated them with silver to enhance the fibrillar structures. These effects of beating can be studied qualitatively and quantitatively. Laamanen et al. [179] obtained a fibrillation index for fibers dried down onto microscope slides. A differential staining technique was developed by Simons [296] to evaluate the degree of fibrillation. Intact fibers stain blue, whereas fibrillated fibers turn orange. This technique was used by Blanchette et al. [23] as a rapid screening tool for evaluating the effectiveness of various species and strains of fungi used to fibrillate fibers in biomechanical pulping. Similarly, Jackson et al. [138] used Simons stain for characterizing surfaces of fibers after treatment with cellulase and/or hemicellulase. Microscopical analysis strongly suggested that cell wall fragments or fibrils were being removed from surfaces by hydrolysis. Jackson et al. [139] also adapted a gold-labeling technique normally used for transmission electron microscopy (see Section IV.E) to see where the cellulases bind to fibers. They enhanced the enzyme-gold complexes with silver so that they were large enough to be resolved using a light microscope. Lackner et al. [180], in their study of wood rot, also employed the silver staining technique to enhance immunogold-labeled ligninases for optical microscopy.

Most paper sheets are too opaque for examination in transmitted light. Surface features can be studied using oblique lighting or vertical illumination methods, but this can be done only at low magnification. For high magnification work, surface contrast must be greatly enhanced in order to reveal fine structural details, and this can be achieved by metal shadowing or surface replication techniques. Williams and Wykoff [358] first proposed the use of metal shadowing for examining surface structures with the electron microscope, and this technique was subsequently adapted for optical microscopy [359]. It entails directional deposition of a thin layer of metal by evaporation under high vacuum onto the surface of the specimen. Raised features intercept the beam and give rise to metal-free regions on the leeward side. Paper sheets that are sufficiently translucent can be prepared in this way and produce a negative image when viewed in transmitted light (the raised features appearing dark and the metal-free depressions light), but a positive image can be obtained by photo-

graphic reversal. Alternatively, replicas of paper or wood surfaces can be made. These were also initially made of metal for electron microscopy, but the replica method was extended to the field of light microscopy, and for this purpose they are usually made of transparent plastic material. Plastic replicas are then metal shadowed and can be viewed in transmitted or incident light. These techniques for studying wood fibers and paper were developed and employed largely by Emerton [79], Emerton et al. [81], and Page and Emerton [239]. Page and Sargent [240] used the carbon replica method to study the fine structure in contact regions of fibers that had been dried onto glass or a steel drying plate and then removed. They examined the same bond areas using both light microscopy and electron microscopy and showed clearly the areas where the fiber surfaces had formed close contact with the substrate. Emerton's classic work [78,79] is illustrated by many examples of replica techniques used by various workers, and Emerton et al. [80] presented an atlas of paper surfaces—light micrographs of metal replicas of a wide range of papers viewed in oblique lighting.

Optical microscopy has been much used for examining cross sections of fibers and sheets. This usually necessitates the use of embedding techniques and mechanical sectioning. The method used for cross-sectioning paper depends on the purpose of the study; Graff and Schlosser [105] review various embedding procedures and their appropriateness for various types of material. Nissan [228] recommended that sedimentation studies of papermaking fibers should be accompanied by direct visual observation of the dimensions and shapes of fibers. Single fibers, placed in a sedimentation cell and timed as they fell through a known distance, were then placed, in a wet state, on a microscope slide for measurement of length and width. They were then dipped in paraffin wax and microtomed so that fiber wall thickness could be measured from cross sections. Page et al. [241] described in detail their methods for obtaining sections thin enough for examination in transmitted light but thick enough to maintain structural integrity and presented some examples of cross sections of various types of papers. Leopold and McIntosh [185] measured the tensile strength of individual alkali-extracted fibers. The fibers were then embedded in resin, and thin sections were cut as close as possible to the break in order to measure the cross-sectional area of the fibers. They showed a correlation between reduction in fiber strength with the removal of xylan-based hemicellulose and also a correlation between decrease in strength and cross-sectional area with an increase in the concentration of the alkali used for extraction.

Robertson and Mason [273] examined cross sections of embedded pulp fibers to study the effect of delignification on fiber collapse by comparing cross sections of spruce fibers from high and low yield pulps when wet, and then after sheet forming and drying. The cross-sectional shapes and transverse dimensions of individual fibers have also been examined for changes in structure arising from beating processes, much of it by Kibblewhite and coworkers [165–168]. Kibblewhite and Shelbourne [169] found that the combination of length and width/thickness ratio of kraft fibers could be used to predict apparent density.

Szikla and Paulapuro [317] developed a method using image analysis for measuring *z*-direction changes in density distribution during wet pressing. They tinted pulp with methylene blue during refining in order to avoid the damage that can ensue from post-staining thin cross sections of embedded samples, and they also tested handsheets made with and without methylene blue to confirm that the staining

treatment did not affect fiber bonding. Mardon et al. [202] investigated changes in paper structure during calendering by examining paper sections at various stages of the process. Bergh and Thomin [19] investigated paper-liquid interactions and penetration of sizing and coating mixtures. Such techniques have been used largely for analyzing the distribution of fillers in sheets, coating thickness, and profile analysis, details of which are given by Elton and coworkers [77,99], and also for examining the effects of coating on the surface roughness of base papers [186,297].

Marton and Crosby [204] cut cross sections of embedded laminating papers in order to study the penetration of dyed resins into the paper sheets and examine the reaction between the resins and the base paper. Quackenbush [259] developed a technique for making precise measurements of individual cells on the metering roll of an offset rotogravure coater. An impression was taken of a small area of the roll on a thin piece of plastic such as cellulose acetate or cellulose nitrate. This was then sandwiched between two blocks of wax for microtoming. Measurements made from the cross sections made it possible to determine the correct coating weight for print roll engraving. This technique could also be applied to studying the corrosion of metal surfaces and the wear and tear of printing plates and of the cutting edges of refining equipment.

Phase Contrast Microscope Phase contrast microscopy makes visible the differences in retardation of light waves as they pass through a specimen, the amount of retardation being proportional to the thickness of the object and the difference between its refractive index and that of the surrounding medium. A phase plate placed in the microscope converts the differences in refractive index into differences of contrast in the image, allowing better observation of transparent specimens. Phase contrast microscopy has been especially useful in biological and medical research because it obviates the need for staining living cells. Robertson [274] used it as a diagnostic tool to identify microbial populations to facilitate the appropriate selection and placement of biocides in papermaking systems. Asunmaa and Marteny [5] used phase contrast microscopy to reveal the manner in which the outer cell wall layer peels off fibers, and Crosby and Mark [57] employed phase contrast microscopy in conjunction with near ultraviolet illumination to determine fibril angle in the S2 wall layer of pulp fibers. Their technique overcame some of the problems encountered in using polarizing microscopy for measurement of fibril angle, which necessitates careful preparation of fibers to expose a single wall layer. Generally, phase contrast microscopy does not appear to have been used much for paper science. There are some references to its use in textile research (see Rollins and deGruy [277]).

Interference Microscope Like the phase contrast microscope, the interference microscope makes visible the relative retardation of light through a specimen, but it is primarily designed to measure the differences in retardation of light rays passing through the object and those passing through a reference area in a mounting medium of known refractive index. Knowing the thickness of the specimen and the refractive index of the surrounding medium, it is then possible to determine the concentration of solids and the dry mass of the specimen. Thus it is generally used for quantitative studies rather than the observation of specimens. Lange [183] described methods for determining mass per unit area of lignin and carbohydrates in different regions of the

cell wall. Page et al. [238] used interference microscopy to measure the compacted thickness of single fibers, in order to determine fiber stress after straining. Howarth et al. [131] describe the use of a modified interference microscope to measure adhesive distribution in pigment coatings on paper.

Polarizing Microscope The polarizing microscope measures and analyzes the effects of a beam of polarized light passing through a transparent specimen, thus determining the orientation and crystalline characteristics of the structure of the specimen. Polarization of the light is achieved by the use of Nicol prisms or polaroid sheets. Two polarizing devices (a polarizer and analyzer) are used. When a polarizing object, such as a crystal or highly oriented fiber, is placed on the microscope stage with the polarizers in crossed position (90°), the parallel-polarized light striking the specimen is repolarized in the two perpendicular directions, and the waves, on striking the analyzer, are repolarized. The polarizing microscope is used principally for determining orientation by measurements of refractive index and birefringence. Many materials polarize light to some extent, and evaluation of this characteristic allows correlation of the optical properties of a material with its physical behavior.

Bailey and Kerr [9,10] were pioneers in elucidating the cell wall structure of fibers. Using polarizing microscopy they showed the concentric layering of the secondary wall of lignified wood fibers and observed the helical orientation of fibrils in cell wall layers. On the basis of observations and measurements made using polarizing microscopy and X-ray spectrometry, Wardrop and Preston [344] proposed a model of the wall structure of tracheids and fibers. Kallmes [156] used polarizing and metallurgical microscopes to examine the structure of wall layers unraveled by prolonged disintegration. His fine micrographs illustrate the fibrillar structure peculiar to the primary, S1, and S2 wall layers, and wall thicknesses was measured using the polarizing microscope.

Alexander et al. [2] used polarized light to measure fibril angle and to determine changes in fibril angle caused by beating and wet pressing, and Leney [184] describes in great detail the technique he employed for measuring fibril angle. Measurements of fibril angle are obtained by rotating the cell wall in a beam of plane polarized light to the major extinction position, which appears black so nothing can be seen. The drawback with this technique is that it requires careful preparation of fibers so that only a single wall layer is exposed because polarized light passing through the two walls of a whole fiber will effectively cancel. However, Page [234] overcame this problem by introducing mercury into the lumina of fibers, which blocked out the other half of the cell wall. Recently, Ye and Sundström [369] described a new technique for determining the fibril angle of the S2 wall layer, based on microscopic transmission ellipsometry using a conventional polarizing microscope equipped with a charge-coupled device (CCD) camera or video camera. Whole fibers, wet or dry, can be examined without any special preparation.

Page and De Grâce [237] used polarized light to observe delamination of fiber cell walls resulting from beating and refining. Pulp fibers differ in their ability to swell during beating, and some delaminate more than others. Page and De Grâce showed that sulfite pulp fibers split into 10 or more lamellae, whereas sulfate pulp fibers split into only two to six lamellae. McIntosh [207] used polarized light to increase definition when examining delamination in cross sections of wet fibers that had been set in gelatin, frozen, and then sectioned on a microtome with a freezing attachment.

A great deal of knowledge of fiber bonding has accrued from the use of the polarizing microscope, much of it from the work of Emerton, Page, and coworkers. Page [233] described a new technique of sandwiching dry fibers between two strips of Scotch tape and using a combination of transmitted and polarized light to study the collapse behavior of fibers. Emerton and Watts [82] proposed the use of polarized vertical illumination as a means of distinguishing the primary wall (which shows bright under crossed polarized devices) from the secondary wall (which shows dark) to study the effects of beating on the removal of the primary wall in spruce tracheids. Page [232] adopted this technique to make direct observations of areas of optical contact between fibers in a paper sheet (where areas of optical contact appear black), and Page and Tydeman [242] made a survey of fiber–fiber bonding in sheets made of various furnishes, both wood and non-wood. Page et al. [244] examined the size and shape of fiber–fiber bonds, looked at their frequency of occurrence in paper sheets, and investigated the effects of beating on these parameters. They also made a quantitative examination of loss of bonded area when fibers in a sheet of paper were strained to rupture [245]. McIntosh and Leopold [208] determined the bonding strength of individual fibers. The area of fibers bonded either to cellulose film or to shives was first measured in polarized light, and then tension was applied to determine the load required to release the fibers. Page and Tydeman [243] also used polarized vertical illumination to examine bond formation in paper during drying. The web was formed in situ, and a modified porous plate apparatus allowed controlled removal of water so that each image was recorded at a known moisture content of the web.

Yang et al. [368] evolved a technique for making direct measurement of the bonded area of a fiber in a sheet. This entailed using an embedding technique developed by Quackenbush [260] and cutting numerous serial sections. The sections were examined using both phase contrast and transmitted polarized light, and many fibers could be followed through a series of sections without any difficulty. Bonded area, aspect ratios, moments of inertia, and bonding state probabilities of the fibers were measured using a point mode digitizer interfaced with a computerized data processing system.

Polarized light has also been used for lignin studies, and Coppick and Fowler [50] developed a silver staining techniques for woody tissue that differentiates degrees of lignification in the cell wall by color reaction. Jordan and O'Neill [154] describe a method of detecting mechanical pulp fines particles composed of lignin and hemicellulose, which are not birefringent and therefore are not detected by fiber length analyzers such as the Kajaani FS series. Quackenbush [261] describes techniques developed to study flaws in coated papers and presents a series of case studies to illustrate the usefulness of the polarizing microscope as an analytical tool for the identification of contaminants in coated papers.

Ultraviolet and Fluorescence Microscopes Ways of using shorter wavelengths of light were developed in an attempt to increase the resolution of optical microscopes. A fluorescence microscope is just a standard instrument that has been modified so that the wavelengths needed to induce fluorescence can be focused on the specimen and the emitted fluorescence observed. This is achieved by the use of filters. An excitation filter is placed between the light source and the specimen, and a barrier filter is placed between the specimen and the viewer. Köhler's original observation of

fluorescence was with UV light, so early workers thought it was always necessary to use wavelengths of < 350 nm, but fluorescence microscopy commonly employs near-UV and short-wavelength visible light, because most fluorochromes that occur naturally in plant tissues fluoresce strongly in these wavelengths. The most commonly used light source for general-purpose fluorescence work is a mercury vapor lamp. Fluorescence microscopy has featured largely in the study of living plant tissues and fossilized plant remains, and fluorochromes have been employed to trace the movement of cytoplasm and the transpiration stream in plants [231]. It is not necessary to embed tissues and cut thin sections for fluorescence microscopy if epi-illumination is used instead of light transmission. Fresh material needs no more than a deft cut with a sharp razor and immersion in a fluorescent stain. This enables rapid screening of large amounts of material.

The main advantage of using ultraviolet light is that it is strongly absorbed by unstained biological material, producing good contrast in the image. The UV microscope has not been useful for cellulose, but it has been frequently used for the study of lignin. Frey-Wyssling [94] used UV optics and fluorescence for quantitative evaluations of the content and distribution of lignin in the cell wall, and Fergus and coworkers [87,288] carried out similar studies using UV light. Goring [104] measured the distribution of lignin in spruce and birch wood and showed the progressive removal of lignin during chemical pulping. Fukazawa and Imagawa [96] used both UV and fluorescence microscopy to study the decay and delignification of wood, using acridine orange stain in conjunction with fluorescence microscopy for qualitative histochemical identification of cell wall components. Boutelje and Eriksson [26] used UV microscopy to determine the concentration of lignin in fragments of a spruce thermomechanical pulp (TMP) and used an interference microscope to obtain the thickness measurements.

Wardrop [343] used a simple piece of apparatus to draw or force liquids through small blocks of wood. A silver staining reagent [50] was added to the pulping medium passing through the specimens. Ultraviolet microscopy of cross sections showed that the pits provided the main path of penetration in both heartwood and sapwood, even when the pits were aspirated.

Confocal Laser Scanning Microscopes Confocal laser scanning microscopes (CLSMs) are optical microscopes that use an intense laser beam, focused to a small point, as a light source. The beam is scanned across the specimen in raster fashion. Unlike images produced by a conventional optical microscope, which contain both blurred and sharp areas, confocal laser scanning microscopic images show only structures that are in focus, and out-of-focus areas are not seen. The confocal scanning microscope makes possible applications that have been difficult or impossible to perform with conventional optical microscopes, such as the nondestructive sectioning of specimens in their natural state. The CLSM is described in detail in Section IV.

B. Electron Microscopes

The advent of electron microscopy (EM) presented greater scope for structural research into fibers. A good general review of electron microscopy is given by Rollins et al. [276], and Parham [248] discusses the advantages and disadvantages

of transmission electron microscopy (TEM) and scanning electron microscopy (SEM) and their appropriateness to different research applications.

In electron microscopes a beam of electrons is used instead of light. The electrons are generated by passing a current through a very thin tungsten wire that is heated to $\sim 2500^{\circ}\text{C}$, at which temperature electrons are emitted from the hot metal. Electrons are accelerated from the filament by applying a high negative voltage to the cathode assembly. The greater the voltage, the greater the energy of the electrons and the higher the resolution that can be achieved. The electron gun consists of a cathode and anode assembly, and the electrons pass through a small hole in the center. The electron beam is focused by electromagnetic lenses. All this takes place in a vacuum column, because air molecules will deflect the beam. For the same reason specimens must be dry so the electrons are not scattered by water molecules.

The drawback with all conventional electron microscopy is that the presence of water prevents direct examination of pulp stock and wet sheets, so water must first be removed from specimens, but in a way that maintains the wet structure. Dehydration of material may be necessary, and this may cause shrinkage, distortion, and collapse of specimens to varying degrees. Embedding techniques necessary for TEM work may cause further structural changes [251], and mechanical sectioning may also cause damage or deformation. Finally, the deposition of a thin layer of metal during sputter-coating of samples for scanning electron microscopy can disproportionately increase the dimensions of very fine structures [37], although this can be advantageous in enhancing very fine fibrillar material, which is otherwise difficult to detect. Watts and Emerton [346] discuss some of the problems associated with interpreting electron micrographs arising both from the preparation techniques, such as embedding and sectioning, and from the conditions of the instrument itself, such as beam damage. Sectioning can give rise to several types of artifacts. Imperfections in the cutting edge of the knife show up as lines scored across the specimen, and knife chatter may give rise to periodic waviness in specimen thickness. Compression in the cutting direction may distort the shape of structures in the specimen and may even cause cracking or delamination of structures, and the subsequent mounting of ultrathin sections may result in wrinkling and creasing of the specimen. Studies undertaken by Davies [61–63] are typical of many that were made to investigate fiber–fiber bonding in sheets and the effects of beating on fiber conformability and bonding. However they also serve to illustrate some of the defects resulting from ultrathin sectioning outlined above.

Transmission Electron Microscope Conventional transmission electron microscopy (TEM) has certain limitations, because the electron beam can penetrate only very thin specimens. The preparation techniques are tedious, usually entailing dehydration, impregnation with liquid resin or plastic, polymerization, sectioning, and staining. Only ultrathin sections ($< 100\text{ nm}$) can be examined, and the size of the specimen is limited to the size of the supporting grid (typically $\sim 3\text{ mm}$ diameter). Sections require staining to increase contrast; salts of heavy metals (e.g., lead citrate, uranyl acetate) do this by creating electron-opaque regions in the specimen. Furthermore, each stage in the preparation of specimens for TEM examination may induce certain physical changes, resulting in shrinkage and/or distortion of a specimen. Some of the problems associated with dehydration can be overcome by freezing the specimen and then embedding it by freeze substitution.

However, certain suitable specimens can be mounted directly onto a sample grid. Fibers can be disintegrated into small fragments, either in a laboratory blender or by ultrasonic vibration. Alternatively, thin replicas of the surfaces can be prepared (see details in Section III.A). Replica techniques were developed as a means of studying the ultrastructure of wood and fiber surfaces. Côté et al. [55] review the techniques for surface replication of samples for examination in the electron microscope and give a detailed description of the technique for making direct carbon replicas of wood and paper samples. This method is recommended for its simplicity and high reliability in representing fine details. Comer et al. [49] present examples of replicas of papers coated with various pigments commonly used in coatings. The excellent structural details of particle size, shape, and orientation help to explain properties such as gloss and ink receptivity.

Despite the limitations imposed by the TEM on the study of papermaking fibers, its great advantage lies in the high resolution that can be achieved—down to 0.2 nm with modern instruments. The earliest reported instance of the use of a TEM for examining pulp was by Sears and Kregel [289], who discussed its application to problems associated with pulp and papermaking. The TEM has been invaluable in characterizing the primary units of native cellulose and showed for the first time the microfibrillar structure of cellulose fibrils [53,86,124,125,263]. Examination of the morphology of cellulose synthesizing bacteria has also helped to shed further light on the structure of cellulose [65]. As with all microscopy, correct interpretation is essential, and Hanna [117] pinpoints some of the pitfalls involved in such studies. Jayme and coworkers [147–150], Côté [53], Asunmaa and Steenberg [4,6], and, more recently, Nanko and coworkers [224,225] are among many workers who made notable contributions to the study of fiber structure and fiber bonding using the TEM.

Ultrathin sectioning, employed for many TEM studies of fiber and sheet cross sections, enabled Stone and Scallan [308] to present direct evidence of internal fibrillation of cell walls during beating (see Fig. 1). Internal fibrillation, a term coined by Campbell [39], is the splitting apart of the cell wall layers into their constituent lamellae, which, according to Gallay [98], are thus “separated or resolved into a series of concentric sleeves, like layers on an onion.” Stone and Scallan postulated that microfibrils were associated laterally into sheets or lamellae and, because the microfibrils had greater adhesion in the tangential direction than in the radial direction, fiber wall swelling and internal rupture of lateral bonds caused the wall to delaminate into coaxial layers. But, because cleavage also occurs in the tangential plane, Scallan [286] extended the concept of concentric lamellae to a “honeycomb” structure. Water-swollen fibers were dehydrated by solvent exchange. The fibers were then embedded in methacrylate and mechanically sectioned. The methacrylate was then dissolved from the sections with chloroform. However, they recognized that their technique was responsible for exaggerating cell wall delamination and therefore precluded quantitative analysis. Tripp and Giuffria [336] had noticed earlier, using the same techniques, that the cross-sectional size of partially acetylated cotton fibers swelled by 200–400%. They suggested that this phenomenon might “be useful for studies where it is desirable and possible to break down the organization of the fiber cell wall,” and Dlugosz [71] took advantage of the expansion effects of methacrylate polymerization to reveal the cell wall structure of cotton fibers. Jayme [147] had earlier shown similar cross sections of coaxially delaminated cell walls in spruce fibers that had been delignified with sodium chlorite after swelling with 5% NaOH.

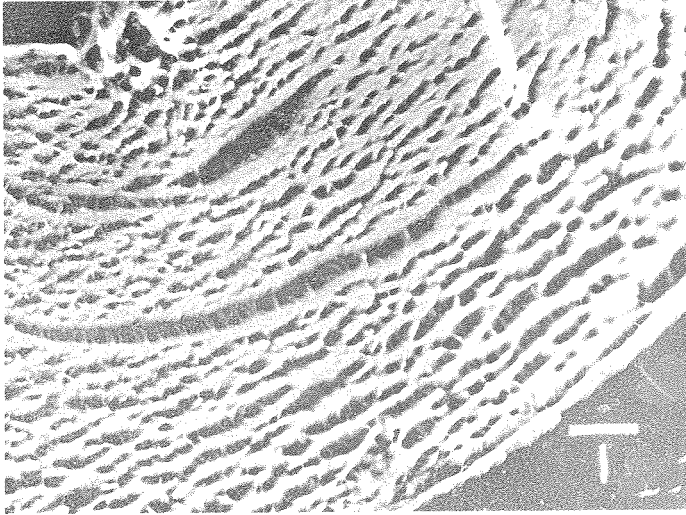


Fig. 1 Cross section of beaten fiber showing internal fibrillation. (From Ref. 308.) (Photo by G. M. A. Aberson.)

Gaining an insight into the structure of the cell wall is an important area of fundamental research. Pulping and refining processes produce changes in the molecular structure and chemical composition of cell wall components. For example, they cause redistribution of hemicelluloses, and knowledge of this is important to an understanding of fiber bonding. A means of labeling hemicelluloses has long been sought. In 1949, Mark (see Ref. 295, p. 115) wanted a substance “containing a heavy atom which reacts specifically with the hemicelluloses” for use with electron microscopy in order to find out something about their distribution in a sample. And in 1970, Page (see Ref. 53, p. 329) reiterated this need to develop “methods for introducing heavy metal atoms into specific sites to provide electron contrast.” He thought that the locations of lignin, hemicellulose, and cellulose could be found by this approach. Even today the interaction of the hemicellulose–lignin matrix with the cellulosic fibrils is not really known. However, some specific labeling techniques have been developed. Enzymes can be tagged with metal particles, and when these enzyme–metal complexes are incubated with the appropriate wood or fiber samples the enzymes bind to the specific polysaccharide. Jackson et al. [139] give full details of the preparation techniques. Ruel and Joseleau [279] used enzyme–gold complexes to study the distribution of xylans in grasses and glucomannans in tracheids of spruce fibers, and Mora et al. [214] employed the same technique to study the redeposition of xylans on birch kraft pulp fibers. Immunolabeling techniques have also been used. Srebotnik and Messner [303,304] used gold-labeled rabbit antibodies conjugated with marker proteins of different sizes to examine the porosity of wood cell walls.

Shijun [293] used a TEM to study the distribution of hemicelluloses in bagasse fibers. He first oxidized the aldehyde groups to carboxyl groups using NaClO_2 and then stained the fibers with KMnO_4 . Potassium permanganate is electron-opaque and is commonly used to provide contrast in TEM sections, but for lignin studies it is

used as a specific stain. The manganese ions react with the carboxyl groups and attach to them, so the presence of hemicellulose is denoted by dark areas.

Energy-dispersive X-ray analysis (EDXA) can also be used in conjunction with the TEM to analyze various elements in a sample and determine their distribution. Saka and coworkers [283–285] undertook comparative studies of lignin distribution using TEM/EDXA and UV microscopy.

Reflection Electron Microscope The reflection electron microscope (REM) was first employed for examination of fiber surfaces by Chapman and Menter [43], who used a commercial TEM modified to operate in reflection mode. In the REM, specimens are illuminated by an electron beam at a glancing incidence. The advantages of REM lie in a greater depth of field, giving images a three-dimensional appearance and allowing easy interpretation of the spatial relationship of structures. However, in early instruments beam damage caused polysaccharides to break down into gases, giving rise to bubble artifacts [3]. It is also necessary to use a higher beam intensity than with the TEM to make the image visible on the screen. The REM was used to examine pulp and paper for only a short period in the mid-1950s.

Scanning Electron Microscope Goldstein et al. [103] provide a comprehensive review of scanning electron microscopy (SEM) and its applications. Vaughan [338] and DeNee and Abraham [64] provide further details of microanalytical techniques. Walbaum [342] gives a clear account of the SEM and its functions and discusses the factors that influence image formation and contrast. Parham [247] outlines the principles of X-ray/SEM analysis and its application to paper.

In the SEM the electron beam is focused into a very small spot on the specimen and traverses over each point of the specimen in turn, one scan line at a time, to form a raster. The electrons emitted from each point on the specimen are collected by a nearby photomultiplier tube and produce a signal on a cathode ray tube that is being scanned in synchrony with the specimen. The electron beam stimulates the emission of electrons from the target spot, and these vary in abundance with the topography of the specimen; crevices emit the fewest electrons and high points the most.

The resolution of the SEM, generally 3–10 nm, is far better than that of the light microscope but inferior to that of the TEM. The great advantage of the SEM lies in its large depth of field—at least 300 times that of a light microscope at comparable magnification. The SEM is ideal for large bulky specimens and those of coarse structure. Small, whole specimens or thick pieces of material may be examined in the SEM, the size of the specimen being limited by the size of the sample holder, usually 1–2.5 cm in diameter, although larger samples can be accommodated. Dry specimens of wood and paper can be examined directly, but, as mentioned earlier, wet or moist specimens that are to be examined by conventional SEM have to be dehydrated. The favored method seems to be critical point drying rather than freeze drying because it is felt that critical point drying is more consistently reproducible; see Parham [249] and Sachs [281,282] for pulp fibers, Boyde [28] for animal tissues, and Parsons et al. [251] for plant tissues. However, it is possible to examine a moist uncoated specimen, such as a fresh leaf, directly in the SEM at a low voltage. This is possible for only a short period because the specimen will dehydrate very rapidly in the vacuum chamber [74,251]. Whichever specimen preparation method is used, it is usually necessary to coat the specimen with a thin layer

(~10 nm) of metal, usually gold or carbon. This provides a conductive surface that allows the electrons to drain off and thus prevents a buildup of electrostatic charge.

The SEM also offers the possibility of elemental analysis using backscatter detection or X-ray analysis. The interaction of the electron beam with the specimen produces, in addition to secondary electrons (SE), backscattered electrons (BSE). As the incident beam enters the sample, secondary electrons are generated, and it is these that are normally detected to give the topographical information. Backscattered electrons are those that re-emerge from the sample and, as they exit, generate their own secondary electrons, which can be collected by a special detector. This is usually referred to as backscattered electron imaging (BEI or BSI). The amount of backscattering that occurs is dependent on the atomic number of the elements present. The higher the atomic number, the more electrons are backscattered. The emerging backscattered electrons carry information about the nature of the specimen over a range of depths, the depth depending on the exact nature of the specimen. Similarly, an X-ray detector can be used in conjunction with the SEM to identify elements, because each element generates characteristic X-rays, and elemental mapping can be used to show the location of an element over the surface of the specimen [51, pp. 87–89]. Scanning electron microscope energy-dispersive X-ray spectrometry (SEM/EDX or EDS) studies have become routine, and quantitative analysis can also be carried out using the appropriate standards and reference materials.

The SEM is best suited for the study of surface structure, and its remarkable depth of field means that the surface of rough or irregular samples can be brought into focus over an area of several millimeters, and dry samples of wood and paper can be examined directly. It has proved to be an invaluable aid to descriptive analysis of wood and non-wood fibers, and several fine books of SEM micrographs have been published [38,51,52]. Details of the applications of the SEM to pulp and paper research can be found in Smith [301] and in Ilvessalo-Pfäffli and Laamanen [135]. James et al. [140] describe some of its applications to the study of Australian newspapers with respect to product performance.

Rezanowich [270] considered that the usefulness of SEM lay largely in its low magnification range, enabling studies of extensive surface areas. It is especially useful for studying large numbers of specimens that can be rapidly screened, with areas selected for more detailed examination. This application of SEM has yielded information about the influence of various factors on fiber–fiber bonding and sheet density, e.g., fiber collapse and conformability, fibrillation, and pulp yield [32,129,273]. Klofta and Miller [172] describe a method for obtaining a fibrillation index from scanning electronmicrographs of freeze-dried fibers. Teder [327,328] observed the effects of beating, drying, and heat treatment on the papermaking properties of spruce and birch pulps using the SEM and found differences between species (spruce and birch), fiber type (springwood and summerwood), and pulping process (sulfate and sulfite). Pye et al. [258] studied the structural changes that occur in papermaking processes and characterized the appearance of fibers at different stages. Samples of the web were taken from different positions along the paper machine, from wet end to reel-up, and freeze-dried for examination in the SEM. Washburn and Buchanan [345] outline the freezing procedure.

Stratton and Colson [311] examined fiber wall damage during rupture of individually bonded fibers. The bonded area was first measured using Page's polarized

light technique, and after elongation failure the surface areas were examined in the SEM for visual assessment of damage. Buchanan and Washburn [33,34] examined the fracture faces of samples of handsheets made of pure chemical pulp fibers and groundwood pulp fibers broken in tensile testing. In general, the number of fibers broken, as opposed to the number being pulled out, was higher in the stronger, chemical pulp sheets. The fracture lines were more sharply defined in the stronger sheets and very irregular in the weaker sheets. Nordman and Qvikström [230] made similar studies but compared handsheets made of pure earlywood and latewood fibers. They showed that rupture zones were clearly distinguishable by broken fibers in the stronger sheets made of earlywood fibers, whereas rupture zones were discernible only as a loosening of the structure in the sheets made of latewood fibers. They also examined the rupture zone in sections of wood subjected to tensile fracture and showed that ruptures proceeded in almost straight lines in earlywood sections but were very irregular in latewood sections. The installation of a tensile stage inside the specimen chamber of the SEM enables in situ monitoring and analysis of the straining behavior of the paper structure. Retulainen and Ebeling [265] employed this technique to examine the effect of sheet structure on the load–elongation behavior of fiber–fiber bonds.

Kučera and Bariska [177] used the SEM to study the structural changes of spruce and aspen wood samples subjected to axial compression and produced excellent scanning electron micrographs showing different types of deformation—microscopic and macroscopic compression failure lines, stress lines, and slip planes. Bergander and Salmén [18] applied load to specimens of spruce sapwood to investigate the effects of compression on the development of cracks and delamination in cell walls. Thayer and Thomas [330] used scanning electron microscopy to examine and analyze the physical characteristics at each stage of the formation of the glue line in corrugated board.

The SEM is the obvious tool for observing the micro- and macroroughness of surfaces, and stereoscopic images give an even greater perception of the surface topography and depth of field. No special equipment is required to characterize the surface structure; the sample is simply tilted, typically at an angle of 30–45° to the beam. Settlemeyer [291] used this method to examine the topography of coated papers and found that conventional measurements of gloss did not agree with visual perception. Enomae et al. [83] used a novel analytical technique, employing four secondary electron detectors, for constructing profile curves in order to investigate the surface topography of sheets and make surface roughness measurements.

Helle and Johnsen [123] used stereo images with BEI for studying the distribution of ink particles on paper and fiber surfaces, the atomic number of the ink particles being sufficiently different to distinguish them from fibers. Gregersen et al. [106] used a combination of electron imaging and BEI to examine ink distribution on paper surfaces at the single fiber level in order to study both variation in local ink coverage and ink penetration into interfiber voids.

The SEM has been used also to characterize filler and coating particles [27] as well as for examining their distribution within sheets. MacGregor [195] discusses the use of BSI to compare surface distribution of clay and calcium fillers in sheets formed on different machines. He also used EDS to map the calcium, illustrating the differences in amount and distribution of calcium on the two sides of the sheets. Peterson and Williams [257] used SEM/BSI with image analysis to determine coating

thickness and base roughness from cross sections of resin-embedded sheets. Klunness et al. [173] investigated fiber loading as a means of minimizing hornification by precipitating calcium carbonate within fiber voids in order to prevent subsequent collapse of the voids during drying. They cut cross sections of pulp fibers and handsheets with a razor blade and used SEM with X-ray microanalysis to observe the calcium carbonate deposits on the surfaces, and within the lumina, of the fibers.

Cross sections of sheets for SEM examination need to be cleanly cut, by using either a razor or a special guillotine or by first embedding the sheet for sectioning in a microtome. Hellawell and Nelson [122] compared, and illustrated, various cross-sectioning techniques they employed for examining coating structures: freeze-fracturing, free-hand razor cutting of paper immersed in a lubricant, and embedding in resin and microtoming. The disadvantage of the latter is that the sections may be distorted by knife chatter. Gibbon et al. [100] developed a new technique for obtaining cross sections of paper sheets for high magnification viewing, which overcomes this problem. Several precut samples of paper are inserted, between spacers, in a plastic mold (30 mm diameter); then resin is carefully added. After the resin has been cured, the block is ground and then polished on a machine to reveal the section plane. This results in a mount with artifact-free cross sections of paper. Gibbon used this technique in conjunction with SEM/EDX to study the distribution of inorganic filler particles in sheets. Williams and Drummond [356] used Gibbon's method of preparing sections of paper in resin blocks and then, after sectioning, removed a thin layer of the supporting resin according to the method of Maxwell [205]. This produces very high quality sections for studying sheet structure, and Williams et al. [357] include examples of these cross sections viewed first in normal transmitted light and then in the SEM. Browne et al. [31] used the same technique to examine the way in which sheet structure responds to calendering. They examined cross sections of uncalendered and calendered samples of a thermomechanical pulp (TMP) newsprint and a bleached kraft pulp paper containing hardwood and softwood fibers for evidence of deformation and fracture of fibers resulting from calendering treatments.

Lignin reacts with potassium permanganate and bromine, and treatment with these chemicals raises the atomic number of lignin, making it detectable in SEM/BEI and SEM/EDX studies. Saka et al. [285] developed a procedure for labeling lignin with bromine gas. The amount of reacted bromine was found to be directly proportional to lignin content and, using SEM/EDX, they made a qualitative and semi-quantitative analysis of lignin concentration and distribution within fiber cell walls. Eriksson et al. [84] and Westermark et al. [351] undertook similar studies in birch and spruce wood, but used a mercurization technique to label the lignin. Gregersen et al. [107] treated paper surfaces and paper cross sections with potassium permanganate or bromine gas to study the distribution of middle lamella on TMP fibers, to identify the mechanical fibers in blended pulps, and to compare kraft pulps of high and low yield. However, the method is not recommended for quantitative determination of lignin. A similar method for locating fines in mechanical pulp handsheets is described by de Silveira et al. [67]. The fines fraction of a mechanical pulp was halogenated with chlorine or bromine and then added to long fibers for handsheet preparation. Handsheets samples were embedded and cross-sectioned. The fines were readily detectable with BEI, the lignin appearing much brighter than the carbohydrates.

Forseth and Helle [93] used the SEM to investigate the effects of moistening on calendered paper such as occur during pigment coating and offset printing. They prepared cross sections of sheets embedded in resin and then dissolved away the resin at the surface, using the method of Williams and Drummond. This enabled them to observe and quantify water-induced changes in cross sections of the same fibers by imaging the same areas before and after wetting. They also exposed samples to bromine gas and used SEM/BEI to differentiate between the chemical and mechanical pulp components of the sheets [90].

Low Temperature Scanning Electron Microscope The low temperature scanning electron microscope (LTSEM) is a conventional SEM to which has been added a special cryogenic unit. Use of the LTSEM obviates the need for dehydration of wet specimens. Instead, the specimen is rapidly frozen and is examined in a frozen hydrated state, its frozen state being maintained at a temperature of -185°C on a special cryostage. It is also possible to use cold stages with the TEM and scanning transmission electron microscope (STEM), but these are confined to specialist fields and do not appear to have been applied to paper science research. The LTSEM is described in detail in Section V.

Scanning Transmission Electron Microscope This uses the scanning beam in a transmission mode, thus allowing the examination of thicker samples than can be examined with conventional TEM.

Environmental Scanning Electron Microscope The ESEM differs from the conventional SEM in that the vacuum column contains a differential pumping system, and a special detector allows examination of specimens in the presence of water vapor. Specimens can therefore be viewed under ambient conditions and no coating is required. In fact, wet, frozen, or dry samples may be examined with the ESEM. The ESEM was designed specifically for examining liquid and hydrated samples, thus enabling the effects of wetting or drying processes to be monitored. Danilatos [59] gives a concise description of the first commercial ESEM and a bibliography [60] of its applications, and de Silveira et al. [66] discuss the advantages and drawbacks of the ESEM. So far the ESEM has been applied mainly to studies of the effects of water on the swelling behavior of fibers [151] and on surface roughening of papers [91,92,108]. Surface profilometry of paper and board is described in detail in Chapter 11. Mott et al. [221] used the ESEM to examine microstraining of single wood pulp fibers. A comparison of fiber images obtained with ESEM and AFM is given in Section VI. Although both techniques revealed image details of the cell wall, the resolution of the AFM was superior to that of the ESEM.

C. Scanning Probe Microscopes

Atomic Force Microscope and Scanning Tunneling Microscope These are the most successful of a series of scanning probe microscopes that were developed for high resolution imaging. A review of scanning probe microscopes is given by Wickramasinghe [353]. They have several advantages over the TEM, including the possibility of atomic resolution and their ability to operate at ambient air pressure and even in liquid environments, allowing structures to be examined in their native

hydrated state. The AFM is now a well-established tool in three-dimensional topographical analysis of various materials at the molecular level. The AFM is described in detail in Section VI.

IV. THE CONFOCAL LASER SCANNING MICROSCOPE

The confocal laser scanning microscope (CLSM) is variously referred to in the literature as a laser scanning microscope (LSM), scanning optical microscope (SOM), confocal fluorescence scanning microscope (CFSM), confocal scanning optical microscope (CSOM), and confocal scanning microscope (CSM). References will also be found to a tandem scanning reflection light microscope (TSRLM or TSM). The latter are real-time, direct-viewing confocal microscopes. Illuminating and detecting apertures are scanned in tandem. This is achieved by using a rotating disk containing thousands of tiny holes (the apertures) arranged in a precise and symmetrical pattern and simultaneously illuminating the specimen with hundreds of scanning beams.

All CLSMs currently on the market are reflection microscopes. Dixon and Cogswell [68] and Dixon et al. [69] reported on a confocal scanning microscope for transmission and reflection imaging, but confocal transmission microscopes are optically complex and not yet commercially available. More recently Dixon et al. [70] described a new confocal scanning beam laser microscope that can image large areas of specimens (7.5 cm \times 7.5 cm). When combined with the confocal microscope this produces a hybrid imaging system, the microscope/microscope, that uses the advantages of small area, high speed, high resolution microscopy. Again, this is not yet commercially available.

The basic principles of confocal microscopy described below are based largely on knowledge and experience of a first generation Leica CLSM. There are several different types of CLSMs on the market, most of which can be used for the applications described here. Their ability to perform certain tasks is usually just a matter of whether or not the appropriate software is installed, but in some cases appropriate hardware may not be available. Lichtman [187] gives a brief general review of confocal microscopes. There are a few reference books that provide detailed accounts of the different aspects of confocal microscopy [253,360,361]. The book edited by Pawley [253] includes chapters that describe and compare each of the main component parts of these microscopes, provides a bibliography of confocal microscopes [347], and, in Appendix 2, gives brief descriptions of the models currently on the market. Centonze and Pawley [42] provide an excellent tutorial on practical confocal microscopy for the novice. There is also a wealth of information in the literature on the application of confocal microscopy, but most of it pertains to cell biology. Of these, a review by Shotton [294] provides the beginner with a good overview of the principles.

A. Basic Principles of the CLSM

The CLSM consists of a conventional optical microscope to which are coupled a laser and associated optical system (mirrors, optic fiber, pinholes), a scanning unit, and photodetectors. A fast central processor controls microscope functions, drives

the scanner, converts detected light to digital form, and controls the subsequent processing of data. A wavelength selector, beam splitters, and a series of bandpass filters enable the microscope to be used in reflection or fluorescence mode. The changeover from conventional use to the confocal mode is achieved simply by moving a lever. This operates a beam-diverting system that prevents entry of laser light into the eyepieces when it is being used in the confocal mode.

In a conventional optical microscope the whole field of view is uniformly and continuously bathed in light and can be viewed directly, but this is not possible with the confocal microscope. The optical system of a CLSM contains two pinholes that are optically separated by a beam splitter (see Fig. 2). The laser beam passing through the illumination pinhole is focused to a fine spot that illuminates only one point in the in-focus plane. Because the detection pinhole is confocal with the illuminated point, only the light that is reflected or emitted from this point can pass through it (placed in front of the detector). Any light emanating from above or below the in-focus plane is eliminated.

Because the laser beam is focused to a single point it has to be moved across the sample. This is achieved by using a scanning mirror to deflect the beam across the specimen, point by point, in raster fashion—the same principle as in the scanning

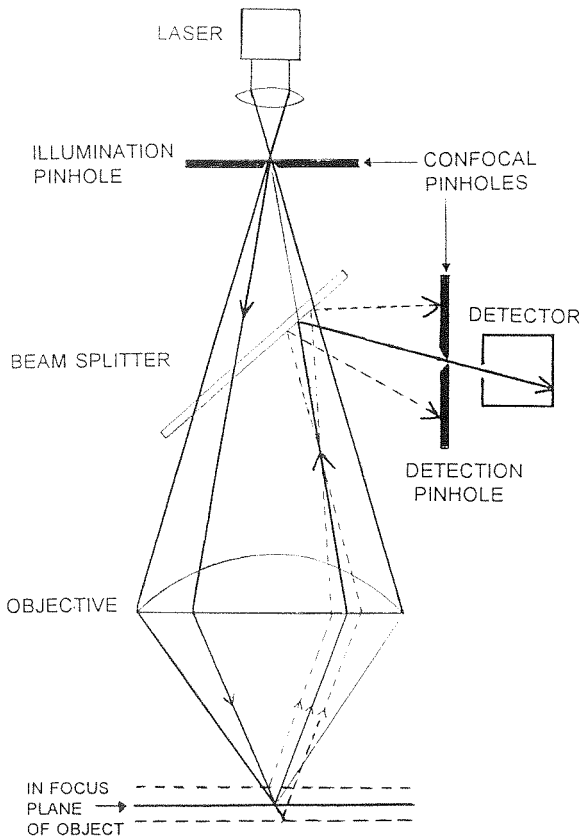


Fig. 2 The principle of a confocal microscope.

electron microscope. This method of scanning (referred to as off-axis scanning) can be very fast, allowing many frames to be built up per second and thus enabling rapid changes within specimens to be observed. In some microscopes, however, it is the object that is mechanically scanned across a stationary point of light (referred to as on-axis scanning). This method produces undistorted images of very high quality.

In this way an image is sequentially built up point by point. Data are recorded as a set of intensity values for every pixel in the area scanned and are stored in the computer for future processing and simultaneously displayed on the image monitor. Thus, the image produced by the beam is a thin slice of just those parts of the specimen that lie in the in-focus plane, i.e., an optical section. So, whereas in a conventional transmitted light image everything in the image field of view can be seen but only part of the image will be in focus (Fig. 3a) in the confocal images only those structures that are in focus will be seen. Elimination of out-of-focus structures means that there are no blurred areas in the image (Figs. 3b–3d). By moving the microscope stage vertically through a set distance, one step at a time, a series of consecutive optical sections can be collected. In short, the CLSM can be considered a 3D sampling instrument for collecting information at different levels. Figure 4 shows a series of optical sections taken in the xy plane through a CTMP shive at incremental steps of $2.4\ \mu\text{m}$ along the z axis.

Nondestructive optical sectioning is the unique feature of the CLSM. It enables detection of structural details that are otherwise concealed by overlying material. The absence of various conformation-influencing preparatory steps allows a more faithful rendering of specimen reality than the conventional optical or electron microscope. Optical sections can be collected not only in the xy plane but also in the xz plane, which gives a cross-sectional view of the sample (Fig. 5). Optical sectioning in the xz plane is achieved by moving the microscope stage very rapidly

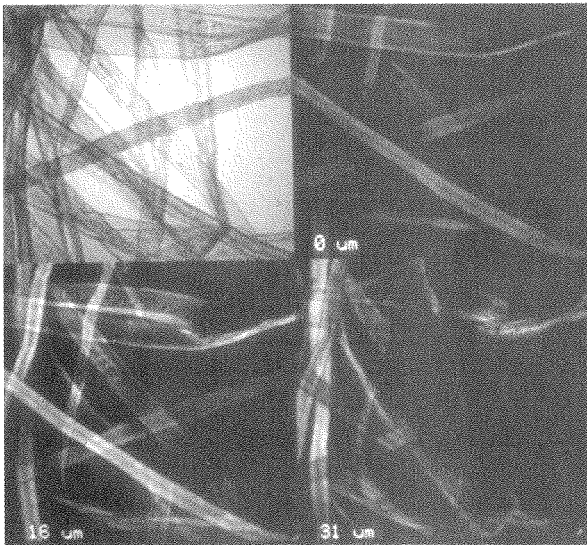


Fig. 3 Pulp fibers seen in conventional transmitted light (upper left) and the same fibers seen in confocal mode at depths of 0, 16, and 31 μm .

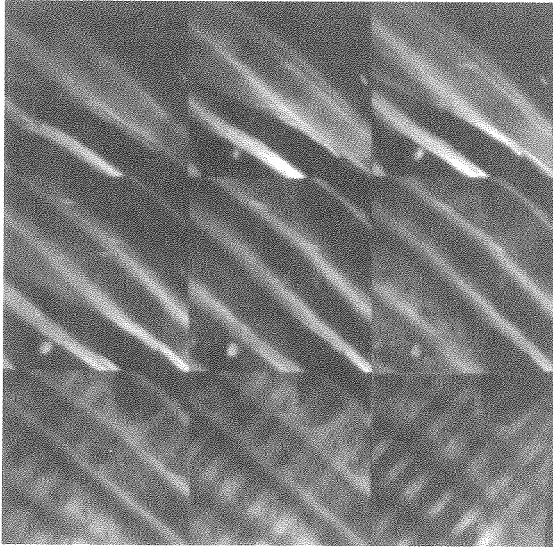


Fig. 4 Nine of a series of 16 optical sections taken through a CTMP shive to a depth of 36 μm . Ray cells can be seen beneath the tracheids.

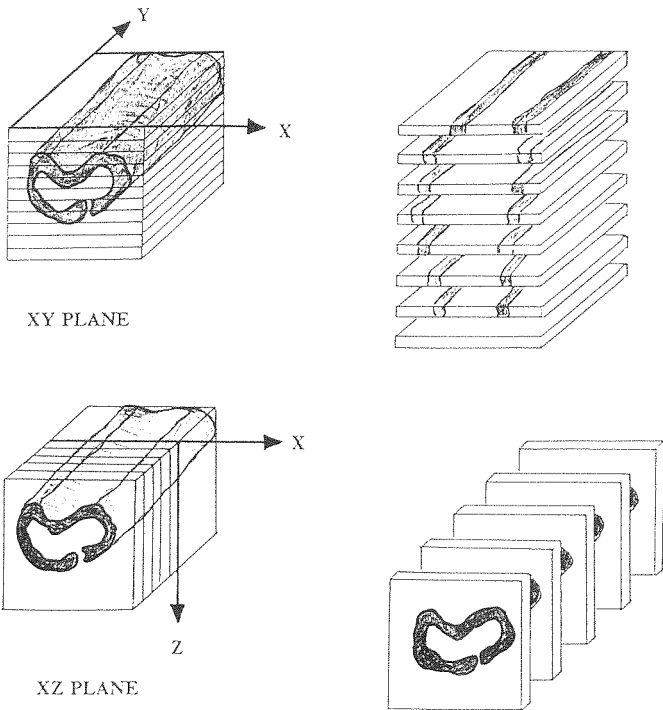


Fig. 5 Samples can be sectioned in the xy plane and in the xz plane.

use to thin specimens or to a thin layer at the surface of a specimen. A hardware zoom function, which can be used during scanning, allows increase in the magnification of the image (by up to a factor of 8 with the Leica CLSM) without having to change the objective.

Choice of objective also depends on the mounting medium being used; ideally, the refractive index of whatever lies between the objective and the glass cover slip should match that of the mounting medium. Therefore, a water immersion objective should be used to examine specimens mounted in water, an oil immersion objective for specimens in commercial mounting media of the same refractive index as oil, and a dry objective for specimens dried down onto microscope slides. If there is a mismatch in refractive indices of the media, then optical aberrations will distort the size and shape of images collected in the xz plane. However, when specimens are being examined under changing conditions, as in drying experiments, the ideal cannot be attained. A compromise may be reached by using a multi-immersion objective. (This problem is discussed further in Section IV.F.)

Step Size When a series of consecutive sections is being collected through a certain distance, it is necessary to select a step size, i.e., the distance the microscope stage is to be moved between successive planes. Choice of step size will depend on the N.A. and consequently on the depth of focus of the objective being used. Therefore the step size should be equal to, or less than, the depth of focus if all available information is to be acquired. This is especially important where height differences are being measured, and it is always better to oversample because undersampling may result in incomplete information. However, when selecting step size, the depth to which the specimen is to be sampled and the number of sections to be collected must also be borne in mind, because some older models of CLSMs may have limitations in data storage capability and computing power.

B. Imaging Modes

The optical system contains beam splitters and bandpass filters that allow the CLSM to be operated in different modes. The majority of CLSMs can be used in reflection or fluorescence mode, and most of them nowadays have two or more photodetectors. This enables simultaneous acquisition in different image modes.

Reflection Mode All available light from the laser is used in the reflection mode. This mode is usually used for dry specimens, particularly for surfaces of paper samples where roughness measurements are to be made. Reflection mode is used where staining for fluorescence work (which requires wetting the sample) is impractical. Reflection mode is suitable for examining dry samples containing filler particles and can also be used for specimens that have been labeled with metal particles. Shotton [294] reports that clear images of individual gold particles of 40 nm diameter have been obtained with confocal reflection scanning microscopy using a $63\times/1.4$ oil immersion objective.

Fluorescence Mode Although there is a wide choice of lasers on the market, most of the earlier models of CLSMs came equipped with an argon ion laser. This has generally been replaced by a krypton/argon ion laser offering better choice of

excitation wavelengths. Although this mode usually requires the sample to be stained with a fluorescent dye, in some cases specimens may have enough autofluorescence to produce a reasonable image without the need for staining. This is particularly true of fresh plant material and lignin-rich fibers such as those of mechanical pulps. As with the reflection mode, the fluorescence mode can be used for localization of fluorescently labeled subresolution particles. Although the particles themselves cannot be resolved, their location can be detected by the emitted fluorescence.

Confocal fluorescence microscopy overcomes the problems associated with conventional epifluorescence microscopy where diffuse light originates from structures above and below the focal plane.

The fluorescence mode is to be preferred for acquiring clear cross-sectional images of fibers in the xz plane. However, in order that the structure of the sample is not affected by the wetting incurred during staining, experiments should be planned so that specimens are stained at the beginning of any beating or sheet-making processes and are therefore ready for examination at any subsequent stage if required.

Conventional Transmitted Light Mode It is also possible to collect non-confocal transmitted light images by using the laser if the specimen is sufficiently thin or translucent. In this case laser light passing through the specimen and condenser is collected by an optic fiber placed below the condenser and goes directly to a second detector, thus bypassing the detection pinhole. It is often very useful to be able to compare the area seen in the confocal image with the same area seen in the familiar transmitted light micrograph.

Dual (or Multiple) Wavelength Imaging If there is more than one photodetector (and modern instruments may have up to four detectors), then it is possible, by the use of bandpass filters, to obtain images in different modes simultaneously from the same scanning spot. Images generated by the same scanning spot are in exact spatial register and can therefore be superimposed to give a complete picture. The fluorescence and transmission modes have proved to be a particularly useful combination. Similarly, two fluorescence images can be obtained simultaneously from a specimen containing structures that have been specifically stained with different fluorescent dyes. Use of appropriate filters separates the emission wavelengths, channeling each to a different detector. This particular technique of double, or even triple, staining is widely employed by cell biologists [120,174], though its application to the study of fibers is very limited, for reasons that will be discussed.

C. Specimen Preparation Techniques

Specimen preparation is the same as for normal light microscopy and therefore relatively simple. Specimens may require staining, and, of course, large samples may need to be cut down to a size that will fit onto the glass microscope slide.

Slide Preparation Wet fibers, or drops of fines material in suspension, are mounted on a microscope slide in the normal way and covered with a glass cover slip. Very small amounts of material are being examined, so it is important that

samples be taken from a well-mixed pulp suspension to ensure that they are as representative as possible.

Cover slips must be firmly secured to the slide so that the sample does not move when the microscope stage is moved during sectioning. Securing can be done simply with strips of adhesive tape, or the cover slip can be sealed in place with rubber solution or nail polish. Care should be taken to ensure that the pressure of the cover slip does not cause mechanical damage or deformation of the sample. Spacers can be used for this purpose, but they have to be of just the right size because for high magnification work the specimen needs to be as close to the cover slip as possible, because of limitations in working distance. Likewise, the microscope slide must be clamped firmly in position on the microscope stage. Optical sectioning in the xz plane involves rapid movement of the microscope stage in the z direction; therefore, failure to secure samples firmly enough will result in blurred or stretched images. This is particularly important when oil immersion objectives are being used because surface tension forces may be strong enough to lift the cover slip from the microscope slide or even lift the whole slide if it is not satisfactorily anchored to the stage.

Generally, for investigations into the morphological structure of fibers and fines material, the best images are obtained if the fibers are stained with a fluorescent stain and examined in a wet state while fibrillar material is spread out. Certain types of paper and board, such as release paper, polyethylene-coated board, coated papers, and papers containing fillers, may contain pigments and fillers that have fluorescent properties and therefore do not require staining. In fact, some, such as polyethylene-coated board, may be impervious to staining, whereas for others, such as coated papers, staining is impractical because the application of an aqueous stain will disturb the structure of both the coating layer and the underlying base paper.

If dry specimens are to be examined with an oil immersion objective, they should, ideally, be mounted either in immersion oil or in some commercial mounting medium of the same refractive index as the oil. (See Section IV.F.)

Staining If staining is required it can usually be done quickly and easily. The stains are usually made up as aqueous solutions (1–2% w/v). Wet pulp and paper samples can be immersed directly in a few drops of stain and then rinsed in distilled water to remove excess stain; dry samples may be wetted with distilled water before staining. Suspensions of fibers or fines material and starch solutions can be stained by carefully stirring stain into the suspension a drop at a time, because it is not easy to wash off excess stain without losing some of the material.

Much biological light microscopy is carried out on specimens of low intrinsic contrast, and staining is needed to increase overall contrast without much concern for staining selectivity. But, more importantly, microscopy is a way of gaining information about small structures. It can tell us what they are, where they are, and how many there are or how much there is. A stain, therefore, is any visual label attached to the specimen that will help answer these questions—dyes, fluorochromes, metal ions, labeled antibodies, and enzyme substrates.

Staining may be selective. Specific stains are those that have an affinity for particular molecules or substances, thus enabling easy identification and localization in a specimen of entities of a particular chemical nature. Staining is widely used for chemical analysis. Microscopical histochemistry (i.e., the localization and identification of substances and enzyme activity within cells and tissues) was pioneered by the

French botanist Raspail as long ago as 1825, and histochemical staining techniques are routinely used by biologists to identify tissues and to make quantitative analyses.

The standard test methods for fiber analysis employ chemical analysis in conjunction with light microscopy. Several stains are used to identify the types of pulp present in a sample. Fibers are identified by the color they assume, thus making it possible to differentiate between fibers of hardwoods and softwoods, chemical and mechanical pulps, bleached and unbleached pulps. Unfortunately, these methods cannot be used with the CLSM, because laser light is monochromatic and cannot show the color differences. Instead, fluorescent stains must be used.

Fluorochromes, the stains most commonly used in confocal laser scanning microscopy, are substances whose electrons are excited to a higher state by a particular wavelength of light. As the electrons return to their normal state they release energy in the form of light of a longer wavelength, and it is this emitted light that is detected. Some substances may be naturally fluorescent, creating primary fluorescence, but in most cases secondary fluorescence is also necessary. High image contrast is important for fluorescence microscopy; the structures of interest should be bright and the rest of the image dark.

There are a large number of fluorochromes available for biological specimens (see Kasten [159]). Acridine orange appears to have been most widely used for both fiber and paper samples and has proved to be a good general stain. Congo red, auramine, rhodamine, and safranin have also been used successfully. Some textile dyes (e.g., Neolan saurerot E-XB and Maxilon brillantflavin 10 GFF, Ciba-Geigy) and optical brighteners (e.g., Resolinbrillantgelb 10 GN, Bayer) are also suitable, and further experimentation with such dyes is recommended. Fluorescently labeled dextrans can also be used. Dextrans are water-soluble polysaccharides of high molecular weight. They are commercially available in fractions of different molecular weights and have been used traditionally as inert colloids in perfusion studies because they are not absorbed significantly by fibers. Stone and Scallan [309] and Scallan [287] used dextran molecules in their solute exclusion experiments to determine the size of pores in cell walls. When labeled dextran is used to stain fiber suspensions or sheets for fluorescence microscopy, a negative image is obtained, the interfiber spaces giving a bright image and the fibers remaining dark.

Photobleaching can be a problem in fluorescence microscopy. Long excitation periods cause a fluorochrome to decompose, creating photobleaching, which results in a loss in intensity in the area being examined. The problem is particularly noticeable with acridine orange but can usually be overcome by using a very low concentration of the stain [145]. However, photobleaching can also be used to advantage, and fluorescence recovery after photobleaching (FRAP or FPR) has become a useful technique for studying the transport of fluorescently labeled substances in living cells. The laser light bleaches the fluorescent label in the small area being examined so that it no longer gives an intensity reading, but, because there is a constant through-flow of the labeled substance, continuous scanning of the same area shows when the intensity rises again as the photobleached material is replaced. Blonk et al. [24] describe methods for measuring the mobility of labeled particles in liquid systems and for calculating diffusion coefficients.

The choice of stain is governed by the excitation wavelengths of the laser and its specificity for a particular specimen. Consequently, the use of CLSM for chemical analysis of pulp and paper samples imposes certain limitations. Most of the earlier

CLSMs were fitted with argon ion lasers, which have excitation wavelengths of 488 and 514 nm. Nowadays krypton/argon ion lasers are more common. These have excitation wavelengths of 488, 568, and 647 nm and thus offer a little more scope. Helium/neon lasers are preferred by some researchers because they are lower powered and heating effects are therefore reduced [223].

Paper scientists are further limited in their choice of stain by the chemical composition of the material they are examining, mainly nonliving plant cells, and although there is a long history of botanical histochemistry, little quantitative work has been done with cell wall carbohydrates despite their importance in the cell wall. Ligning, cellulose, hemicelluloses, and pectins are the main constituents of the cell walls of wood. Lignins are fairly easy to deal with, because there are some stains, e.g., Schiff's reagent [152], that will preferentially stain lignin, and they also exhibit primary fluorescence in UV and blue light. It is the cellulose and hemicelluloses that present the difficulties; there are many of them with considerable chemical similarity and, more important, they rarely occur singly. The cell wall contains large numbers of complex polysaccharides, and it is difficult to find a stain specific to a particular polysaccharide.

However, some specific labeling techniques have been developed for TEM studies (see Section III.B). Jackson et al. [139] describe methods for the preparation of enzyme-gold complexes enhanced with silver for observing the effects of cellulase attachment to secondary fibers of a bleached softwood pulp with an optical microscope. Also, immunolabeling techniques are available for determining the presence and location of specific polysaccharides. Monoclonal antibodies are highly specific probes that can be directed against a range of substances. The application of this technique to the study of pulp fibers is still in its early stages, and there are some problems. The antibodies are not always as specific as could be desired and may bind to other polysaccharides. Lackner et al. [180] employed the silver staining technique to enhance immunogold-labeled ligninases for optical microscopy. However, any labeling techniques using fluorochromes or metals can be used for confocal microscopy. A detailed account of the use of confocal reflection microscopy for imaging immunogold labels is given by Cogswell [48].

D. Fluorescence Quantification

Quantitative fluorescence analysis is widely used in cell biology. The amount of fluorescence emitted from specifically stained structures is related to the amount of the particular substance present. A densitometric program can display the distribution of fluorescence intensity in specifically labeled structures along a selected line, and the volume of fluorescent material can be determined. However, as far as is known, this has not yet been applied to pulp and paper research though it could be employed in conjunction with specific staining and immunolabeling techniques.

E. Image Acquisition and Processing

Reduction of signal noise is important both for image quality and for accuracy of subsequent measurements. Filtering can be achieved during image acquisition either by frame averaging or by scanning in a line accumulation mode, and the user can observe the improvement of the image quality during its acquisition. The noisier the

image, the greater the number of times it will have to be scanned. A fluorescently stained specimen should give a clean image, whereas an unstained or weakly autofluorescent sample will be noisy and may require a large number of scans.

Raw confocal images are often less than perfect, but it is possible to enhance them by computational processing. Electronic contrast facilities enable observation of very fine structural detail in both weakly stained and unstained samples. This can be achieved with a variety of standard image analysis techniques. For example, linear filters can enhance the visual appearance of an image by smoothing or accentuating the edges of structures. There are also many logical and arithmetical image processing operations that can be used to increase contrast or enhance certain features. Laser light is monochromatic; therefore images are black and white, so pseudocolor is used. Because the human eye can perceive many more colors than gray levels, the use of pseudocolor may be considered a further technique for image enhancement.

Once a series of images (or optical sections) has been collected it can be processed in different ways to make a three-dimensional representation of the image. A series of sections can even be viewed rapidly as a movie to give a more realistic idea of the depth of a sample as well as to show the relative positions of different structures. Although the principles of confocal imaging and methods of image collection are common to all makes of CLSMs, there will be differences in the methods of processing data, depending on the software used. Cox [56] gives details of data storage and of various systems for obtaining hard copies of images.

Three-Dimensional Reconstruction Most CLSMs are supplied with basic image processing software and sufficient power to reconstruct a 3D image. White [352] gives examples and details of some of the multidimensional imaging systems on the market. Each set of consecutive optical sections is in spatial register and can readily be superimposed to construct the three-dimensional structure. This can be done in a number of ways.

Extended Focus Image An extended depth of focus image is produced by simply adding all the sections together and scaling down the intensity. Features hidden beneath overlying structures are revealed by this method. Various algorithms can be used that take into account the intensity values of pixels in the z direction through the image stack and thus emphasize different features in the image.

Simulated Fluorescence Process This method of 3D image reconstruction simulates the fluorescence that would be produced by an incident light source angled obliquely. The intensity level is corrected for each section in the image stack according to its depth and to preset absorption and emission levels. This produces a shadowed effect (not unlike that produced by a scanning electron microscope) that emphasizes structural features on the surface.

Topographical Image A topographical image is color-coded for height; the uppermost structures are the brightest, and the deepest are the darkest. Voids are black. This application takes advantage of the fact that as the object passes through focus, the image intensity shows a sharp maximum. The x , y , z coordinates of every point in the sample are determined automatically by through-focusing, and the focal level where maximum intensity is recorded is determined for each pixel. It is from this information that the topographical image is derived, showing the relative positions of structures within the volume sectioned. Points of equal height on the topographi-

cal image can then be joined to produce a cartographic representation of the height structures (i.e., a contour map), or a three-dimensional surface plot can be produced to show the surface roughness profile.

Stereo Images All the sections in the image stack are sequentially shifted by a constant number of pixels to the left or right and then combined pixel by pixel to generate a black-and-white stereo pair of images. A pair of images can be combined to give an anaglyph (two-color) stereo pair. Such images can be viewed directly in three dimensions by using special spectacles and give an excellent impression of depth and spatial structure. Figure 8 shows some of the different images, described above, that have been generated from the same data stack. Martínez-Nistal et al. [203] give some nice examples of 3D reconstructions of hardwood pulp fibers.

Rotation A stack of optical sections can be rotated about any, or all, of its axes so that the sample can be viewed from different angles. The rotation program calculates a series of projection images of the data stack calculated at different tilt angles, with rotation and projection being performed simultaneously. Tilt angles are first selected and set. The best results will be obtained from a series of images having a small step size. Figure 9a shows CTMP fibers constructed from a stack of 16 sections collected in the xz plane. The same image stack rotated through 20° about two of the axes (Fig. 9b) reveals a pit in a fiber (top left-hand corner) not visible in Fig. 9a. It is also possible to cut an optical slice at any angle through the image stack. This enables cross-sectional (i.e., xz plane) views to be made through a stack of images collected in the xy plane if it is not possible to scan in the xz plane.

F. Artifacts of CLSM Imaging

Artifacts must be avoided. Therefore, when a specimen requires some special preparation it is necessary to check the sample for any changes that might have been induced by the preparation technique. One way is to measure the specimen before and after treatment. Stelzer and Bacallao [307] suggest that, for fluorescence microscopy, an evaluation of the quality of the preparation procedure should be based on images recorded by conventional fluorescence microscopy; images recorded with a conventional fluorescence microscope using an objective of high N.A. (> 1.25) will provide a standard against which images derived from a confocal fluorescence microscope may be tested.

Diatoms have been traditionally used for testing the resolution of microscopes. Wilke [354] used the diatom *Amphipleura pellucida* recorded at a wavelength of 488 nm to show periodic structure resolved with good contrast using a Zeiss Plan-Apochromat $63\times/1.4$ objective. Tsien and Bacskai [337] mixed small quantities of a commercial preparation of diatomaceous earth in solutions of fluorescent dyes. They used different fluorochromes in different solvents of varying concentrations to compare the effect of varying wavelength, signal strength, and refractive index.

Aberrations are inherent in all optical microscopes. These may be optical (due to the design of various components), chromatic, or geometric (due to diffraction phenomena). Image fidelity can be affected by curvature-of-field effects. This produces distortion in 3D reconstruction; therefore, plan or flatfield (F) objectives should be used. The thickness of the glass cover slip (normally $170\ \mu\text{m}$) is also very important, because it has a severe impact on xz resolution. Aberrations in

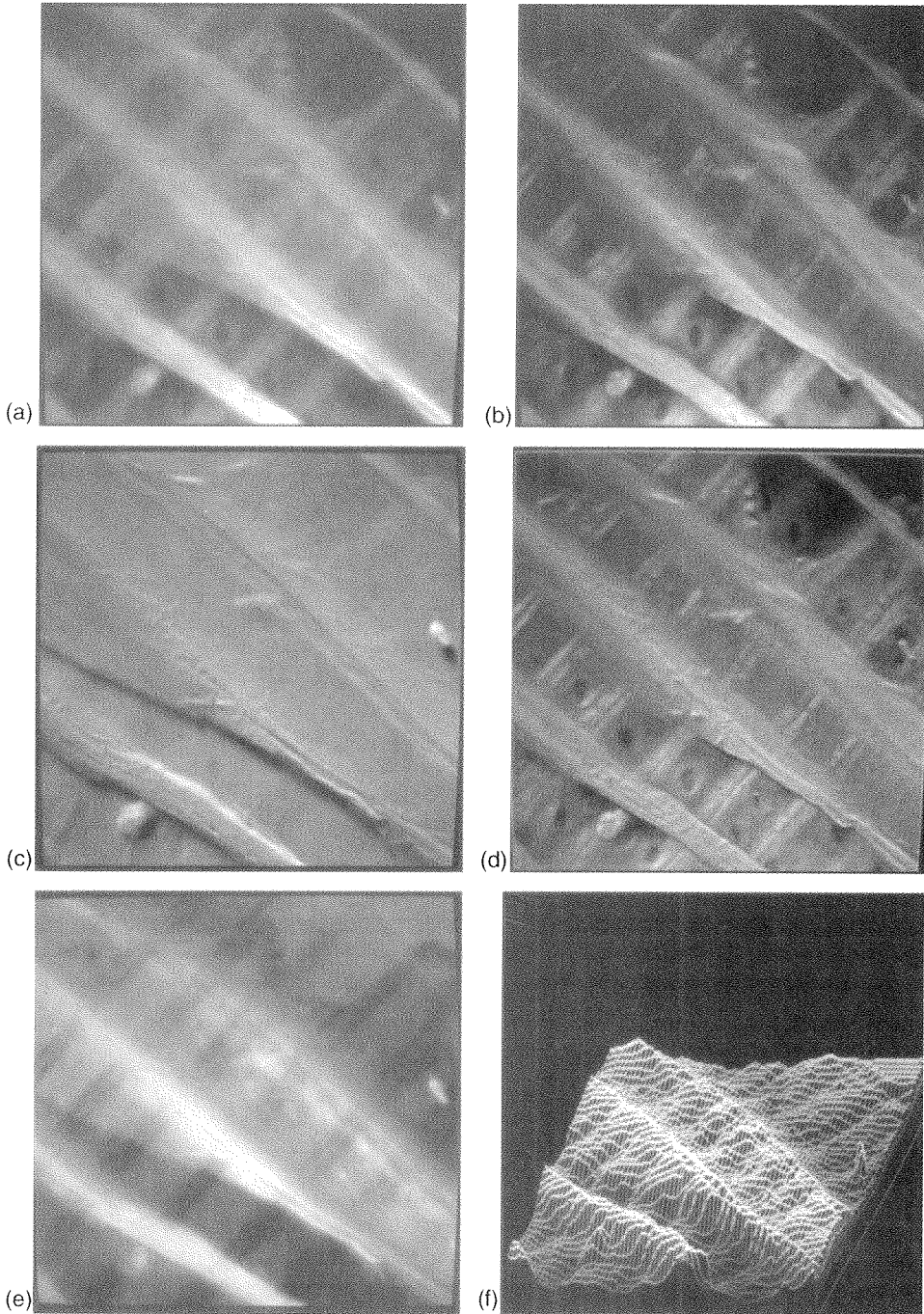


Fig. 8 The series of optical sections shown in Fig. 4 processed in different ways. (a) An extended focus image; (b) an extended focus image where weighting has been given to maximum intensity values; (c) a simulated fluorescence image; (d) a combination of a stereo image and simulated fluorescence process; (e) a topographical image; and (f) the surface profile constructed from it.

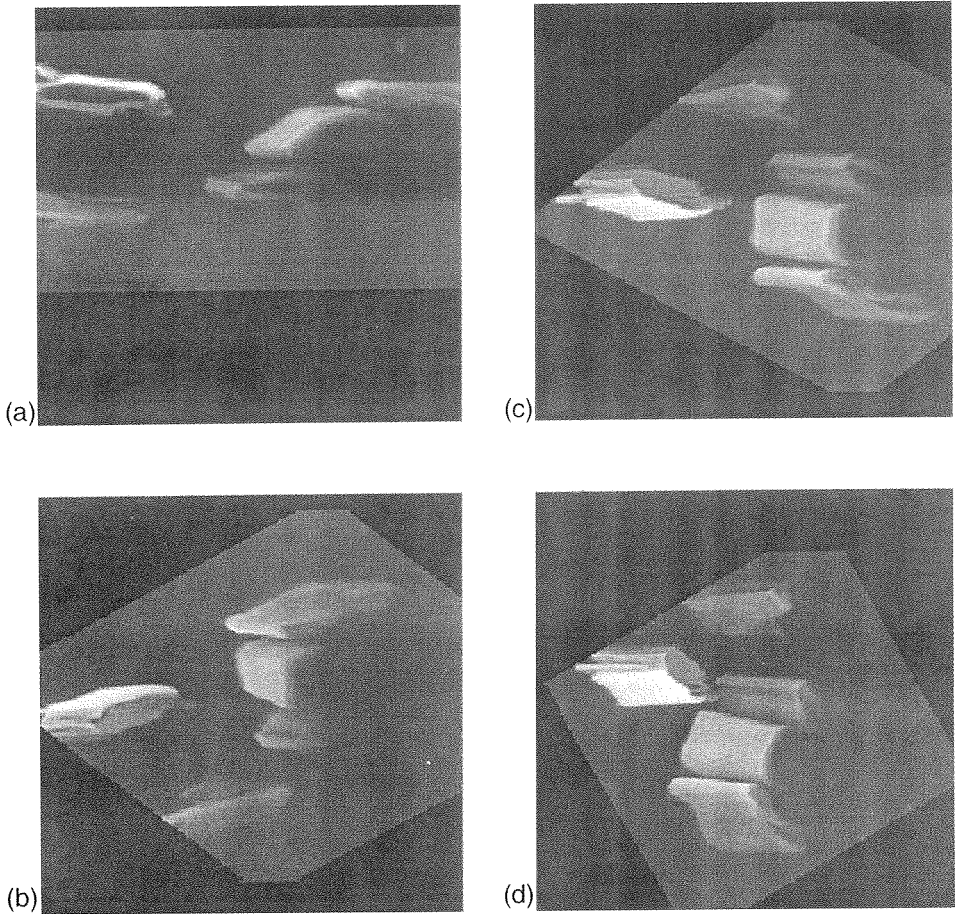


Fig. 9 (a) An extended focus image of a series of optical sections collected in the xz plane. (b)–(d). Views from different angles when the image stack is rotated 20° through the x and z axes, which reveal that the bright fiber in the top left-hand corner of (a) has a bordered pit.

cross-sectional images collected in the xz plane are probably the main potential source of error in the analysis of confocal scanning microscopy images. Therefore images must be calibrated against a standard of known dimensions before any measurements are made.

If the refractive index of the immersion medium for the objective does not match that of the mounting medium (see “Choice of Objective,” Section IV.A), then spherical aberrations will distort the size and shape of the xz plane image. A mismatch of media produces significant distortion in the depth measurements, but lateral measurements are not affected. Such aberrations are described in more detail by Hell et al. [121] and Visser and Oud [340]. Consequently, careful calibration of the xz plane images is necessary. Fluorescently labeled latex spheres, or man-made fibers, of known dimensions can be used, and a few can easily be included with pulp or sheet samples in order to check image shape in the z direction. Figure 10 illustrates the differences in apparent size and shape of cross-sectional images result-

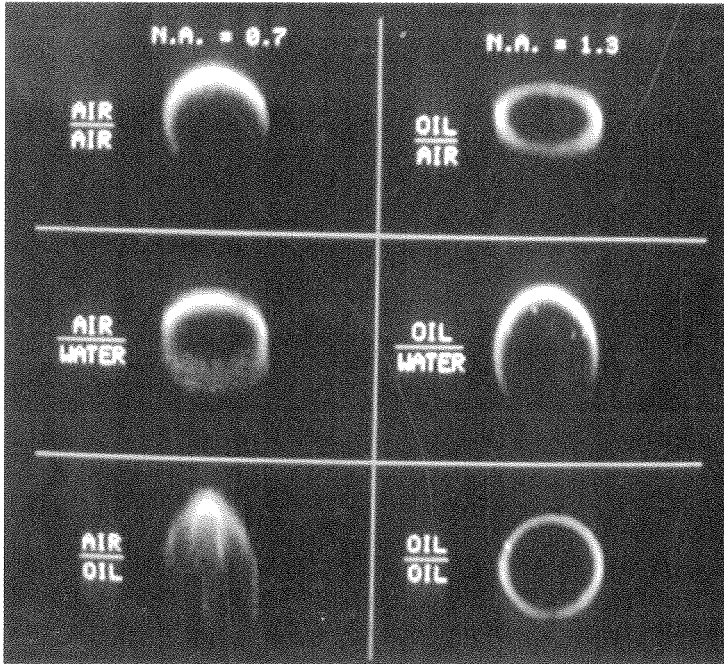


Fig. 10 A cross section through a polyamide fiber showing the spherical aberrations caused by mismatch of media.

ing from the use of different mounting media. Polyamide fibers, which are hollow with a circular cross section of $20\ \mu\text{m}$ diameter, have proved to be very suitable for calibration purposes. The effects of using a $40\times/0.7$ dry objective to examine a polyamide fiber mounted in air (top), water (middle), and oil (bottom) are shown on the left-hand side of Fig. 10, and the corresponding effects produced by using a $40\times/1.3$ oil immersion objective to examine a fiber are shown on the right-hand side. This shows clearly that the optimal conditions are obtained by using an oil immersion objective to examine a specimen mounted in a medium of the same refractive index. When in situ monitoring is being carried out under changing conditions, the refractive indices of the objective and mounting medium will not always match. This is a common problem with studies involving measurement of fiber shape and cross-sectional dimensions during drying.

Distortion of cross-sectional images also occurs if an objective of low N.A. is used, and topographical images constructed from images collected with such an objective will give inaccurate height measurements. A step-height standard can be used for checking the height discrimination of objectives. Alternatively, a piece of paper of known thickness but translucent and thin enough for the laser to penetrate fully can be used. Lens cleaning tissue, and similar thin tissues, are suitable for this purpose. Experiments were undertaken to compare measurements obtained using a $40\times/0.7$, a $16\times/0.45$, and a $10\times/0.3$ objective. A piece of lens cleaning tissue with a mean thickness of $39\ \mu\text{m}$ was optically sectioned in both the xy and xz planes. Topographical images were constructed and height measurements made, and the

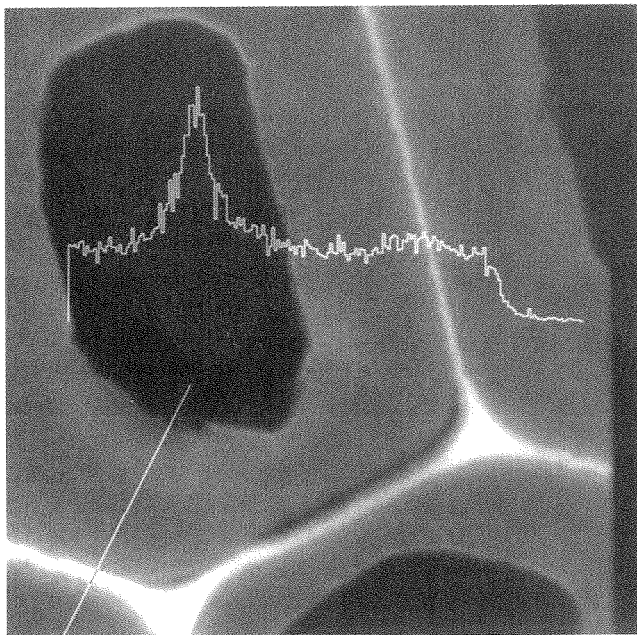


Fig. 13 A cross-sectional image of Douglas fir wood showing lignin distribution across the cell wall.

were labeled with *o*-phenylenediamine to produce fluorescent phenazine derivatives that could be clearly detected in cell corners, middle lamellae, and tori.

The CLSM has been used to study the distribution of lignin in fiber cell walls and to monitor changes with bleaching [218]. The embedding, grinding, and polishing technique described in Section III.B was used to obtain clear cross sections of handsheets made of unbleached and bleached kraft pulp fibers. The intensity of fluorescence was assumed to correlate to lignin concentration, and this embedding technique was employed to eliminate the loss of intensity with depth that occurs when fibers are optically sectioned in the xz plane. Lignin exhibits primary fluorescence at 488 nm; therefore the fibers did not require staining. Commercial preparations of glucose, cellulose, xylose, and mannose, examined under the same microscopic operating conditions as for lignin, gave negligible fluorescence emission signals, thus verifying that the fluorescence was emanating from lignin components of the cell wall. Figure 14 shows the distribution of lignin in the fiber walls of (a) an unbleached pulp (kappa number 25.4), (b) an oxygen-delignified pulp (kappa number 16.9), and (c) a TCF-bleached pulp (kappa number 4.7). Cross-sectional images of a fully bleached pulp (not shown) were barely discernible.

The CLSM lends itself well to the study of fiber morphology and the characterization of fiber types. Basic fiber properties, such as length, width, and curl, are most readily determined by using existing methods. However, since the CLSM can be used to generate cross-sectional images of fibers, it offers better possibilities for measuring width and coarseness (see Jang et al. [144]). Confocal microscopy has also been used to monitor the structural changes that occur when pulp fibers are subjected to cyclical loading. Hamad and Provan [112] observed the propagation of

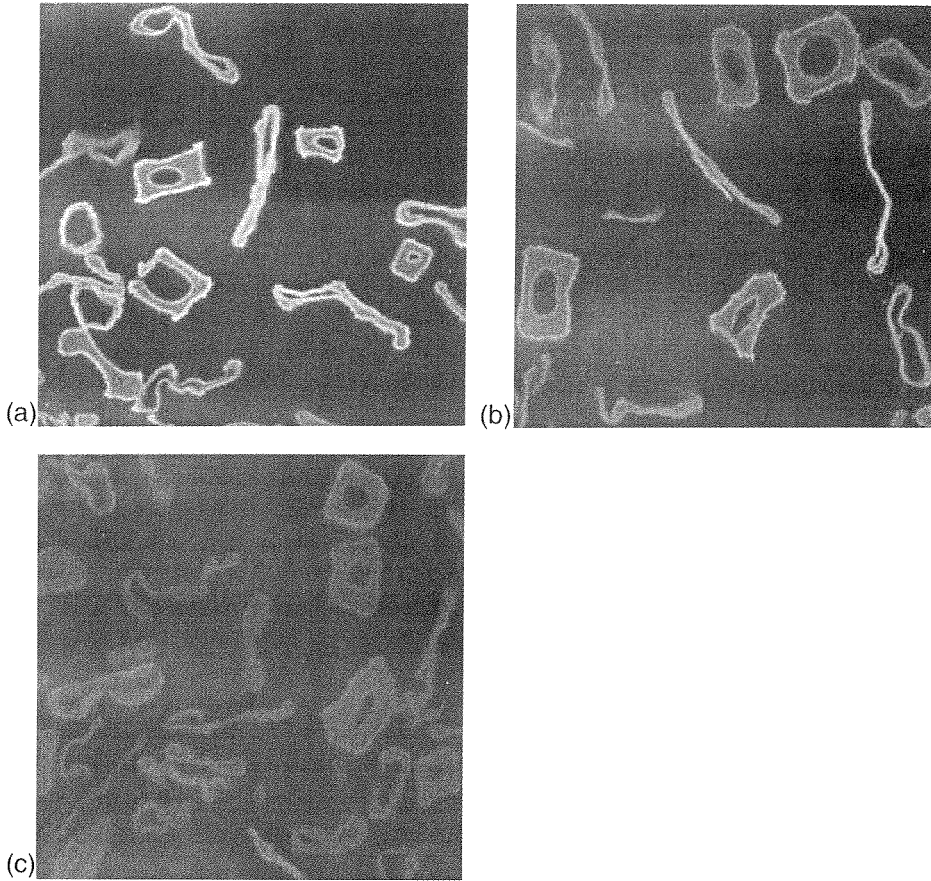


Fig. 14 Differences in lignin content of fibers can be measured using the CLSM in fluorescence mode. (a) Unbleached pine kraft pulp, kappa 25.4; (b) oxygen delignified pulp, kappa 16.9; (c) TCF bleached pulp, kappa 4.7.

cracks during straining of individual fibers. Groom et al. [109] used a CLSM to determine the cross-sectional area of individual fibers that had failed during tensile testing in the ESEM.

The CLSM can be used to measure fibril angle of wood pulp fibers using the classical crossed polaroid technique. This overcomes the problems encountered in measuring the fibril angle of whole fibers using a conventional polarizing microscope (Section III.A), because with the optical sectioning capability of the CLSM only the wall layer of interest is focused. Verbelen and Stickens [339], using the CLSM in fluorescence mode, inserted a polarizing filter between the laser and the scanning unit of the microscope to determine the fibril orientation in the walls of leaf cells cultured from *Nicotiana tabacum*. The cells were stained with Congo red. Jang [141] used both Congo red and acridine orange stains to measure fibril angle in the softwood and hardwood fibers of mechanical, chemical, and bleached pulps. Batchelor et al. [14] describe their method of measuring the fibril angle of the S2 wall layer in wood fibers using a CLSM in reflection mode.

Pulp Characterization and the Effects of Beating The CLSM is particularly useful for characterizing pulps and examining various structural changes brought about by pulping and refining processes. Wet samples can be observed in their natural state before fibrillar material has dried down onto fiber surfaces.

Xu et al. [365] used a CLSM to measure the wall thickness of mixed eucalypt kraft fibers. Jang et al. [142] characterized the collapse behavior of mechanical fibers produced under different refining conditions, and Sundin et al. [315] determined the collapse and coarseness of mechanical fibers in laboratory handsheets. Similarly, the effects of recycling can be examined and quantified. Jang et al. [143] used confocal microscopy to study the effects of laboratory recycling on the transverse dimensions of fibers, evaluating the degree of collapse resulting from the recycling of mechanical and kraft pulp fibers. Seth et al. [290] measured and compared the transverse dimensions of kraft pulp fibers obtained from a variety of tree species. This information allows selection of fiber sources for properties most appropriate for various end uses.

Nanko et al. [223] undertook a carefully controlled experiment to measure shrinkage of individual fibers using an SLM. The microscopy was carried out under controlled temperature and humidity, and a low power helium/neon laser was used to minimize heating effects. Fiber measurements were made at points where two fibers crossed and also in free segments of fibers. Fiber cross-sectional area measurements were made using the surface profile measurement system of the SLM. A real-time sample-weighing system was used to obtain a wet weight corresponding to each image collected, so that changes in fiber width and cross section could be correlated with moisture content. The experiments undertaken by Page and Tydeman [243] to monitor controlled drying of fibers using the porous plate apparatus (Section III.A) could perhaps be adapted for use with a CLSM to control the removal of water from a wet web during drying. This would allow easy observation of cross-sectional views of bond formation in fibers.

External Fibrillation External fibrillation is an important effect of beating, and the CLSM has been used to characterize external fibrillation of different types of fibers and the effects of different laboratory beaters [370]. Fibers are best examined in a wet state when fibrillar material and peeling sheets of wall lamellae are still spread out. Fibers need to be fluorescently stained in order for the fine fibrillar material to be identified, but even then this material can prove difficult to detect simply because much of it is too fine to take up enough stain to give a sufficiently strong signal. However, it is possible to obtain good images, and image enhancement techniques can be used to bring up details of the finer structures.

Ferrofluids (Ferrofluidics Corp., Nashua, NH) have been used to enhance fibrillation. Ferrofluids are colloidal suspensions of very fine particles of magnetite (average particle size 10 nm) that when added to a suspension of fibrillated fibers appear to bond to fine fibrillar and colloidal material. A sample of highly beaten kraft fines was stained with acridine orange, and a little of the ferrofluids suspension was then stirred into the fibers. A drop of this mixture was mounted on a microscope slide and examined wet. The sample was scanned simultaneously in the reflection and fluorescence modes. The reflection image (Fig. 15a) indicates that there is a great deal of fibrillar material to which the magnetite particles have bonded. The fluorescence image (Fig. 15b) shows the basic fiber shape, although thick aggregations of particles have prevented detection of the fiber surface in some areas.

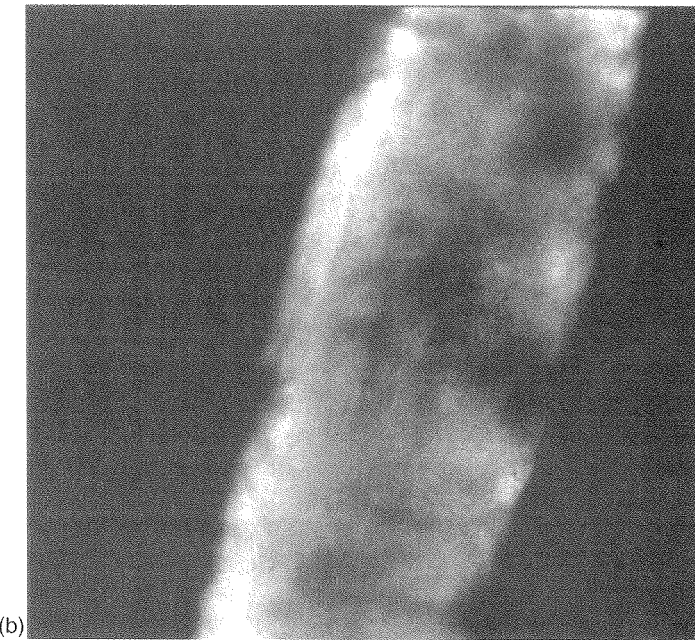
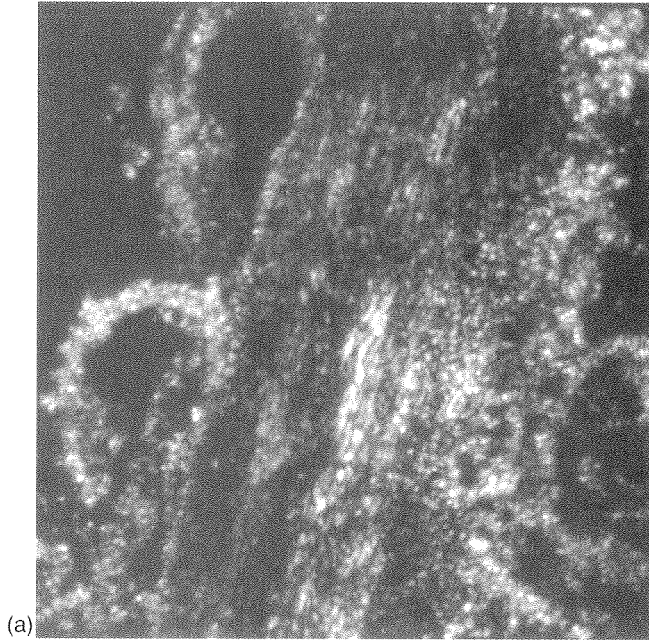


Fig. 15 (a) A confocal reflection image of a fluorescently stained beaten kraft softwood fiber shows nanoparticles of magnetite binding to fibrillar and colloidal material. (b) The fluorescence image reveals the basic fiber shape.

Image analysis can be used to quantify fibrillation. Laamanen et al. [179] obtained a fibrillation index for fibers dried down onto glass microscope slides, and the method described by Klofta and Miller [172] for obtaining a fibrillation index from scanning electronmicrographs of freeze-dried fibers could well be applied to CLSM images of wet fibers.

Internal Fibrillation (or Cell Wall Delamination) Another important effect of beating, but one not as easy to study as external fibrillation and more difficult to quantify because of the scale involved, is internal fibrillation. Stone and Scallan's model (see Section III.B) describes internal fibrillation on a microscale in which the pores are only a few nanometers in diameter. It has been suggested that although these are important in effecting local plasticity in the cell wall, it is the larger visible splits in the cell wall that are important for increasing plastic flexibility in fibers [78,236]. Internal fibrillation has been extensively studied, because it is believed by many workers to be the most important effect of beating [1,138,164,209,332]. Page [236] drew attention to the large cracks that are seen in a delaminated cell wall and pointed out that no technique had been developed to measure these cracks. Quantification of their surface area would be relevant to determining the relative importance of pores and cracks to fiber flexibility and fiber-fiber bonding. Figure 16 shows what is achievable with the CLSM. Compare these cross sections with those obtained with TEM (Fig. 1) and LTSEM (Fig. 31). Measurement of pores in the cell wall is clearly beyond the scope of optical microscopy, but the larger cracks that occur during cell wall delamination could perhaps be quantified using a program such as that developed by Kibblewhite and Bailey [166].

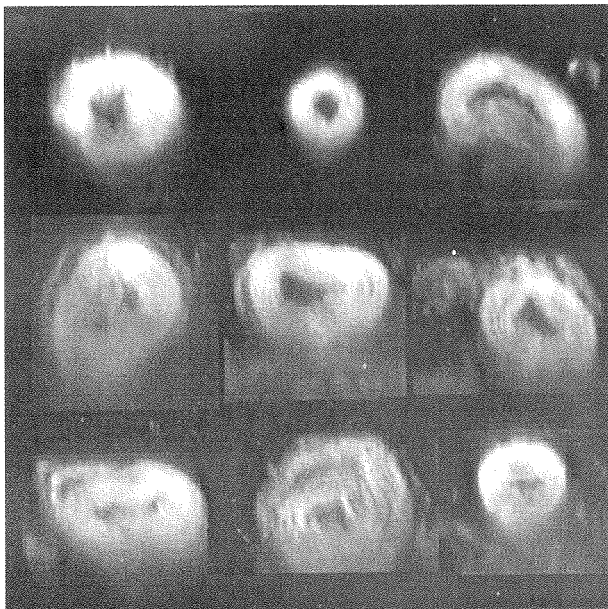


Fig. 16 Cross sections of fully hydrated bleached birch kraft fibers beaten to 4000 rev in a PFI mill.

Investigations into wet fiber flexibility such as those described earlier (Section III.A) could be employed using the CLSM, and, in addition to measuring fiber flexibility, the cross-sectional appearance of the fibers could also be monitored as they dried. Abitz and Luner [1] concluded, after examining the effects of refining on wet fiber flexibility and its relationship to sheet properties, that wet fiber flexibility might not depend solely on the amount of internal fibrillation. This could be verified using the CLSM in conjunction with Steadman's method. Lammi and Heikkurinen [181] studied the effect of refining on the stiffness of latewood and springwood fibers and the relationship between fiber stiffness and cross-sectional shape. Fiber flexibility was measured using the method of Tam Doo and Kerekes [318]; then, for some of the pulp samples, a CLSM was used to obtain a series of 10 cross-sectional images of each fiber after it had been deflected. From these Lammi and Heikkurinen determined cell wall thickness and calculated the moment of inertia. They concluded that fiber stiffness cannot be predicted from the cross-sectional shape.

Fines Material The importance of fines material is being increasingly recognized. The characteristics of a fines fraction vary with pulp type. Fines material also differs greatly according to whether it is from a mechanical or a chemical pulp, and further differences arise from subsequent refining processes. Image analysis can be used to characterize different types of fines on the basis of size and shape [193]. Fines vary in their chemical composition, and the distribution of lignin in mechanical pulp fines can be studied using dual-channel imaging in the CLSM. Mechanical fines are stained with acridine orange, and images are collected using the fluorescence mode and nonconfocal transmitted light. The transmitted light image shows all the structural components of the fines material, including fine fibrillar material, whereas the fluorescence image shows just the lignin-rich areas. The combined image shows the location of lignin on the fines particles, and the proportion of surface area that is lignin-rich can be quantified.

Luukko et al. [194], who used an optical microscope for measuring fines particles, assumed that light transmission attenuated exponentially in proportion to the thickness of the particles. They then tested this assumption using a CLSM to measure the cross-sectional thickness of particles and an optical microscope to take normal gray tone images of the same particles. The thickness values of the particles plotted against gray tone values showed a clear correlation.

The effects of fines on sheet properties were investigated by Moss and Retulainen [219] and Retulainen et al. [266]. They found that additions of fines to the long fibers of a TMP pulp produced handsheets of greater density and higher tensile strength properties than sheets made of just the long fibers, and that the addition of kraft fines was even more effective. The CLSM was used to examine the cross-sectional appearance of potential bond sites in crossing fibers, first in wet-pressed sheets and then in exactly the same areas after drying. This showed that fines were necessary to help wet-pressed fibers maintain contact during drying and that better fiber-fiber contact was achieved with kraft fines, shown in Fig. 17, than the bulkier TMP fines, as shown in Fig. 18. However, the bulky elements of TMP fines help to improve the optical properties by increasing light scattering.

Distribution of Cell Wall Components Immunolabeling techniques, such as those described in Section IV.C, have been applied to investigations into the redeposition of xylans in kraft pulping using dual-channel scanning. Antibodies to xylanase were

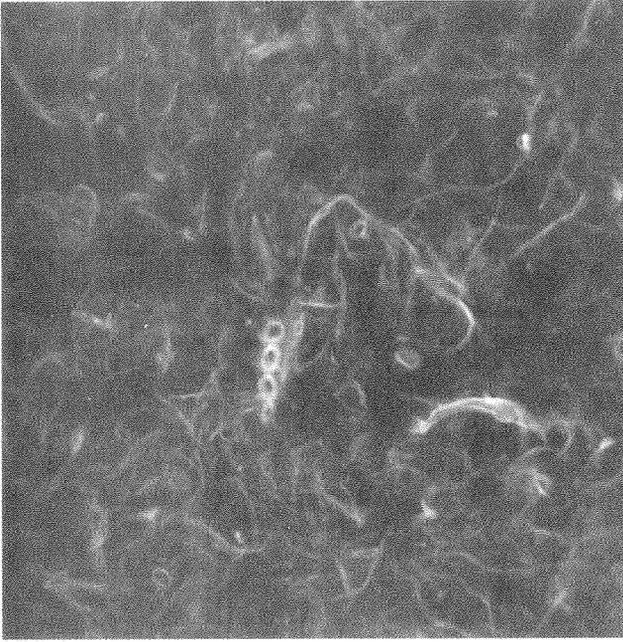


Fig. 17 Secondary fines of a bleached pine kraft pulp beaten for 60 min in a Valley beater. (From Moss and Retulainen [219].)

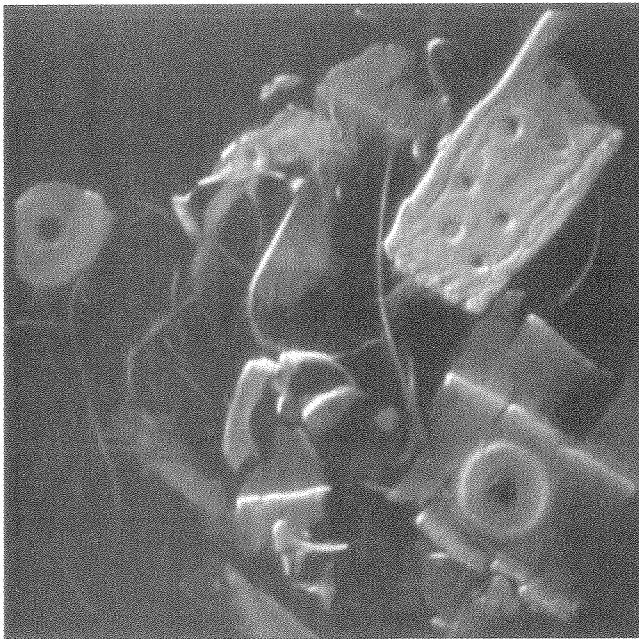


Fig. 18 Primary fines of a spruce TMP. (From Moss and Retulainen [219].)

raised, labeled with acridine orange, and then conjugated with the xylanase. The enzyme-antibody complex was then added to birch kraft pulp fibers and left to bind to xylans present in the kraft pulp. Images collected simultaneously in nonconfocal transmitted light and fluorescence mode were combined to show the location of the xylans. Fluorescently labeled cellulases have also been used in an attempt to elucidate the mechanism of enzymatic attack on fibers.

Sheet Structure The CLSM can be used to study network structure (pore volume, fiber orientation, density, etc.) and to monitor changes that occur during sheet drying and the effects of humidity on network structure. Distribution of fines material and fillers within a sheet and coating structures can also be examined. The CLSM can be used for examining surface roughness and is an excellent tool for height measurements and three-dimensional surface profiling. The effects of calendering and wetting treatments can be monitored, and changes in sheet structure resulting from compression can be directly observed.

Network Structure The nondestructive optical sectioning capability of the CLSM makes it eminently suitable for investigating network structure in both the xy and xz planes. However, there are limitations on the size of the area that can be sampled and the depth to which it can be sampled.

The CLSM offers great potential as a means of assessing paper quality by direct measurement of fiber orientation. Söremark et al. [302] used the CLSM to investigate the cause of fiber orientation streaks affecting the quality of a kraft liner. Xu et al. [366] used confocal microscopy in conjunction with image analysis to evaluate fiber orientation distribution in three dimensions. In-plane variation of fiber distribution has important implications for paper properties such as printability and dimensional stability, and Xu et al. [367] employed the same techniques to determine fiber distribution in the z direction. Naito et al. [222], in a study of the delamination resistance of paper, used the CLSM to determine the depth to which fibers penetrate in the z direction of a sheet.

Sheet density can be measured from images reconstructed from a series of sections, and sheet two-sidedness can also be investigated [220]. Distribution of surface pore area as a function of depth can be calculated from topographical images. Mangin and Béland [200] calculated surface pore areas of various newsprint samples and of a base stock (coated and uncoated) before and after calendering, to investigate structural changes induced by calendering. Løvhaugen [190] also used the CLSM to make quantitative evaluations of pore volume of different unprinted newsprint samples, and Løvhaugen et al. [191] related pore volumes of newsprint and uncoated liners measured by the CLSM to measurements made using the Parker Print-Surf and Bendtsen air leak instruments.

Kunnas et al. [178] used the CLSM to investigate the effect of Condebelt drying on the structure of fiber bonds. Under the high pressure Condebelt conditions, crossing fibers appeared to weld together, with excess surface material (lignin and hemicellulose) flowing and filling the angles formed between the crossing fibers. It was surmised that these bonds were better able to resist water than the thin, fibrillate bonds seen in the conventionally dried sheets.

Nanko and Wu [227] studied the mechanisms of paper shrinkage during drying using a reflection-type SLM. They used silver grains as location markers

on fiber surfaces and collected images of the sheet surface, before and after drying, to measure how much the fibers had shrunk longitudinally. They also obtained surface profiles along fibers and examined the effects of restrained and free drying on the longitudinal shrinkage of fibers. Optical sectioning in the xz plane allows easy monitoring of changes in drying sheets. Figure 19 shows an extended focus image and a cross section through a sample of handsheet at the just-formed stage (top) and after drying (bottom). Collapse of fibers and their relative movement during drying are clearly indicated. Nanko and Tada [226] cut cross sections of sheets with a razor and used the SLM to observe deformation of fibers due to changes in relative humidity. Samples were placed in a chamber into which the objective of the microscope could be inserted, and humidity-controlled air was supplied. They measured cross-sectional and longitudinal hygroexpansion of fibers in the sheets.

Mangin et al. [201] developed a special piece of apparatus to apply static compressive stress to the paper surface while imaging with the CLSM. Pressures of up to 5 MPa were applied during in situ studies of changes in surface compressibility. They applied this technique both to the effects of calendering and to the evaluation of surface roughness and compressibility in relation to printing processes. Ting et al. [335] also designed and manufactured their own compression rig in order to characterize network changes in paper under compression in the z direction. Direct visual observation of the cross-sectional shapes and locations of the fibers enabled them to study the effect of loading rate and fiber cell wall thickness on compressibility of the sheet.

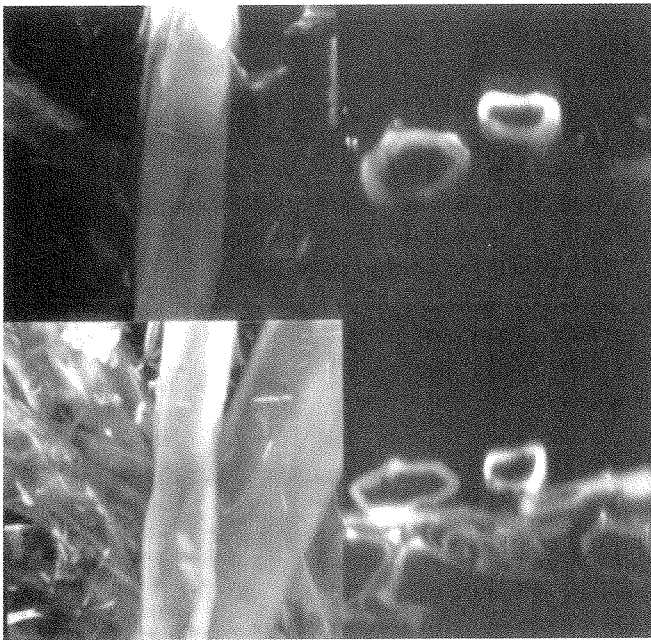


Fig. 19 Extended focus image and a cross section of a wet handsheet made of spruce TMP (top) and the same area after drying (bottom).

Many earlier microscopists developed sophisticated techniques for investigating various properties of pulp fibers and paper, many of which could be adapted for use with the CLSM. These include, for example, control of humidity in drying experiments [243,348] and techniques used for studying porosity. A study of relative porosity in paper, similar to that described by Lindsay [188], could be usefully undertaken using confocal microscopy. Lindsay observed and measured the movement of a dye injected into paper samples. One of the dyes he employed was blue dextran 2000, but fluorescently labeled dextran solution could be used to investigate the movement of the stain in both the xy and xz planes of the sheet. The rate of flow of a liquid through a sheet could be measured using the FRAP technique described earlier (Section IV.C). High magnification examination of fiber cell walls, seen in cross-sectional view, could be made in solute exclusion studies. Experiments could also be designed for use in conjunction with compression apparatus, such as that developed by Ting et al. [335], to study sheet permeability and the effects of pressing on the movement of water. Carlsson et al. [40], for instance, used dextran solutions of different molecular weights to demonstrate from which cavities in the fiber matrix water was expressed during pressing.

Distribution of Fines and Fillers in Sheets The simultaneous generation of images in fluorescence and nonconfocal transmitted light modes (see earlier) can be used to examine the distribution of fines material within a fibrous network providing that the fiber and fines fractions are sufficiently different chemically. One component needs to be from a mechanical pulp and the other from a chemical pulp, to enable differentiation of the components [220]. The same technique can be applied to investigations into the distribution of fillers, using the reflection mode with the nonconfocal transmitted light mode, or the reflection mode with the fluorescence mode if the fillers have fluorescent properties.

Coated Papers Coated papers offer a challenging area of application. Much research has been done on the distribution of coating thickness that involved embedding sheets in resin and cutting thin sections (see Sections III.A and III.B). Cross-sectional views of coated sheets can be obtained with the CLSM, but only to a limited depth due to the opaqueness of the coating layer. However, as shown in Fig. 20, the interface of the coating layer with the base paper can be clearly discerned. Measurements of variation in coating can be readily obtained from such images, and the void volume, critical to coating processes, can be calculated. Clearer cross-sectional images are obtained if the sample is stained with a fluorescent dye, but the application of an aqueous stain would not only affect the coating itself but also disrupt the structure of the base paper. This can be overcome if the sample is stained during sheetmaking. However, unstained samples can be examined quite successfully using the fluorescence mode, because coating layers usually include optical brighteners or other pigments that have fluorescent properties, and the base papers are often made of lignin-rich mechanical pulps that are inherently fluorescent. Polyethylene coatings, such as those used on drink cartons, and the adhesive layer of labels (see Fig. 21) can also be examined. Lange et al. [182] used several microscopical techniques, including conventional optical microscopy, CLSM, SEM, and AFM, to examine defects in solvent-free organic coatings that require rapid curing time. The AFM and CLSM both proved useful for characterizing coatings,

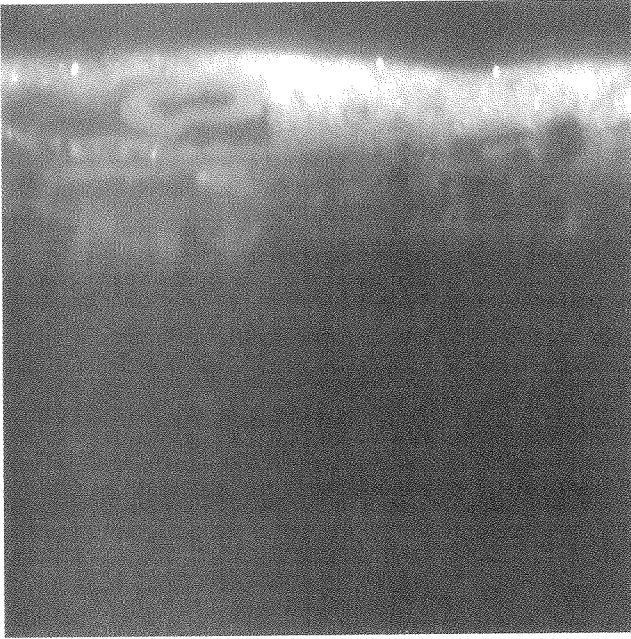


Fig. 20 Cross section through an LWC sheet showing the interface of the coating layer with the base paper.

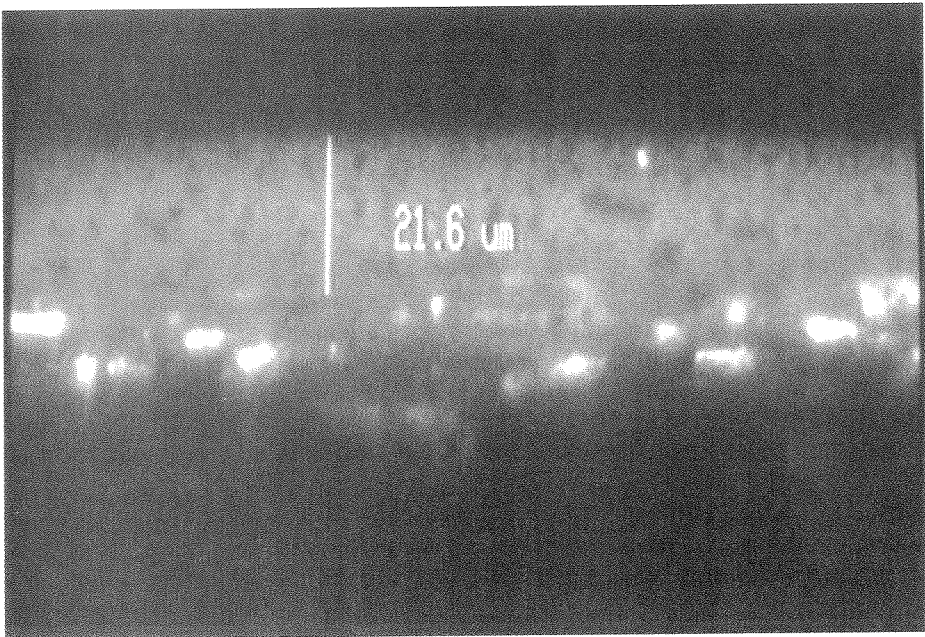


Fig. 21 Cross section through the adhesive layer of a label.

but the CLSM was particularly useful in that the internal structure of transparent coatings could be viewed.

Analysis of Surface Topography Surface roughness is an important property of paper in relation to printability, and the CLSM offers a non-contacting method of surface profilometry. This has certain advantages over conventional stylus instruments, which can cause damage to samples due to stylus pressure [83,341] (Chapter 11). This is even more true where there are raised or loose pieces of fibrillar or fines material, and the use of a laser overcomes these problems. The CLSM not only gives roughness values but also enables visual assessment of changes that occur at the fiber level, because the same areas can be examined before and after treatment.

The software for the Leica CLSM includes a program based on the international and DIN standards for the measurement of surface roughness parameters using stylus instruments, and such a program could be easily written for other makes of CLSMs that do not include it in the standard package. The Leica program calculates the arithmetic mean deviation from the profile, root-mean-square deviation from the profile, difference between maximum height and maximum depth of the profile, and skewness. Surface roughness measurements are made from topographical images constructed from a series of sections collected in the xy plane using the reflection mode. Samples should be dry, and a dry objective should be used. A $40\times$ objective is recommended for such measurements. This shows a very small field of view ($125\ \mu\text{m} \times 125\ \mu\text{m}$) with the Leica CLSM but is better able to discriminate height differences than objectives of smaller magnification, which have a greater depth of field and consequently give falsely high values. Step size (see Section IV.A) should be kept as small as possible, and, in order to measure as accurately as possible, it is better to oversample than to undersample.

There are no standards pertaining to image acquisition using a CLSM. This means there will be problems with reproducibility using different laser scanning microscopes. Experimentation is therefore necessary to determine the most suitable combination of microscope settings. Many variables (voltage, laser power, pinhole size, step size, objective, image format, the number of sections to be collected, and the number of scans needed to reduce noise) can affect the quality of topographical images. Optimal conditions may vary greatly for different paper surfaces, so these parameters should always be kept the same for any given paper so that meaningful comparisons can be made. Laser power is important and can affect the results of work being undertaken if there are fluctuations. Løvhaugen [189] outlines some of these problems in relation to paper surface measurements.

Because the area examined is very small, a very large number of areas would need to be sampled in order to acquire statistically meaningful data. However, if changes in roughness are being monitored and exactly the same areas are being re-examined after various treatments (as described in the following section), then a smaller sample size may suffice.

Fjerdings et al. [90] used a CLSM to investigate the effect of fiber wall thickness on paper surface characteristics. The CLSM has been used by many workers to examine and measure changes in surface topography, some of which are detailed below.

Monitoring the Effects of Calendering and Wetting Treatments Retulainen et al. [267] undertook a series of experiments to characterize the effects of calendering on the microstructure of the paper surface. They studied the effects of calendering

treatments applied to handsheets made of earlywood fibers and to others made of latewood fibers, with and without fines. Areas in an uncalendered paper sample were measured, then the same areas were measured again after calendering. The areas were randomly selected, but to facilitate location of areas for subsequent reexamination a few lines were lightly penciled onto the samples to serve as location markers. Roughness measurements were obtained and visual analysis was made of the topographical images and three-dimensional surface profiles in order to see how calendering affected the surface structure. Figure 22 illustrates the surface profiles of an uncalendered handsheet (a) and then exactly the same area after calendering treatments (b)–(d). After the first calendering, flattening of fibers and increases in fiber width are observed. (Fig. 22b). Height differences are further diminished after the second calendering (Fig. 22c), but there is little change after the third calendering treatment (Fig. 22d), just some displacement and rearrangement of material in the lateral direction.

Retulainen et al. [267] applied the same technique to study the effects of wetting printing papers, such as occurs during coating processes or in offset printing. A KRK printability tester was used for the dampening treatment. This tester simulates practical coating or printing processes and was used in these experiments to investigate the wetting behavior of calendered sheets and the effect of moisture on surface roughness. Roughness was measured, and images of the areas were examined for evidence of changes in fiber dimensions, for fiber swelling, fiber rising, breaks at bonded areas, and redistribution of material. They found that in handsheets made of a furnish typically used for printing papers (a kraft pine whole pulp plus 60% spruce groundwood), the final roughness and thickness of calendered sheets after wetting and redrying approached those of the uncalendered sheets. The higher areas on the surface were more compressed in calendering and more affected in subsequent rewetting.

MacGregor [196] examined the roughening effect of water on the surfaces of untreated, water-treated, and printed papers and its relationship to reduction in gloss. In subsequent work [197] the CLSM was used to complement image analysis measurement of small-scale gloss variation in printed paper. Topographic data acquired with the CLSM were directly compared with gloss images of the same areas.

Heat Conduction During Calendering A novel method was developed by Luong and Lindem [192] to determine the temperature distribution through the z direction of paper during calendering. Paper samples included monodispersed fluorescently stained latex spheres with an average diameter of 9.5 μm and a melting point of 125°C. Paper samples were calendered at various temperatures and speeds, and the calendered samples were then optically sectioned using a CLSM. The transient temperature distribution through the z direction of the sheet was determined by measuring the distances between the paper surface and the unplasticized spheres.

Related Research

Printing and Deinking Béland and Mangin [17] used the CLSM to study ink transfer mechanisms, comparing the same newsprint printed at high and low ink levels. They also examined the adhesion of toner to paper using reflection and fluorescence modes to record halftone dots before and after the samples were subjected to a peel test. Topographical images indicated whether halftone dots were situated on raised or depressed areas of the surface, whereas the fluorescence images showed the areas

of the dots. Images of the same areas taken after the peel test show clearly where toner had been detached from the surface.

Christiani and Bristow [44], in a study of the drying mechanism of waterborne printing inks, used a CLSM to examine the diffusion of water within paper and observed a tendency for the water to follow the fiber direction.

Analysis of contaminants removed during recycling of waste paper is necessary for determining the efficiency of recycling equipment. The problem with characterizing toners and other three-dimensional particulate matter using conventional optical microscopy is that the size and shape of the particles cannot be fully ascertained from the two-dimensional binary images produced for image analysis. Borchardt et al. [25] found the CLSM to be a useful tool for studying the particle geometry of ink removed from laser printed and photocopied papers. It was thought that because the ink particles are three-dimensional, image analysis of particle length dimensions might not give a sufficiently accurate measure of the actual mass of ink in particles. They used stereo images and simulated rotation to view the morphology of ink particles.

Synthetic Polymers Furuta et al. [97] studied the structure of cellophane using both an SEM and a CLSM. They found the CLSM to be demonstrably more useful in the determination of three-dimensional structure. A major difficulty with investigating the interface regions of heterogeneous materials is that the interface cannot be separated from the sample but must be studied in situ. Thomason and Knoester [333] used both polarized light microscopy and CSOM for in situ investigations of the interface region of the polymer composites. A series of optical sections taken through an aramid fiber in polypropylene revealed structures not seen in polarized light. They also studied glass fiber reinforced epoxy composites to see whether failure cracks in samples had propagated along the fiber/matrix interface or through the matrix. An advantage of using CSOM was that samples required no further preparation other than cutting; also, the roughness of the cut surface disappeared at a depth of 5.3 μm and fibers were clearly discernible. Previous methods of preparation had included polishing the cut surface, which often resulted in cracks getting filled in.

Microbial Contamination of Pulp and Paper There is a great deal of interest in cellulose-related products, mainly because of the biodegradability of cellulose. Plastic films used in food packaging have to be resistant to bacteria and fungi. Samples of film made of discrete layers of starch and polyvinyl alcohol were incubated in soil for several days. They were then lightly stained with acridine orange and examined with the CLSM. Various species of bacteria and fungi were detected. Figure 23a shows the ramification of fungal hyphae at a depth of 35 μm from the surface, and scanning in the xz plane revealed that the fungi appeared to have a preference for specific layers, as shown in Fig. 23b.

Microorganisms exist everywhere and are responsible for decomposition of both organic and inorganic substances. They cause decay in the wood used for production of pulp and are present in all systems in pulp and paper, producing damaging slime deposits. Work has been done to investigate the growth of bacteria on the metal surfaces of headboxes and also on the wires of paper machines and in the recirculating white water, which all provide ideal conditions for the growth of bacteria and fungi. Robertson and Taylor [275] describe their techniques for examining and evaluating bacterial biofilms and biofilms containing particulate calcium carbonate by using CLSM and ESEM. Bacterial flocs from paper mill effluent have

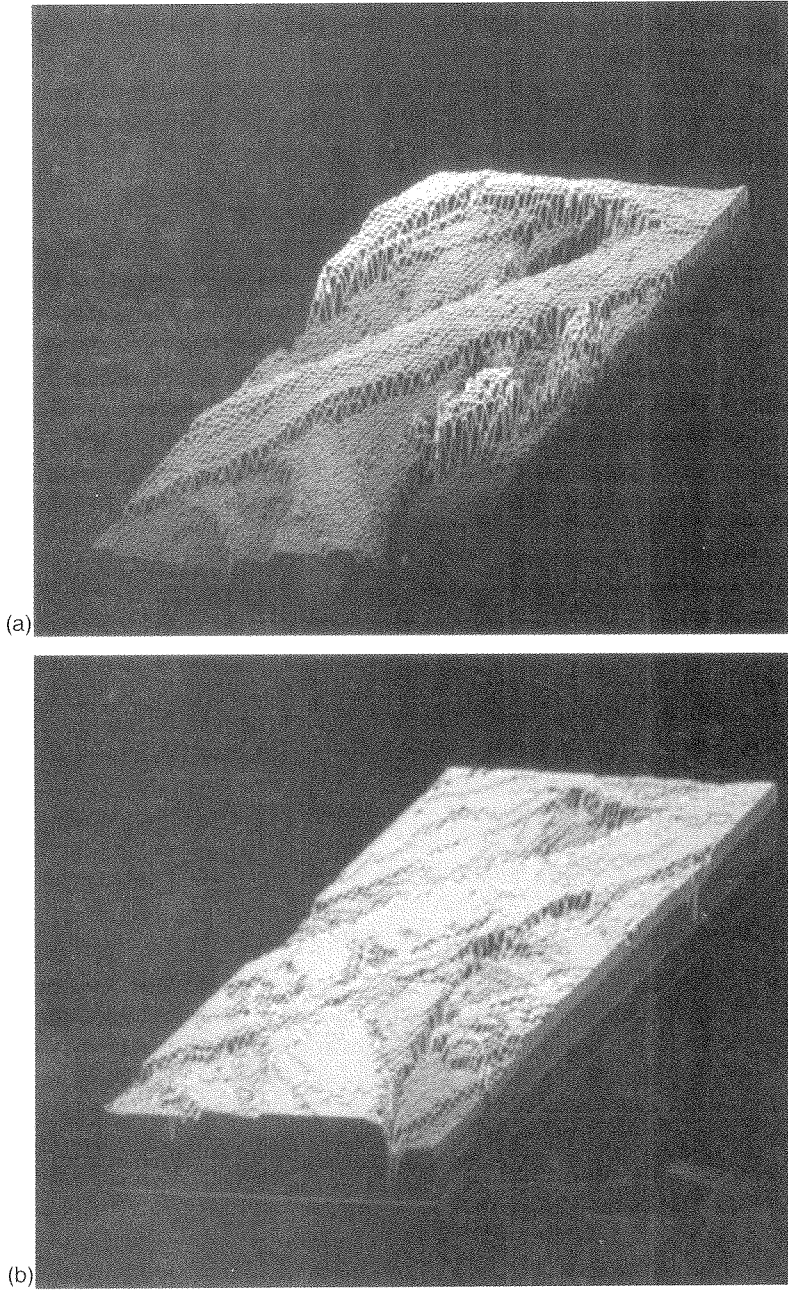
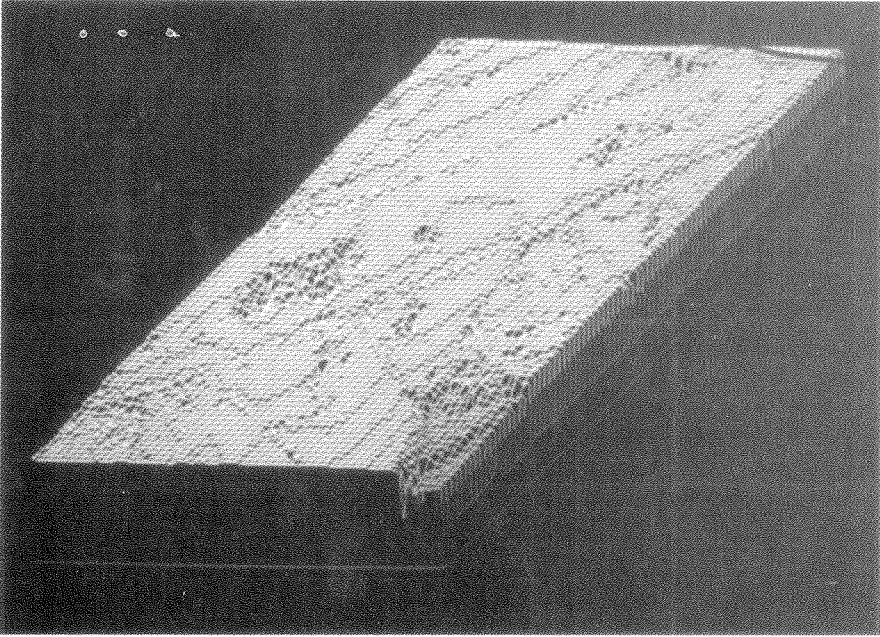
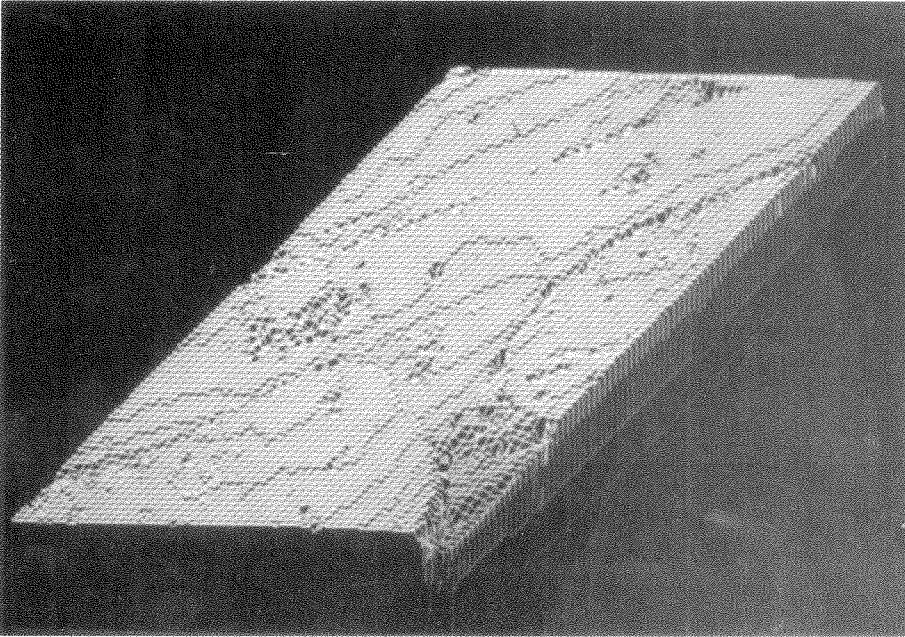


Fig. 22 The surface profile constructed from the topographical image (a) of an uncalendered handsheet made of summerwood fibers of a pine kraft pulp and (b)–(d) of exactly the same area after repeated calendering treatments.



(c)



(d)

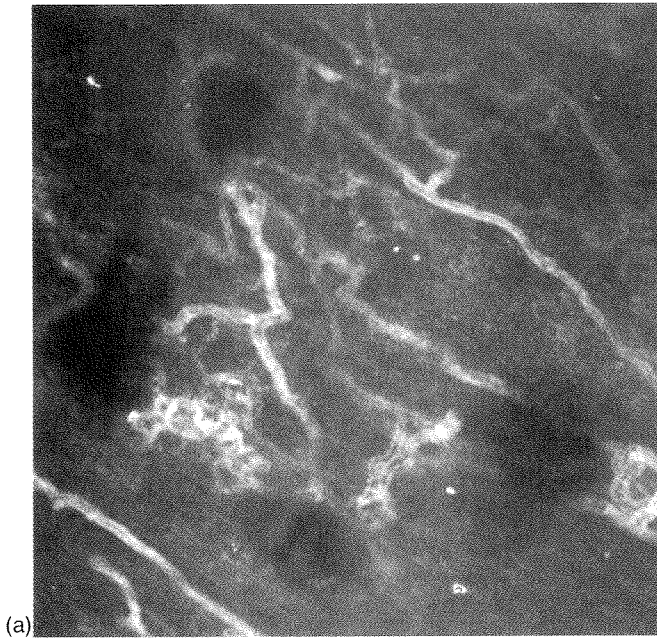


Fig. 23 (a) A single optical section taken at a depth of $35\ \mu\text{m}$ below the surface of food packaging film showing fungal hyphae and (b) a cross section showing that the fungal hyphae tend to be confined to discrete layers. The protuberance seen in (b) is a fungal spore that prevents the penetration of light and is the cause of one of the apparent voids seen in (a).



Fig. 24 Bacteria deep inside the base board of a polyethylene-coated milk carton. (Photo courtesy of I. Suominen.)

also been examined and analyzed, the size of the flocs being an important factor in how quickly the bacteria break down the sludge.

Suominen et al. [316] examined the growth and migration of bacteria in food-packaging paperboards. Their study showed that microbially contaminated starches used as surface sizes and contaminated mineral pigment coatings posed a threat to hygiene, because the polythene layer separating the food from the paperboard displayed pores and indigenous damage. Base board used for milk cartons was also examined for bacterial contamination. The bacteria shown in Fig. 24 were located quite deeply in the base board and would not have been possible to detect directly using any other microscopical technique.

Studies of delignification are becoming of increasing environmental concern due to the rapid depletion of landfill space. The degradation rate of laminated chip boards such as those used in modern furniture has been studied using compost heaps to simulate rubbish dumps. Fungi found in lignified samples were isolated and cultured for identification.

V. THE LOW TEMPERATURE SCANNING ELECTRON MICROSCOPE

Fernández-Morán [88] reviewed early investigations into low temperature techniques for electron microscopy, but low temperature scanning electron microscopical (LTSEM) (also referred to as cryogenic or cryo-SEM) techniques were first demonstrated for biological specimens by Echlin et al. [76]. A comprehensive account of

low temperature scanning electron microscopy is given by Beckett and Read [15], and de Silveira et al. [66] discuss its application to the analysis of pulp and paper.

Until the advent of LTSEM, and later the ESEM, only fully dehydrated specimens could be examined satisfactorily in a scanning electron microscope because the electron beam is strongly scattered by air or water molecules. Unlike the conventional SEM, which entails rather elaborate and lengthy preparation for the examination of wet pulp and sheet samples, a low temperature stage makes it possible to examine fully hydrated material within a very short time—a specimen can be frozen, sublimed, coated, and examined in less than an hour. It also enables the examination of many previously “impossible” samples such as emulsions, oils, and inks. Material prepared in this way for examination with the LTSEM is usually referred to as frozen hydrated (FH).

Low temperature scanning electron microscopy, which had been widely used in biological sciences for many years, was first applied to the study of papermaking fibers by Howard and Sheffield [130] in 1987. Because the conversion of wood to paper is carried out almost entirely in water, the interactions of fibers with water are of fundamental importance. Therefore, at that time, LTSEM seemed the most appropriate method to use for examination of wet samples. Howard also recognized the potential of developing a technique for obtaining cross sections of fully hydrated pulp and paper samples. An evaluation of the LTSEM as a means of examining the fully hydrated structures of fibers and wet sheets was subsequently undertaken by Moss [216].

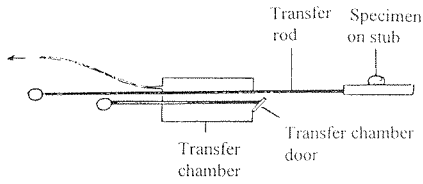
A. The Cryosystem

The cryosystem of an LTSEM consists of a cryopreparation chamber (with cold stage, nitrogen dewar, fracturing device, sputtercoating head, airlock gate, and valve) and a cold stage (with nitrogen gas dewar and anticontaminator) interfaced with a conventional SEM. Figure 25 illustrates a typical system and shows the steps involved in cryopreparation. The use of an evacuated transfer system allows the frozen specimen to be placed directly onto the cold stage of the preparation chamber and then into the vacuum chamber of the SEM without coming into contact with the atmosphere or being returned to room temperature.

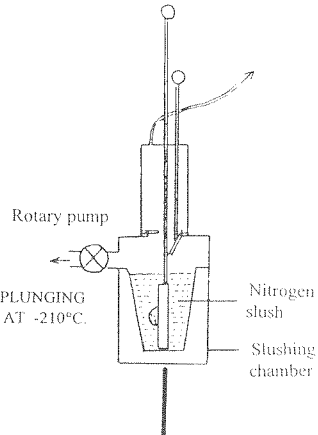
The specimen is maintained, ideally, at -185°C by the circulation through the cold stage of nitrogen gas that has been cooled to -190°C with liquid nitrogen. It is essential that the temperature of the cold stage be maintained well below -130°C , because above this point sublimation begins to occur. Ice then has to be sublimed from the surface of frozen hydrated specimens, and this is achieved by heating the cold stage to a temperature of between -80°C and -60°C . An anticontaminator plate (shown at step 5 of Fig. 25) cooled to about -190°C prevents any recondensation of water molecules onto the specimen. The whole process can be monitored in situ and sublimation stopped when the relevant features of the specimen have been revealed. After sublimation of the surface ice, the specimen is withdrawn into the preparation chamber for sputtercoating and then returned to the cold stage for examination.

Providing sublimation is not allowed to continue for too long there should be no morphological changes arising from shrinkage, and there should be little or no collapse because the bulk of the material is frozen, thus providing physical support.

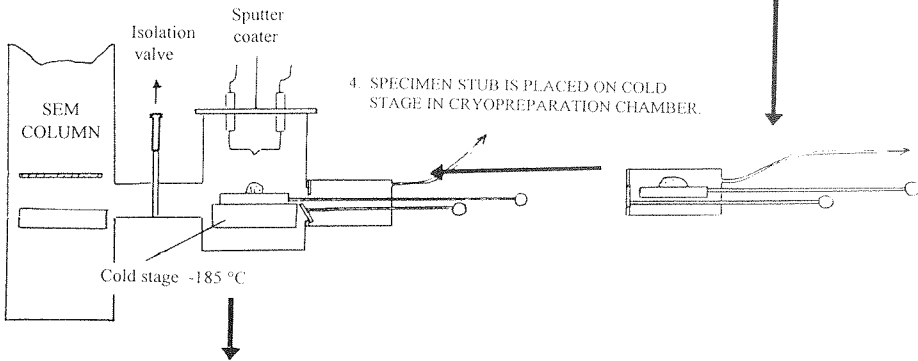
1. SAMPLE IS PLACED ON STUB IN COPPER HOLDER.



2. SAMPLE IS FROZEN BY PLUNGING INTO NITROGEN SLUSH AT -210°C .



3. STUB IS WITHDRAWN INTO TRANSFER CHAMBER.



4. SPECIMEN STUB IS PLACED ON COLD STAGE IN CRYOPREPARATION CHAMBER.

5. THE SAMPLE IS TRANSFERRED TO THE SEM COLD STAGE FOR SUBLIMATION OF ICE (VIEWED *IN SITU*). IT IS THEN RETURNED TO THE CRYOPREPARATION CHAMBER FOR COATING.

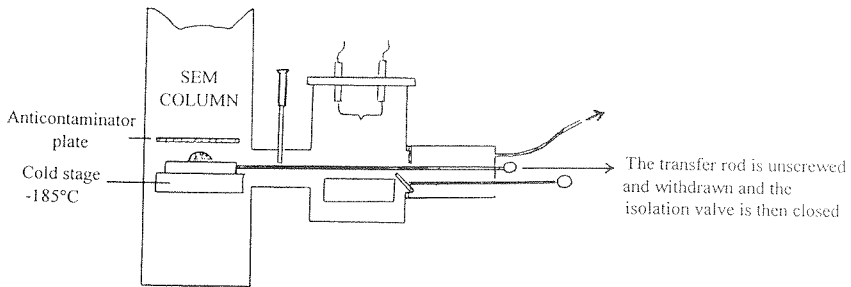


Fig. 25 A typical cryosystem and preparation methods for LTSEM.

B. Specimen Preparation

A small stub, similar to that used for conventional SEM work, is placed in a copper holder. The specimen, which may be a droplet of pulp suspension, a few wet fibers, or a small piece of wet or couched sheet, is placed on the stub. A long rod (the transfer rod) is screwed into one end of the copper plate (see Fig. 25). This is used to plunge the specimen holder into the slushing chamber for freezing. It is then used for the subsequent transfer of the specimen to the cryopreparation chamber and to and from the cold stage. The size of the stub limits the size of the sample that can be examined, but this is not a real disadvantage because the smaller the sample, the faster the freezing.

Special techniques are needed for obtaining cross sections of fully hydrated pulp and paper samples. Figure 26 illustrates the technique used for sectioning wet sheet samples. Here an SEM stub has been cut in half and the wet sheet sample is placed carefully between the two halves. The stub is inserted into the copper holder, and the sample is plunged into liquid nitrogen. The sample is then transferred to the cryopreparation chamber where the sheet is fractured. This is achieved by using a cooled scalpel that is inserted through the wall of the preparation chamber and manipulated from outside.



A circle of just-drained wet sheet (half inch diameter) is carefully placed in a split stub.



The stub is inserted into its copper holder and plunged into liquid nitrogen slush. The frozen specimen is then transferred to the cold stage of the SEM.

A pre-cooled scalpel blade cuts cleanly through the frozen-hydrated sheet.

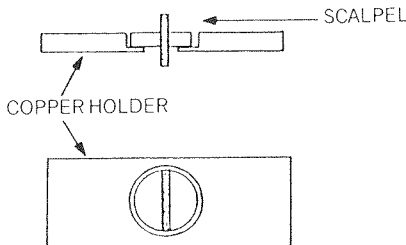


Fig. 26 Technique for obtaining cross sections of wet handsheet samples.

Figure 27 illustrates the technique developed for sectioning wet fibers. Fibers are inserted into a hollow split rivet (2 mm diameter), the two halves of which are held together by a spring clip. Ideally, the fibers are inserted into the rivet so that their long axes lie parallel to the long axis of the rivet. This method requires careful manipulation and considerable practice to achieve a uniform distribution of fibers at an appropriate density; too many fibers closely packed together make analysis difficult, and too few fibers necessitate the processing of a large number of samples. The rivet is then inserted into a special stub that has a hollow center. This is placed in the copper holder, and the sample is plunged into liquid nitrogen. The transfer chamber is not immediately positioned over the top of the slushing chamber as it should be, and after a few seconds the frozen hydrated fibers are fractured by giving the top half of the rivet a sharp blow with an appropriate tool (a spanner works well!)—all done while the fibers are fully immersed in the liquid nitrogen. The transfer chamber is then fitted over the top of the slushing chamber, and the rest of the procedure is as normal.

Pretreatment of specimens is not necessary because they are physically fixed by freezing rapidly in a liquid cryogen. Freezing specimens in liquid nitrogen slush at

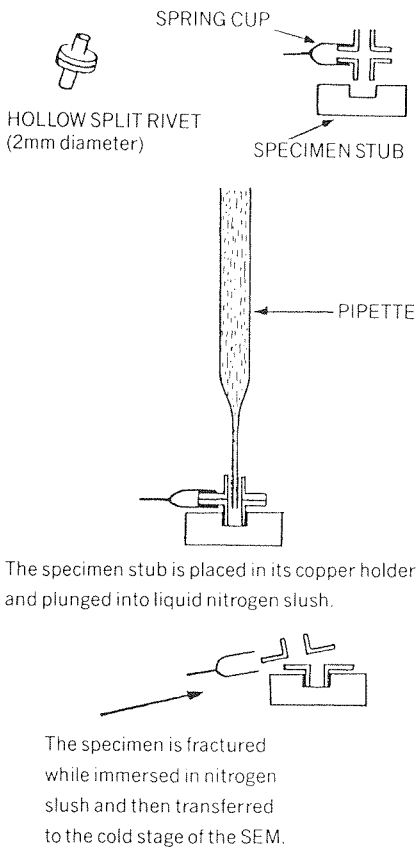


Fig. 27 Technique for obtaining cross sections of wet pulp fibers.

-210°C was one of the earliest methods of freezing biological specimens and is one of the most commonly used today because it is cheap and safe to use. Other cryogens can be used that have a better freezing efficiency than liquid nitrogen, but they are not as readily available or are disadvantageous in some way or another. Likewise, other methods of freezing are available, but they generally require complex and expensive equipment [272].

C. Comparative Evaluation of Preparation Techniques for LTSEM

Examination of wet pulp and paper samples in a conventional SEM necessitates dehydration of specimens either by air drying (AD), critical point drying (CPD), or freeze drying (FD). Many workers [e.g., 8,29,30] have reported on the deleterious effects of dehydration techniques. These include shrinkage, collapse of nonrigid cell walls, distortion, and even rupture of whole cells. Comparative studies should always be made of the different techniques being used, particularly if quantitative work is being undertaken.

Ideally, objects of known dimensions should be used for calibration purposes. Pulp fibers themselves are unsuitable because they are far too heterogeneous. Moss [216] used a single-cell alga, *Euglena gracilis*, to determine how much shrinkage and distortion of delicate structures was caused by air drying, critical point drying, and freeze drying compared with frozen hydrated cells. Light microscopy of living cells was undertaken as an experimental control.

Euglena has been much used as an experimental organism, and its structure is well documented [36,102,111,278,364]. It was chosen for this evaluation because its relevant properties are in many respects similar to those of wet pulp fibers. It has a protective membranous exoskeleton (the pellicle) that exhibits great flexibility and a distinctive, striated structural pattern. It also has a long, delicate flagellum. Comparison of the different methods of preparing *Euglena* for SEM examination indicated cryopreparation to be far superior to either FD or CPD.

D. Advantages and Disadvantages of Cryopreparation Techniques

All dehydration techniques used in preparing wet fibers or sheets for examination using a conventional SEM cause shrinkage, collapse, and distortion of fibers and networks to varying degrees. This is probably the reason electron microscopy has never been considered a satisfactory way of studying phenomena such as fiber swelling. Critical point drying involves solvent exchange procedures, which may cause redistribution or loss of certain components. These problems do not occur in cryopreparation techniques, and samples can be examined in conditions more closely related to their natural state. Furthermore, cryopreparation is quicker and simpler.

Cryopreparation obviates the need for chemical fixation, and if specimens are rapidly frozen and maintained at a temperature below -130°C there should be no shrinkage or swelling. The shape and size of the specimen, the rate at which the specimen enters into the cryogen, and the depth to which it penetrates all have a pronounced effect on the cooling rate, so the choice of freezing technique ultimately depends on the nature of the specimen. The ideal method of cryofixation should be such that the specimen retains good morphology, ultrastructure, and distribution of particulate components. However, cryopreparation does produce artifacts of its

own, namely the creation of eutectic membranes, which may be indistinguishable from genuine fibrillar material and sheets of fine lamellae peeling from the fiber wall.

Cryopreparation techniques appear to have yielded some excellent results. Cryofixation physically fixes and immobilizes dynamic processes and preserves the spatial distribution of particles, etc. within a sample. Many workers have found that this method gives a far superior state of specimen preservation compared with the standard dehydration techniques required for conventional SEM work [85,153,264]. A major disadvantage is that the specimens are very short-lived; unlike dried specimens, they cannot be stored in a desiccator and viewed again after an interval of weeks or months.

E. Artifacts of Cryopreparation

Artifacts Arising from Freezing Cryofixation of specimens can cause problems, and the success of the process is largely dependent on the rate of cooling and the size and shape of the specimen. If freezing is not rapid enough there may be some redistribution of small cellular components or particles in suspension. The fastest rate of freezing currently available gives good fixation to a depth of only about 10 μm . A slow rate of cooling produces large ice crystals that may disrupt cellular structure. It may also result in ice crystallization in the extracellular medium, and further slow crystal growth then causes water to be withdrawn across the cell wall. This may lead to shrinkage and deformation of the cell wall. Cryoprotectants, e.g., glycerol or DMSO, may be used to reduce ice crystal size for a given cooling rate, but their presence may pose further problems with artifacts, as described below.

Cryofixation of wet samples involves phase separation. As ice crystals form and grow, any solutes present in the sample become more concentrated. Consequently, freezing of solutions causes solutes to become concentrated into the liquid phase surrounding the growing ice crystals. This unfrozen solution (the eutectic phase) reaches a critical concentration (the eutectic concentration), at which point the solutes and remaining water freeze as a single component. Eutectic materials do not generally sublime, because their vapor pressure is relatively low. These eutectic regions remain and form a network surrounding the ice crystals.

The process of cryofixation and subsequent sublimation can produce a whole spectrum of artifacts [265], which may have repercussions on structural interpretation. Kistler and Kellenberger [171] demonstrated the formation of eutectic membranes during freeze drying of aqueous solutions, where the eutectic assumed the form of thin perforated sheets that, when completely dehydrated, appeared as a network of strands. Miller et al. [210] presented some very impressive electronmicrographs of lacy artifacts created by rapid freezing of buffer solutions commonly used in the preparation of biological material. Moss [216] and Moss et al. [217] demonstrated effects similar to those described above by freezing sugar solutions. Figure 28 shows a eutectic membrane formed by freezing a 0.03 mM solution of xylose. The membranous sheet seen in Fig. 28a splits apart as sublimation proceeds and forms the reticular structure shown in Fig. 28b.

Other experiments showed that substances dissolved in the filtrates of beaten pulp suspensions also produced similar membranous and lamella-type structures that can mimic thin sheets of lamellae peeling off the walls of beaten pulp fibers and produce fine strands that could easily be mistaken for external fibrillation [217].

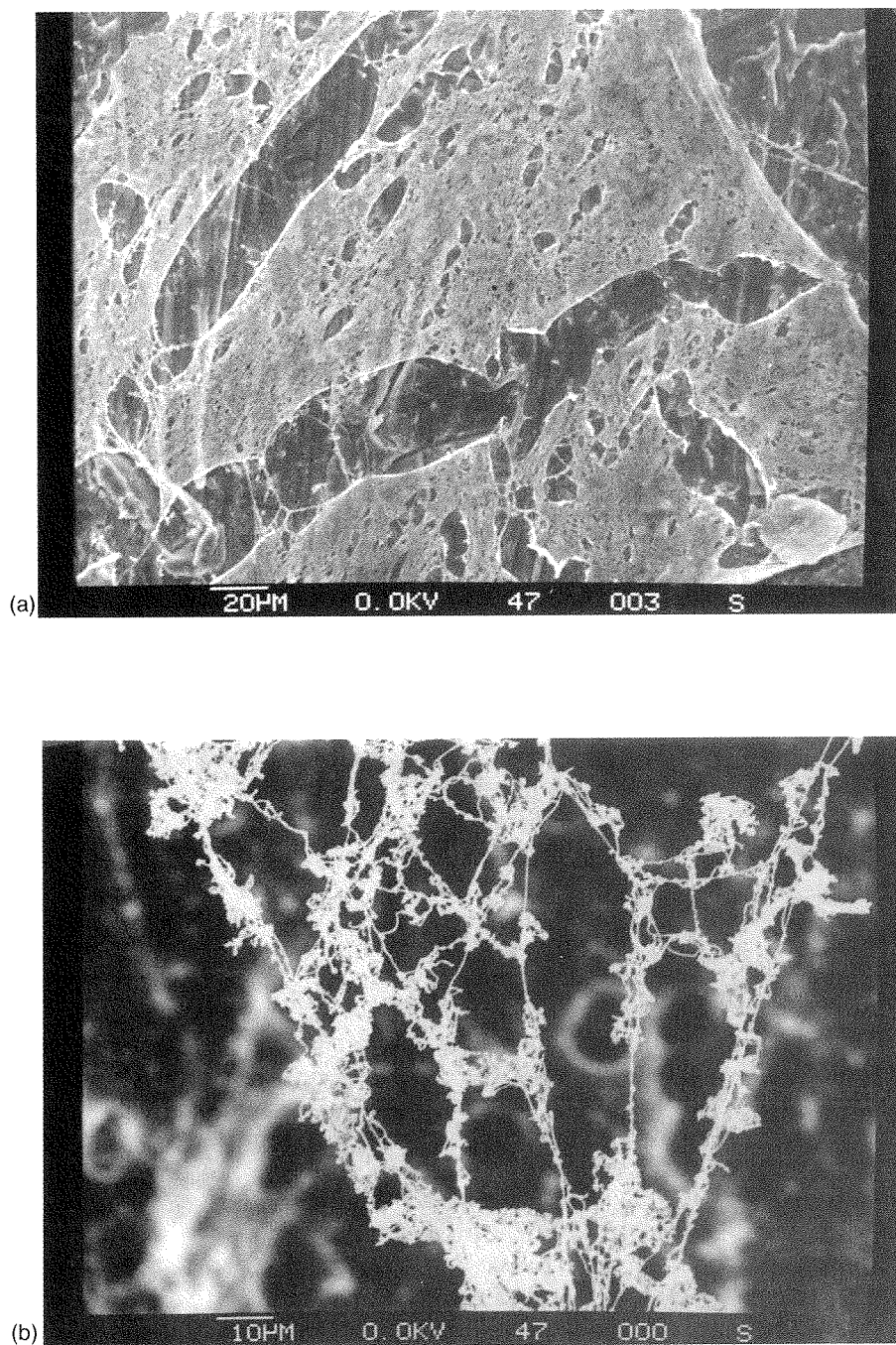


Fig. 28 (a) Eutectic membrane formed during sublimation of a 0.03 mM xylose solution, which forms a reticular structure (b) as sublimation proceeds. (From Ref. 216.)

The disruption of cell wall layers during beating and the production of fibrillar and membranous material is a phenomenon that has been well documented in the literature (see, e.g., Giertz [101] and Iwasaki et al. [137]). Although no chemical analysis was made to determine the hemicellulosic content of the pulps used in the experiments, such membranous and fibrillar structures were attributed to the presence of soluble wood carbohydrates, and certainly the circumstantial evidence is strong. In a pulp suspension much of the fibrillar and membranous material will be of cellulosic origin and not an artifact of cryofixation; the problem lies in distinguishing between fact and artifact. This therefore poses problems in the use of LTSEM for analysis of external fibrillation or classification of fines material. Furthermore, it takes very little dissolved material to produce artifacts, as evidenced by studies of cotton fibers, which have a very low hemicellulosic content. Likewise, the use of cryoprotectants can produce similar effects. These problems are also encountered in the examination of freeze-dried material using a conventional SEM.

Artifacts Arising from Fracturing Techniques Fracturing a FH sheet involves planing the surface with a cooled scalpel blade. Use of knives in fracturing techniques may result in scuff marks across the fracture face and also “smearing,” due to localized surface melting, leading to loss of detail in parts of the specimen.

Fracture methods that cleave the specimen in a single step, such as that employed with the split rivet, produce fracture faces that lack scuff marks but have a coarser surface topography. There is a greater tendency with such methods for fractures to occur along planes of weakness. Plastic deformation, a phenomenon that has been investigated by a number of workers, may also occur. Dunlop and Robards [73] experimented with polystyrene latex spheres in aqueous solutions of glycerol that they froze and fractured. Many of the spheres stretched by up to 50% before they fractured, whereas others were pulled out from the frozen matrix. However, Kellenberger et al. [160] reported that where plastic deformation had occurred the broken surfaces were usually heavily distorted with a rough appearance, and thus easily recognized.

To quote Echlin [75],

It has been said that in biology, image as related to truth is inseparable from artifact as related to the act of observing. It would appear that cryobiology is going to permit us to get nearer the truth than most of the methods we have been using in the past.

F. Applications of the LTSEM to Pulp and Paper Research

Compared to other microscopes such as the CLSM, the LTSEM has been less used as a research tool for studying pulp and paper and may well be superseded by the ESEM, which can look at wet and moist samples directly.

Fiber Structure Papermaking raw materials, both wood and non-wood, can be examined without the need for dehydration. Freeze-fracturing of fibers provides a method by which comparisons can be made between the internal structure of the raw material, never-dried, once-dried, and recycled pulp fibers.

External Fibrillation and Fines Material The LTSEM would seem to be the ideal instrument for detailed examination of fibrillation and fines material, because cryofixation preserves the spatial arrangements of the fibers and fibrillar material in a pulp suspension. However, the rate of development of external fibrillation cannot be accurately assessed owing to the fact that cryopreparation techniques can produce fibrillar material that may be mistaken for genuine fibrillation, as illustrated in Figs. 29 and 30.

Cell Wall Structure and Internal Fibrillation It is in the study of cell wall structure and internal fibrillation that LTSEM would seem to offer the greatest potential. The relatively simple method by which cross-sectional views of frozen hydrated fibers can be obtained for examination has enabled a study to be made of the internal changes in cell wall structure brought about by beating. It has also shown that differences exist between beating methods. In this application the presence of fibrils that may, in fact, be artifacts does not affect interpretation of cell wall delamination. Although the CLSM allows the fibers to be cross-sectioned in their fully hydrated state without any pretreatment, the LTSEM allows observation of structures at a far higher resolution than can be achieved with optical microscopy.

Examination of internal fibrillation of wet beaten fibers has, in the past, meant that fibers have had to be dehydrated, embedded, and mechanically sectioned—with all the attendant repercussions. Cryofixation of specimens for use with the LTSEM overcomes these problems, as Figs. 31–33 show. The appearance of internal fibrilla-

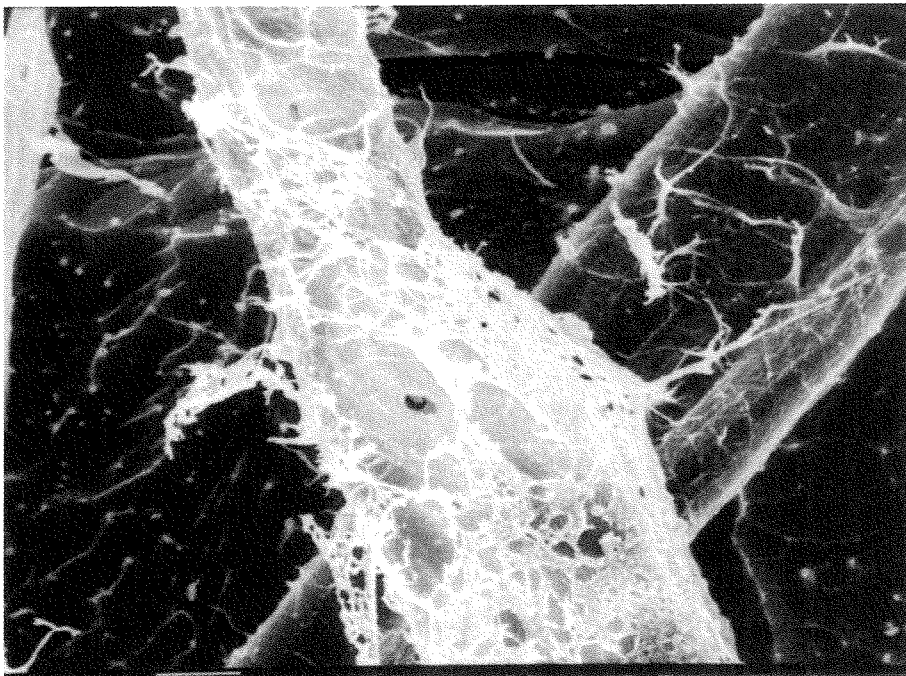


Fig. 29 Fibrillar material seen in a suspension of bleached sulfite fibers beaten for 45 min in a Lampen ball mill.

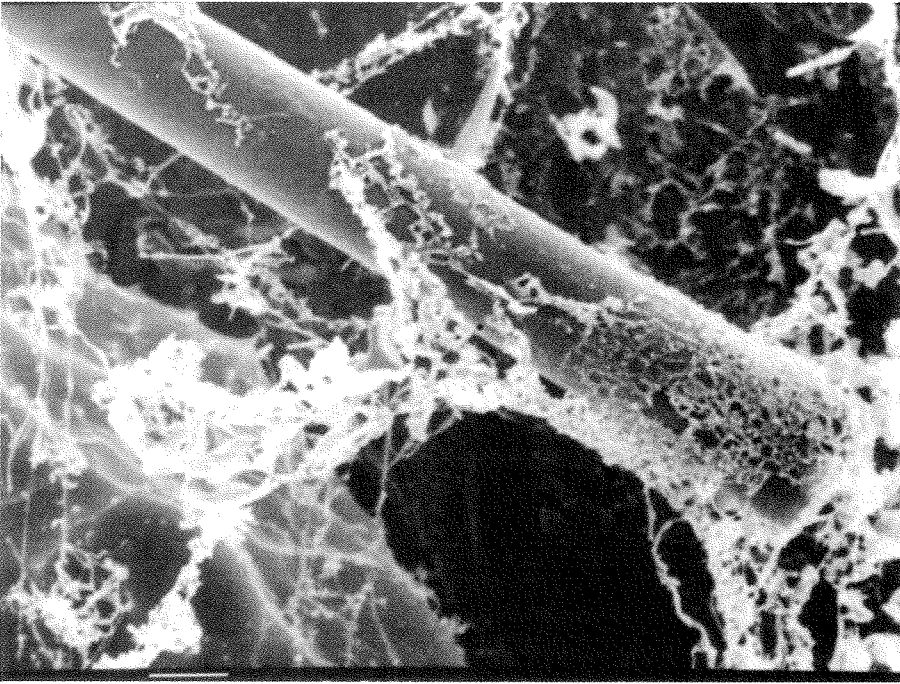


Fig. 30 Fibrillar material formed on nylon fibers suspended in a solution of 2 mM arabinose solution.

tion in Fig. 31 clearly resembles Scallan's honeycomb model (cf. Fig. 1) except that the cell wall has separated into fewer lamellae. One cannot determine whether the fibrillar material spanning the cracks between wall layers is really part of the honeycomb pattern, but it is clear that the cell wall has separated into many distinct layers. It has been suggested that if the fibers are not frozen rapidly enough then water within the cell wall could split the wall lamellae during the freezing process, but since the amount of delamination correlates so closely with the degree of beating there is no reason to suppose this has happened. Also, cell wall delamination was rarely observed in unbeaten fibers even though they had been soaked and disintegrated according to the prescribed methods [319,331] (Fig. 32). However, with the subsequent advent of the CLSM it is now possible to verify whether or not cryopreparation techniques are inducing structural or dimensional changes in cross-sectional views of fibers. Wet fibers can be examined first with the CLSM and then the same fibers can be frozen and fractured and examined in the LTSEM.

Quantification of Cell Wall Delamination Experiments carried out by Moss [216] showed that the ratio of delaminated to flat fibers in dry lap pulp samples correlated well with tensile index properties, and this ratio was proposed as a predictive index for the development of tensile strength. Unbeaten pulp fibers consisted largely of collapsed fibers in which the lumina were clearly visible but with the cell walls showing very little or no sign of delamination. Beaten fibers showed a variety of cross-sectional shapes, from flat, through stages of swelling, to fully swollen, with

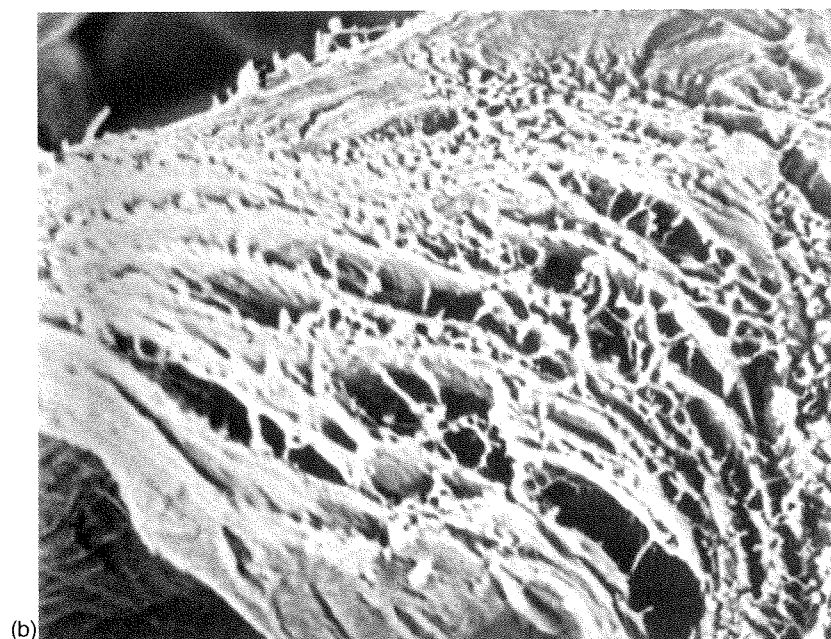
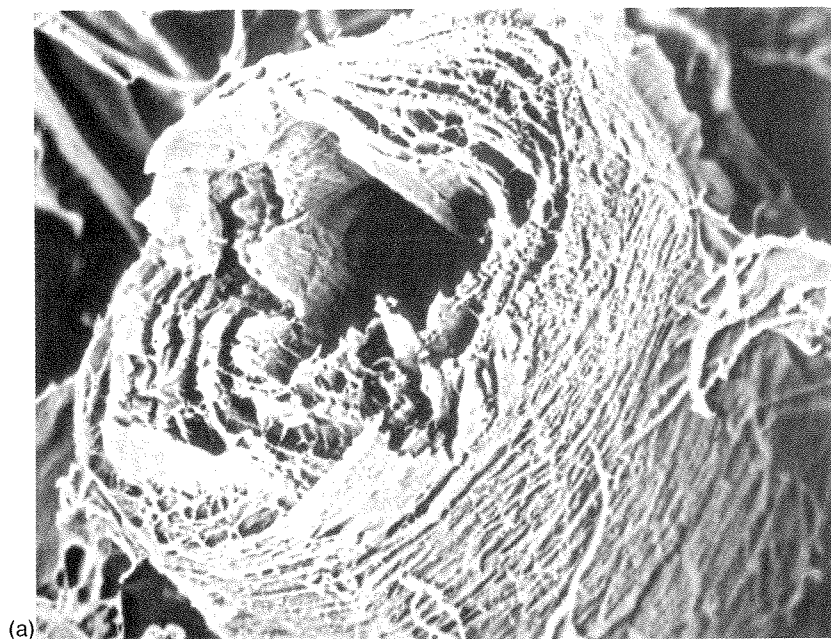


Fig. 31 (a) Cross section of internal fibrillation in a frozen hydrated bleached sulfite fiber beaten for 120 min in a Lampén ball mill. (b) A close-up of the cell wall. (From Ref. 216.)

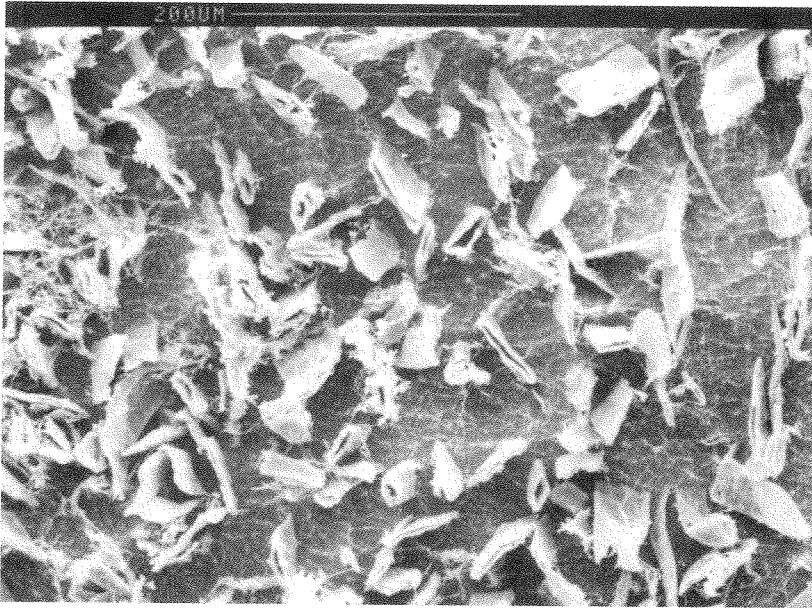


Fig. 32 Cross sections of frozen hydrated fibers of an unbleached softwood sulfite pulp showing little evidence of cell wall swelling or delamination. (From Ref. 184.)

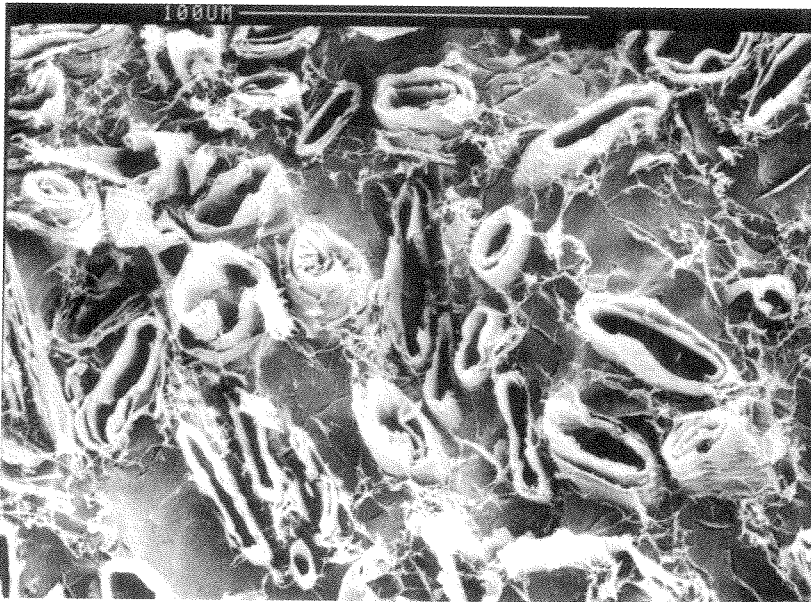


Fig. 33 Cross sections of frozen hydrated fibers of an unbleached kraft pulp beaten for 90 min in a Lampén ball mill showing various degrees of wall swelling and delamination. (From Ref. 216.)

the cell walls showing various degrees of delamination (see Fig. 33). The number of fibers showing swelling and cell wall delamination varied with beating time and method of beating. It must be emphasized that only internal fibrillation on the macroscale, i.e., what Page referred to as cracks, was being examined in this study.

Sheet Structure Pye et al. [258] used a conventional SEM to study the structural changes that occur in paper during pressing and drying. In their experiments the wet sheets were critical point dried or freeze-dried, which would have induced shrinkage and changes in the geometry of the wet web as well as loss of fines through the solvent exchange process. LTSEM offers a better way of observing the changes that occur at the different stages in sheet consolidation from just-drained through couching to pressing and drying. However, although examination of frozen hydrated samples eliminates the effects of shrinkage and changes in microstructure incurred during dehydration, interpretation of fine detail may be confounded by the presence of artifacts. The technique of freeze-fracturing and examining cross sections of frozen hydrated sheets offers considerable potential for studying two-sidedness, both in terms of structure and in the distribution of fillers such as titanium dioxide and calcium carbonate, particles of which are readily identified in the LTSEM. It could also be used to investigate lumen loading. The LTSEM is probably the best method currently available for such studies, because preparative techniques used for conventional SEM can bring about a redistribution of the particles during dehydration.

Coating Structure Sheehan and Whalen-Shaw [292] used high magnification cryo-SEM to examine microstructures in aqueous suspensions of coating components. They were able to observe associations between clay and latex pigments in coating suspensions containing kaolin, styrene-butadiene latex, and carboxymethyl cellulose in different combinations. They demonstrated how freeze-fracture techniques provide the visual link between wet and dry particles and how mechanisms of colloidal interactions can be deduced. Their paper also provides illustrations of the metal-coating and prepump chambers of the cryosystem they used.

VI. THE ATOMIC FORCE MICROSCOPE

Microscopes have been an integral part of material characterization since the early seventeenth century with the development of the first optical microscope (see Section II). There have been many changes in optical microscopy, the most notable being altering of the light path via prisms, mirrors, and slits and the use of various light sources allowing fluorescent and optical sectioning. However, the basic operation of the optical microscope remains unchanged: an image is generated by passing light through, or reflecting it off, a sample. Although functionally quite different from optical microscopes, electron microscopes operate on a similar principle: an image is reconstructed from a scanning sequence acquired from a sample being illuminated with an electron beam rather than light. The resolution of the electron microscope is far greater than that of the optical microscope, primarily due to the short wavelength of electron radiation. The electromagnetic lenses used in electron microscopes are subject to the same type of diffraction limits as the lenses of optical microscopes.

Optical and electron-based microscopes have serious shortcomings with regard to the study of biological materials: optical microscopes are limited by their resolution, whereas electron-based microscopes generally require extensive material preparation, result in material degradation, or must be operated in nonambient conditions. These limitations can be overcome by the use of a new type of scanning probe technique referred to as atomic force microscopy, which allows for the visualization of topographic features from the macroscopic scale down to the atomic scale.

The atomic force microscope (AFM) belongs to a family of microscopes known as scanning probe microscopes. These operate on a completely different principle than either the optical or electron microscopes: images are computer-generated by monitoring the x , y , and z positions of a probe scanning at or near the sample surface (Fig. 34). The microscope functions interactively to simultaneously monitor the position of the probe and maintain a desired tip-sample distance.

The topografiner was the first functional device to study surface imaging at near-atomic resolution [372]. This was the first device that allowed surface imaging using the quantum-mechanical phenomenon of electron tunneling [198]. The topografiner was composed of a conductive tip attached to a piezoelectric scanner and was scanned over the surface of a conductive sample with a feedback-controlled motion. A similar apparatus was developed by Binnig and Rohrer [21]. They improved the feedback mechanism and electronics and were better able to monitor tip location such that resolution was improved to several angstroms. The scanning tunneling microscope was the first instrument to generate images of surfaces with atomic resolution. An STM image is generated by monitoring the current of electrons flowing between a sample and a conducting tip that are separated by a distance of no more than about 10 Å. The STM, invented by Binnig and Rohrer and for which they were awarded the Nobel prize in physics in 1986, is the modern precursor of all scanning probe microscopes.

The stunning images, resolution capability, and material characterization findings prompted the rapid development of similar types of probe-based microscopical techniques. These microscopical techniques are generally lumped under the banner of scanning probe microscopy and include atomic force, interatomic force, electrochemical scanning tunneling, frictional force, near-field scanning optical, surface compliance, magnetic force, scanning thermal, and scanning capacitance.

A prerequisite for this tunneling of electrons to occur across a bias voltage is that both the tip and sample must be conductors or semiconductors. This restriction limits the applicability of the STM in wood fiber investigations due to the electrical insulating characteristics of lignocellulosic fibers. The AFM is not subject to the same restrictions as the STM because tip displacement rather than current flow is the primary sensor measurement. Therefore, this section deals with the applicability of atomic force microscopy to the study of lignocellulosic fiber surfaces.

A. Principles and Operation of Atomic Force Microscopy

Principles of the AFM The AFM generates images by scanning the sample surface with a sharp tip mounted on the free end of a flexible cantilever (Fig. 35). The tip is lowered to the surface of the sample until sufficient force is encountered to result in a deflection of the cantilever. Deflection of the cantilever is monitored by reflection

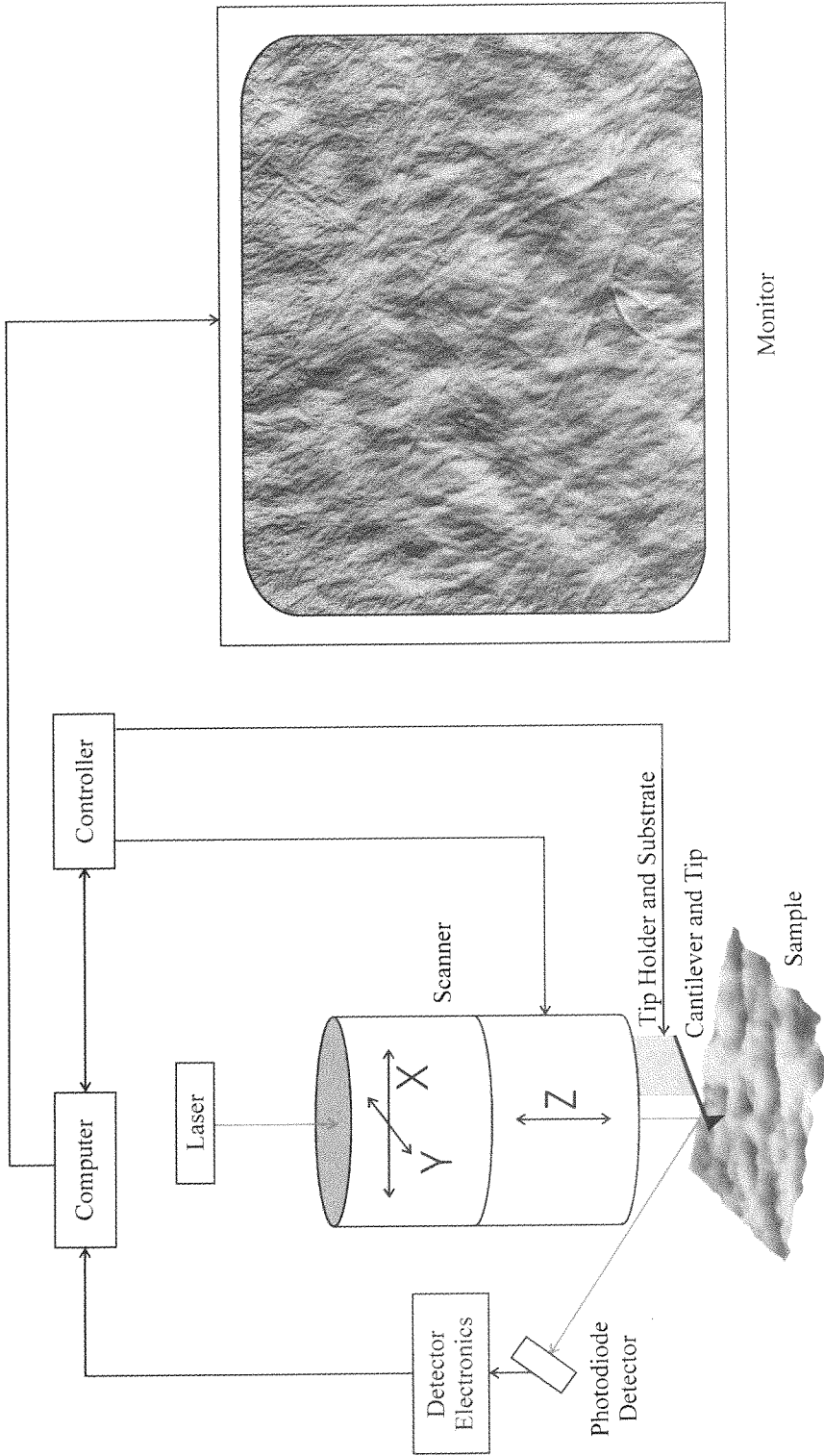


Fig. 34 Schematic of an atomic force microscope. (Adapted from image courtesy of Digital Instruments, Veeco Metrology Group.)

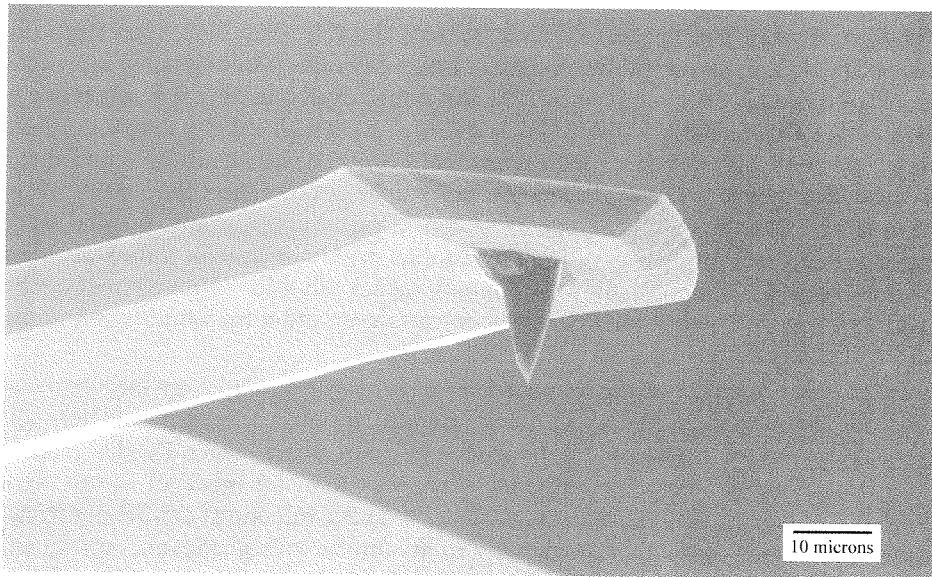


Fig. 35 Side view of an intermittent contact cantilever and tip. (Courtesy of T. C. Pesacreta.)

of a laser signal from the back of the cantilever to a position-sensitive photodetector. Tip deflection data are necessary to carry out two primary functions: (1) to computer-generate a three-dimensional map of surface topography and (2) to establish the tip setpoint and subsequently maintain a constant tip-sample interaction. The photodetector signal, which thus monitors the deflection of the probe tip, is used for feedback to control a piezo-based scanner. For example, if the probe encounters a relatively high feature, the photodetector will monitor the upward probe displacement. This feedback signal will be relayed to the scanner, which will retract the tip enough to restore a predetermined tip-sample force setpoint. The same signal that controls the tip-sample setpoint is also used to generate the three-dimensional topographic representation of the sample surface.

Hardware All AFM techniques depend on four components: probe, scanner, detection mechanism, and feedback electronics. A general description of each component is presented in the following sections.

Probe The probe directly determines the type of image acquired and the ultimate lateral resolution possible. The probe is the least expensive AFM component and is therefore generally considered expendable after a certain number of scans have been obtained. A “probe” is actually a unified assembly of two elements: a “tip,” which is a stylus with an extremely fine point that is in contact (or near contact) with the sample, and a “cantilever,” which is a flexible arm linking the tip to the scanner.

The most common AFM tips are commercially fabricated from silicon or silicon nitride and are pyramidal, tetrahedral, or conical [198]. Tip selection is crucial, because the tip radius, along with the step size of the image, determines the lateral resolution of AFM images [132]. Conical tips are the sharpest and thus the most fragile, with tip radii as small as 50 Å. Pyramidal and tetrahedral tips have tip

radii of a few hundred angstroms but are very durable. The high aspect ratio of conical tips makes them ideal for imaging samples with deep troughs or sharp edges.

Probe selection depends on the sample being imaged and the operating mode of the microscope. The majority of AFM imaging is done with either a contact or non-contact probe. Contact probes require intimate contact with the sample and therefore have cantilevers with low spring constants so as not to deflect the surface of the specimen. Contact probes are made of silicon nitride with a durable tip that has a large tip radius and low aspect ratio. Non-contact probes operate in forced vibration and must be rigid enough to allow for high frequency vibration. Non-contact probes are generally composed of an etched silicon cantilever and a tip with a small radius and high aspect ratio.

Scanner The function of the scanner is to either move the tip over the sample or move the sample under the tip and is controlled by user-defined parameters and feedback regarding tip-sample interactions. Scanners are generally designed to allow translation in the three principal directions and are made of piezoelectric materials. Thus, scanner movement in the x , y , and z directions can be controlled by expansion and contraction in response to an applied voltage. Scanner movement is generally in a raster or back-and-forth pattern.

The size of the scanner tube dictates the limits of lateral motion as well as vertical resolution [132]. Generally, lateral movement is restricted from a minimum of a few nanometers to 100 μm to a maximum of 100–200 μm . The range of vertical displacements are from 5–10 μm down to the subangstrom range.

Detection Mechanism The choice of detection mechanism depends on the operating mode of the microscope. Traditional AFM is based on the vertical displacement of the tip and is monitored by the reflection of a laser beam from the back of the cantilever to a photodetector. The z -displacement photodetector data are then used to control the vertical response of the piezoscanner.

Detection mechanisms that monitor such variables as probe rotation, lateral resistance, and disruption of vibrational integrity are also necessary to allow material characterization using various operating modes outside of traditional AFM. Examples of nontraditional AFM operating modes include force calibration, phase shift, and lateral force. Specifics of these detection mechanisms are beyond the scope of this section.

Feedback Electronics The function of the feedback system is to maintain user-defined tip-sample specifications by controlling the actions of the tip and the scanner. The maintenance of constant tip-sample interactions is necessary to collect accurate morphological representations of surface images. A constant interaction also ensures representative non-height data for techniques such as phase and force modulation.

B. Operating Modes

Atomic force microscopic images are generated by maintaining a constant deflection between the tip and the sample. Deflection is held constant by monitoring the tip-sample force, which can be either attractive or repulsive. There are various AFM techniques that take advantage of these opposing forces. Contact AFM requires repulsive forces, non-contact AFM exists in the repulsive regime, and intermittent

contact (also known as “tapping”) AFM is governed by the repulsive force but also resides in the attractive domain. These forces are summarized in Fig. 36.

Contact Mode The contact mode of AFM is a nonvibrational technique that brings the tip of the probe to within a few angstroms of the sample surface. As the tip and sample are brought closer together, their atoms begin to attract each other; then their respective atoms encounter each other’s Coulombic (repulsive) forces. This repulsive force prevents further intrusion by the tip and causes the cantilever to deflect due to the low spring constant of the cantilever. Surface topography is then determined by scanning this tip over the sample while monitoring tip deflection, maintaining a constant repulsive force.

Non-Contact and Intermittent Contact Modes Non-contact AFM relies on monitoring the deflection of a vibrating cantilever as it is brought into close proximity of the sample surface. A rigid cantilever is vibrated at or near its resonance frequency, typically between 50 kHz and 1 MHz, and with a magnitude of 3–20 nm. This vibrating tip is lowered toward the sample surface. The tip encounters several boundaries during engagement before reaching the region dictated by molecular potential energy: fluid film, electrostatic, and fluid surface. The fluid film boundary

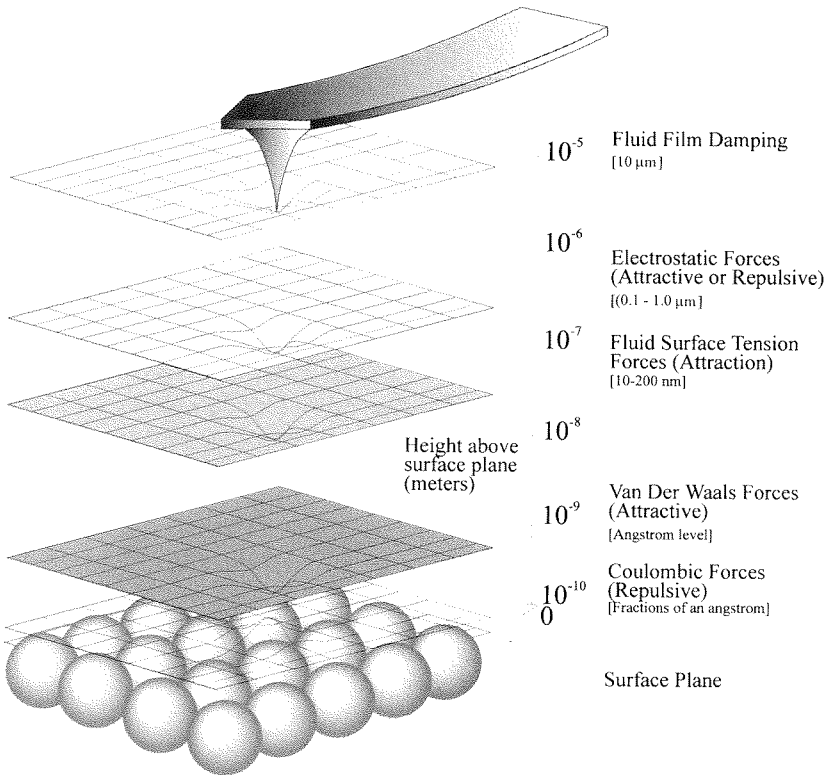


Fig. 36 Tip-sample interactions. (Adapted from image courtesy of Digital Instruments, Veeco Metrology Group.)

dampens vibration approximately 10 μm from the sample surface. However, this damping is temporary and disappears as the probe passes through the boundary. Electrostatic forces begin within 1 μm of the sample surface and can be either attractive or repulsive. Electrostatic forces in wood pulp fibers tend to be rather high, due in part to their low conductivity. The final pre-engagement boundary is the fluid surface boundary, which begins about 100 nm from the sample surface. This is an especially significant layer in wood pulp fiber investigations owing to the hydrophilic nature of the cellulosic material. This attractive force has the capability to pull the tip down onto the sample surface with a force strong enough to cause indentations.

The probe is lowered until the tip begins to encounter van der Waals forces, typically 20–200 \AA from the sample surface. In a modified version of non-contact atomic force microscopy referred to as intermittent contact microscopy, the oscillating tip is moved toward the surface until it begins to lightly touch or “tap” the surface. The tip is considered to contact the sample surface when the amplitude apex enters the repulsive regime of the molecular potential energy curve. In either non-contact mode, the force on the sample is automatically set and maintained by the feedback control mechanism. The vibrating tip is then scanned over the sample surface to determine topography. These modes are generally used for soft or elastic materials because the tip exerts very low forces on the sample surface.

The intermittent nature of intermittent contact microscopy is most ideally suited for cellulosic fibers. The oscillation amplitude is sufficient to overcome any tip-sample interactions due to bound surface water. Also, sample damage is minimized by the vertical tip loading, there being no shearing forces to laterally displace the sample surface.

Other Variants of AFM Many variants of conventional AFM techniques have evolved that either alter the detection mechanism or modify the probe. The variants are too numerous to describe in detail. However, those techniques most applicable to the examination of cellulosic fibers are presented in this section.

Lateral Force Microscopy Also known as frictional force microscopy, lateral force microscopy measures the twisting of the cantilever that arises from forces parallel to the plane of the sample surface [132]. Lateral force microscopy is useful for imaging variations in surface friction attributable to surface inhomogeneities. Further frictional studies can be conducted by coating the tip with various substrates.

Force Modulation Microscopy This technique, also known as surface compliance microscopy, allows the user to ascertain the resistance of a sample to a load applied normal to the surface. The force applied to the sample surface is modulated with respect to z displacement. Traditionally, the AFM is operated in contact mode for force modulation microscopy, but recent advances in electronics allow for the intermittent contact mode to be employed. Changes in cantilever amplitude, which are a function of the elastic properties of the sample surface, are collected and converted to a compliance or elasticity image. Topographic data are collected simultaneously with force modulation data to maintain a constant tip-sample distance. The application of force modulation microscopy for wood pulp fibers may prove useful in mapping various surface components.

Phase Detection Phase detection is done in intermittent contact mode AFM and monitors the difference between the cantilever driving signal and the cantilever output signal [132]. The phase lag, in part, indicates the surface adhesion or viscoelastic properties of a sample. In lignocellulosic fibers, this technique can serve either to differentiate between bulk components such as lignin and cellulose or to identify surface contaminants. Phase detection, also known as phase imaging, can be conducted simultaneously with force modulation microscopy.

Near-Field Scanning Optical Microscopy One of the newest and fastest growing variants of conventional AFM, near-field scanning optical microscopy (NSOM) uses an aluminum-coated optical fiber as the scanning probe and produces visible light images. Laser light is guided through the fiber, which acts as a subwavelength aperture to the sample, and is detected from either a transmitted or reflected signal. Scanning this laser light source over the sample allows for optical images with resolution up to 150 Å. Various types of illumination (e.g., polarization, fluorescence) can be used. The primary significance of this technique lies in ultrahigh resolution optical imaging and single-molecule spectroscopy. A review of the technique and its applications is given by Harris et al. [119].

Electric Force Microscopy Electric force microscopy operates in a non-contact mode and measures the locally charged domains of the sample surface. A voltage is sent between the scanning tip and the sample, with cantilever deflection being proportional to the charge density of the sample surface. Although several offshoots of this technique exist, the primary purpose in lignocellulosic fiber research would be to map static charges on the fiber surface for fiber–fiber or fiber–substrate compatibility.

Scanning Thermal Microscopy Thermal scanning microscopy is a non-contact mode AFM variant that utilizes a specialized cantilever composed of two different metals to ascertain the thermal conductivity of a sample surface. The difference in thermal conductivity responses of these metals causes the cantilever to deflect. Scanning the sample and monitoring this deflection results in a thermal conductivity map of the sample surface. Changes in vibrational amplitude are also collected simultaneously to map surface topography.

Additional AFM Variants Several other techniques that may prove useful in the understanding of wood and other lignocellulosic fibers include

- Chemical force microscopy, which uses chemically modified tips to quantify adhesion and functional group distributions in molecular assemblies

- Magnetic force microscopy, which is similar in principle to electric force microscopy but uses a magnetically charged tip to image weak magnetic interactions

C. Environmental Conditions

The AFM can image samples in one of four conditions: liquid, air, vacuum, and electrochemical. Electrochemical imaging is not relevant in pulp and paper research because it is used primarily for investigating metallic samples and biological materials in electrolytic solution. Imaging in a vacuum environment is predominantly for STMs but is also applicable for AFMs. The purpose of the vacuum is to minimize

electrostatic interference and debris contamination. The applicability of vacuum atomic force microscopy to wood pulp fiber research is questionable due to the nonambient conditions and additional preparation time with little to no increase in image quality.

Ambient air is the simplest, least expensive, and thus most popular scanning environment for the AFM. Sample preparation for this environment is minimal; samples are adhered to a magnetic AFM “puck” with a viscous adhesive or double-sided sticky tape. This type of environment is ideally suited for surface characterization of lignocellulosic fibers, primarily because composites made from these materials are used in ambient conditions. Although AFM imaging of lignocellulosic fibers is affected by various attractive and repulsive forces near the surface (see Fig. 36), it is still possible to get high resolution images of various fiber types imaged in air.

Imaging in liquids eliminates the fluid surface tension forces encountered with imaging in air, resulting in images with improved detail. There are a few disadvantages to imaging in fluids. Lignocellulosic fibers cannot be imaged in their dehydrated or near-dehydrated condition, with features possibly being obscured or distorted due to swelling of the cell wall. In addition, sample adhesion to the AFM puck must be adequate and able to withstand the liquid media. It should also be noted that liquid imaging requires more sample preparation time and is cumbersome due to the difficulty of moving between samples within and among AFM pucks. However, the increased effort is rewarded in many cases by improving surface topographic details.

D. Applications of the AFM to Pulp and Paper Research

The applicability of the AFM to the pulp and paper industry lies in two general areas: qualitative and quantitative analysis. Qualitative analysis is necessary for observations of physical features and overall surface topography, often at extreme magnifications. Collected data exist in the form of a three-dimensional array, thus allowing the development of algorithms that can then quantify individual features such as microfibrils and crystallites as well as more global properties such as surface roughness and spectral type analyses.

It should be noted that most of the research done on cellulosic fibers has been conducted in intermittent contact mode. The relatively rough surface of cellulosic fibers can be problematic in contact mode, causing severe rotational stresses on the cantilever and tip as well as scratching and altering the surface of the specimen. The tapping nature of the intermittent contact mode results in negligible specimen damage and in images of high spatial resolution. Most of the AFM images shown in this section were obtained in intermittent contact mode.

Qualitative Analysis There currently exist only a limited number of publications linking the art of atomic force microscopy and cellulosic fibers. Excellent summaries of the applicability of the AFM to biological samples are given by Morris [215], with specific examples relating to wood and pulp fiber research given by Béland [16]. A summary of the technique and the imaging of polysaccharides and organics in general can be found in Kirby et al. [170] and Radmacher et al. [262]. These publications stress the fact that the most common type of AFM analyses have been qualitative,

owing to the simplistic manner of image collection and analysis as well as the wealth of information generated. In essence, the qualitative analysis allows the investigator to ascertain the effect of various pulp generation schemes on the surface of cellulosic fibers.

Comparison with Various Scanning Microscopes Although the confocal laser scanning microscope (CLSM) is capable of characterizing surface details of cellulosic fibers and networks, it is limited in its magnification and is therefore used primarily in the investigation of subsurface features as described in Section IV. The family of microscopes that most closely parallels specimen characterization by atomic force microscopy is that of electron microscopes. Some of the earliest transmission electron microscopical (TEM) work characterizing cellulose microfibrils was conducted by Asunmaa [4] on pine holocellulose and by Revol [268] on high resolution diffraction contrast images of transverse sections of the green algae *Valonia ventricosa*. Subsequent TEM studies by Revol [269] and Sugiyama et al. [312] confirmed the earlier work. Hanley et al. [114] compared the images produced by AFM and TEM of *Valonia ventricosa* cellulose microfibrils. They found those microscopes to be complementary: specimen preparation for the TEM was more laborious but provided true detail of subsurface microfibril structure, whereas the AFM provided information about surface features. Resolution for the AFM and TEM is similar, around 2 Å. Generally, TEM stains do not show cellulose well, if at all, except for negative stains of isolated cellulose strands. The SEM is more directly comparable than the TEM to the AFM because both the SEM and AFM use a raster-type motion to scan the surface of a specimen. In general, the surfaces to be studied in the SEM and AFM are similar. The primary differences in producing SEM and AFM images have been outlined by Béland [16] and are summarized as specimen preparation, field of view, and resolution. Traditional SEMs require that specimens be conductive, thus requiring metal coating. However, this coating greatly restricts the level of detail attainable due to the size of the granular metal coating [110,355]. The 5–20 nm thick coating of gold typically used in SEM sample preparation often obscures the surface details of individual cellulosic fibers, as can be seen in Fig. 37. A cotton fiber (*Gossypium hirsutum* L.), with the waxy cuticle and pectin removed with an Updegraff reagent, was first imaged with the AFM in intermittent contact mode (Fig. 37b). The fiber was then sputtercoated with gold and imaged at a corresponding magnification with an SEM (Fig. 37a). It can be seen that the clarity of the cellulose microfibrils has been masked by the conductive coating. The problems associated with conductive coatings were minimized by Patnaik et al. [252] in evaluating thin films of hydroxypropyl cellulose with an AFM and a low-voltage high resolution SEM (LVHRSEM) using a 2 nm layer of tungsten applied with a dual ion beam coater. However, the resolution and quantitative capabilities of the AFM were necessary to determine fibrillar trajectories.

Figure 38 illustrates a direct comparison of an uncoated loblolly pine (*Pinus taeda* L.) macerated fiber as imaged with an ESEM and an AFM. Figure 38a was imaged in an EnviroScan ESEM at a magnification of 170×. The dashed region of Fig. 38a was rescanned at a higher magnification of 540×, but it is still apparent that there is insufficient contrast to define individual microfibril features. This fiber was removed from the ESEM chamber, and the boxed region of Fig. 38b was imaged with the AFM (Fig. 38c). The AFM image shows much greater detail than the

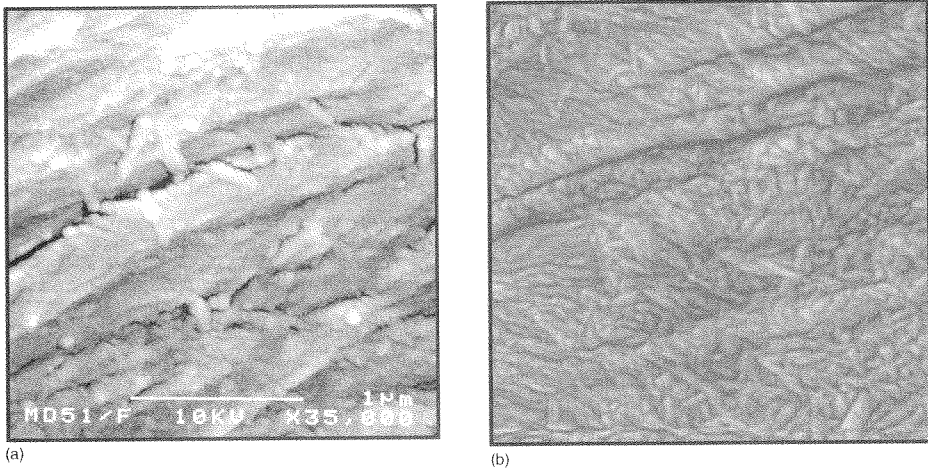


Fig. 37 A cotton fiber with the cuticle removed after treatment with 6% NaOH and Updegraff reagent and imaged with (a) a scanning electron microscope and (b) an atomic force microscope (amplitude data, 2.5 μm scan). The fiber was first imaged with the AFM, sputtercoated with gold, then imaged in the SEM. (Courtesy of T. C. Pesacreta.)

original ESEM images, with individual microfibrils clearly evident. This increase in image detail was also observed in an investigation of cellulosic fiber conducted by Suleman [314] in which the author compared uncoated cellulosic fibers, primarily softwood pulp fibers, with the AFM and the ESEM.

Fiber Characterization The AFM is a surface probe, so the characterization of cellulosic fibers is a direct function of the manner in which the fibers were generated

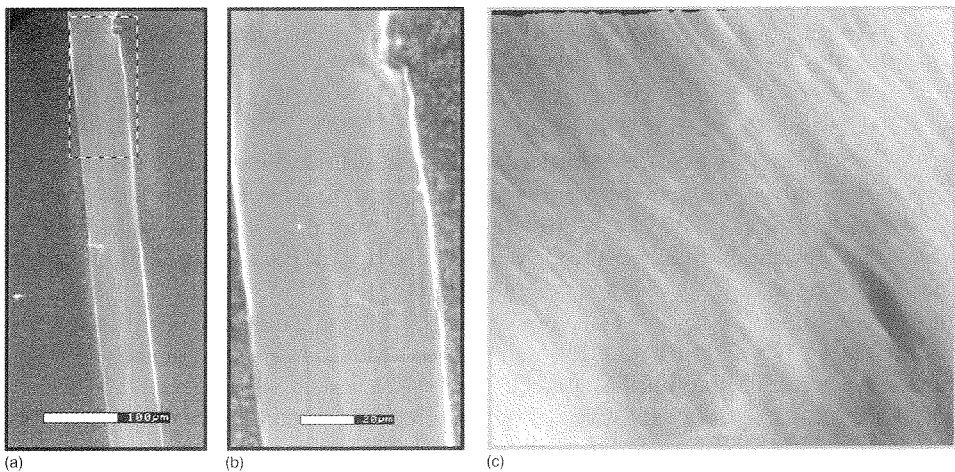


Fig. 38 Varying levels of magnification of an uncoated macerated loblolly pine juvenile, latewood fiber as imaged in (a) and (b) an environmental scanning electron microscope and (c) an atomic force microscope (amplitude data, 2.5 μm scan). [(a) and (b) courtesy of L. Mott and S. M. Shaler.]

and subsequently treated or modified. Thus, the applicability of the AFM to cellulosic fiber characterization becomes most meaningful in the area of pulping and its effect on surface properties. Although the potential for cellulosic fiber characterization with the AFM is immense, little published information is available, primarily because the use of AFM is in its infancy in regard to biological sampling. Recent theses by Suleman [314] and Hanley [113] greatly expand our knowledge base of fiber surfaces. Suleman evaluated the effect of sulfite versus sulfate processes, recycling, beating, and bleaching. In a complementary publication, Hanley and Gray [115] focused more on fundamental characterization, specifically with the description of cellulose microfibrils.

The imaging of solid wood and cellulosic fibers in the AFM involves a relatively simple procedure. The specimen of interest is adhered to an AFM puck by means of an adhesive or double-sticky tape and is then positioned under the AFM head. Figure 39 shows the height data of a typical AFM scan operating in intermittent contact mode of a macerated loblolly pine fiber pit. The fibrillar structure of the pit chamber is clearly evident, as are remnants of the middle lamella and depositions from the maceration process.

The applicability of the AFM to the pulp and paper industry will lie primarily in the ability of the AFM to ascertain surface features and properties of individual cellulosic fibers as a result of the pulp generation method and subsequent treatments

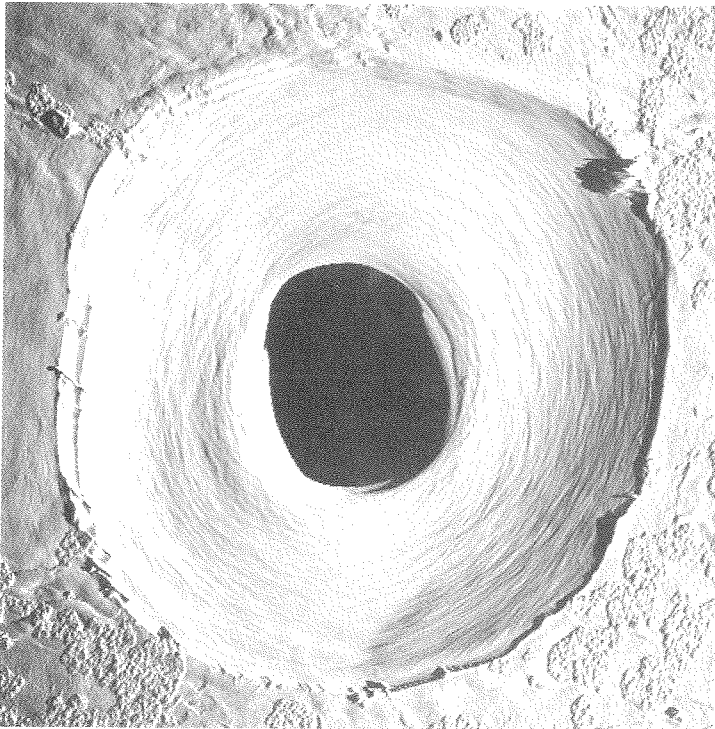


Fig. 39 Intermittent contact mode 25 μm scan showing the primary cell wall, remnants of the middle lamella, and pit chamber of a single macerated loblolly pine fiber.

and modifications. Nissan and Sternstein [229] state that paper strength is directly related to the frequency and strength of fiber bonding. This reliance on fiber-to-fiber bonding for the development of paper strength was reiterated by Page [235]. Some factors governing fiber-fiber bonding are the surface topography and the primary constituents on the surface of individual fibers. Figure 40 demonstrates the difference between fibers that were generated mechanically and chemically. The fiber in Fig. 40a was generated in a pressurized disk refiner at a refining pressure of 40 psi and an ambient temperature well below 95°C, the reported glass transition temperature of lignin [271]. The conditions resulted in intrawall damage as observed with the CLSM as well as a splotchy lignified surface. The fiber in Fig. 40b was chemically generated in a rather extreme kraft pulping regime, with an overall fiber yield of 35%. The resulting pulp fibers have had essentially all of the hemicellulose and lignin removed, thus revealing the random nature of the cellulose microfibrils of the primary cell wall.

Figure 41a shows a typical mature loblolly pine pulp fiber generated from a potassium/anthroquinone (KAQ) pulping regime to a pulp yield of 47% retain. The pulping was mild enough to not remove all of the lignin (pulp yield 47%), thus obscuring the microfibrillar network. Figure 41b shows a mechanically refined fiber analogous to the conditions of Fig. 40a but under a refining pressure of only 10 psi. The longitudinal fiber axes in Fig. 41 run horizontally and show the lamellar undertones of the S1 secondary cell wall layer.

Steam-exploded fibers and high yield kraft pulp fiber exhibit similar surface details, as can be seen in Fig. 42, in which the longitudinal axis is oriented horizontally. Drying deformation in the form of wrinkles and creases can be seen as macro features. The microfibrils are present but not easily discernible in Fig. 42a, due most likely to a thin uniform coating of lignin. The high yield (kappa number of 100) commercial kraft pulp retained much of its original lignin, which formed a thick coating that masked the fibrillar network.

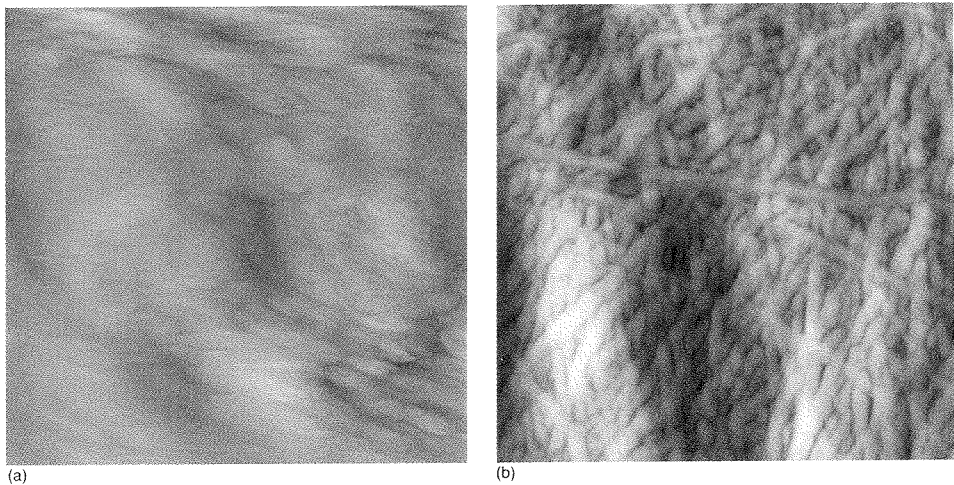


Fig. 40 Comparison of mechanically and chemically generated mature loblolly pine fibers, showing 1 μm scans of (a) fiber refined at ambient temperatures and at a refiner head pressure of 40 psi and (b) low yield kraft fiber (yield 35%).

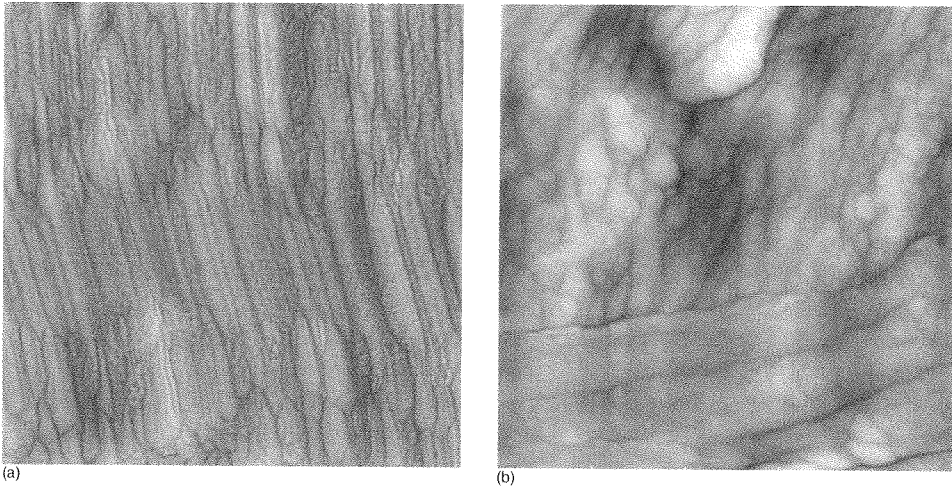


Fig. 41 Scans ($2.5\ \mu\text{m}$) of individual mature loblolly pine fibers generated from (a) a potassium/anthroquinone pulping regime (yield 47%), and (b) a disk refiner at ambient temperature and at a pressure of 10 psi.

The AFM is also important for distinguishing the manner in which various types of fibers respond to pulping regimes. Figure 43 shows the response of juvenile and mature segments of a single loblolly pine to identical Franklin maceration schemes [246]. The surface features of the juvenile wood pulp fibers (Fig. 43a) exhibited no signs of a primary cell wall, showing a flat microfibril angle customary with the S1 secondary wall layer. In contrast, the mature wood pulp fibers (Fig. 43b) possessed a random network of microfibrils, indicating that the primary wall was present. It is unclear whether the primary wall of the juvenile wood fibers was present in the first place or was so thin that it was removed during the pulping process.

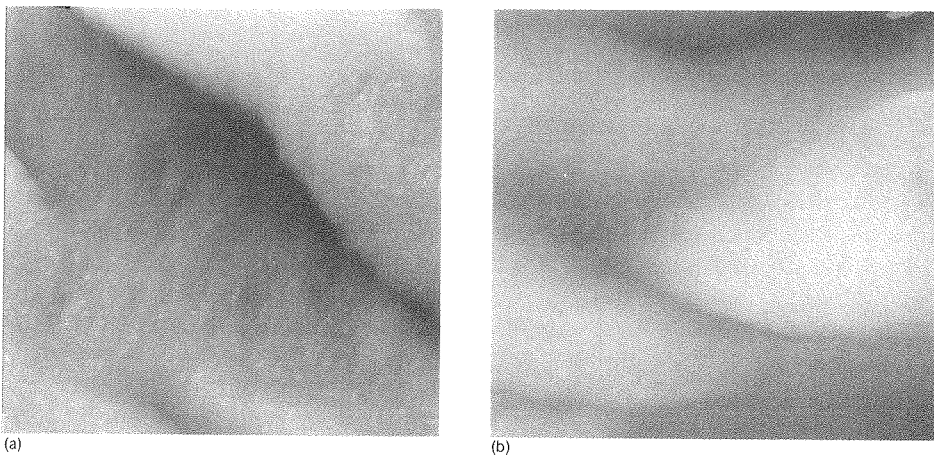


Fig. 42 Scans ($2.5\ \mu\text{m}$) of (a) a steam-exploded loblolly pine fiber from growth ring 20, and (b) an unbleached linerboard pine fiber generated by the kraft process.

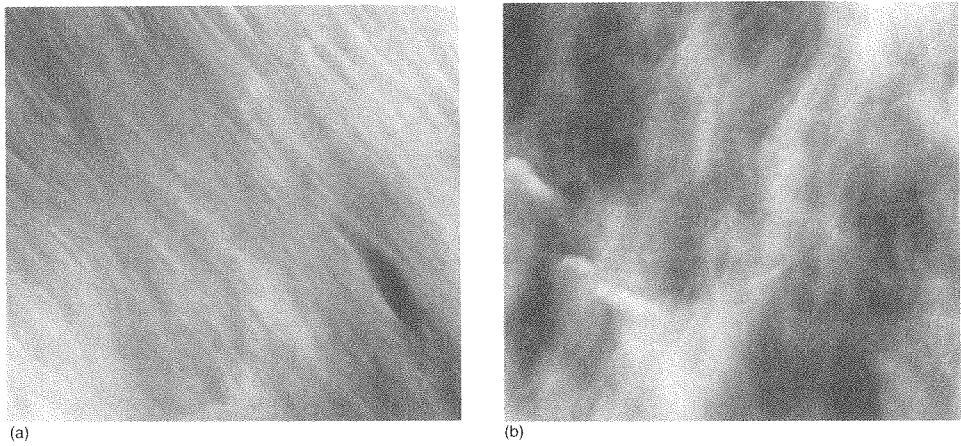


Fig. 43 Intermittent contact mode $2.5\ \mu\text{m}$ scans of loblolly pine fibers subjected to identical maceration schedules of glacial acetic acid and hydrogen peroxide, showing (longitudinal fiber axis oriented horizontally) (a) a juvenile and (b) a mature fiber.

Although the AFM is used exclusively to evaluate surface features and topography, it is possible to image internal cell wall features by physical removal of outer layers. The S3 and S2 layers of mature loblolly pine fibers are shown in Fig. 44, in which the longitudinal fiber axis is oriented vertically. The S3 layer image was obtained by longitudinally splitting a fiber with a knife, then mounting that bisected fiber lumen side up (Fig. 44b). The S2 layer was imaged by initiating a cut with a knife and then peeling the fiber back with forceps, thus removing the S1 layer and a portion of the S2 layer. In both cases, the microfibrils are clearly evident and are oriented accordingly.

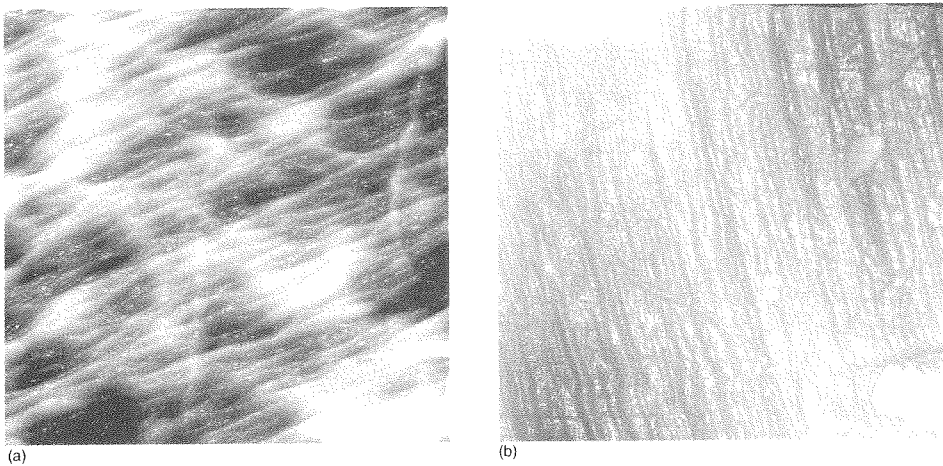


Fig. 44 Intermittent contact mode $2.5\ \mu\text{m}$ scans of macerated loblolly pine fibers. Longitudinal fiber axis runs from top to bottom of the images that show (a) the S3 layer as viewed from the lumen, and (b) the S2 layer, with the S1 layer physically removed.

The effects of chemical and physical treatments of the surfaces of various types of cellulosic fibers can also be studied. Figure 45 shows the surface topography of macerated and refined loblolly pine fibers. The macerated fibers were chemically generated in a solution of acetic acid and hydrogen peroxide; specific details of the pulping regime are outlined by Groom et al. [109]. The refined fibers were generated in a pressurized disk refiner at 4 bar. The difference in the pulp generation method is evident from the surface topography. Individual microfibrils are evident on the surface of the macerated fiber. Microfibrils are not visible on the surface of the refined fiber surface because they are overshadowed by a coating that is more likely lignin in nature.

It should also be noted that the AFM is being used to study native cellulose in situ, as demonstrated in the example of the green algae *Valonia ventricosa* (Fig. 46). *Valonia ventricosa* is commonly used in the study of cellulose because of the arrangement of its fibrils [126] and the high degree of crystallographic perfection within the fibrils [312]. In addition to qualitative assessment of cellulose microfibrils, current efforts are under way to quantitatively assess cellulose and its corresponding crystallites. This work is discussed in the next section.

Level of Magnification The ability of the AFM to resolve features down to the angstrom level is one of the features that makes the AFM most useful for fundamental fiber research, especially with respect to the constitution of cellulose microfibrils and their subsequent components. An illustration of the applicability to cellulosic fiber research is shown in Fig. 47. A commercially processed cotton fiber was adhered to an AFM puck and imaged at low, medium, and high magnifications, with the fiber longitudinal axis oriented horizontally. The 6 μm scan (Fig. 47a) reveals what appears to be a fibrillar network. Subsequent scans of 1.7 μm (Fig. 47b) and 530 nm (Fig. 47c) show that the undulating network was not fibrillar in nature but were wrinkles caused by processing and/or shrinkage, with the cellulose

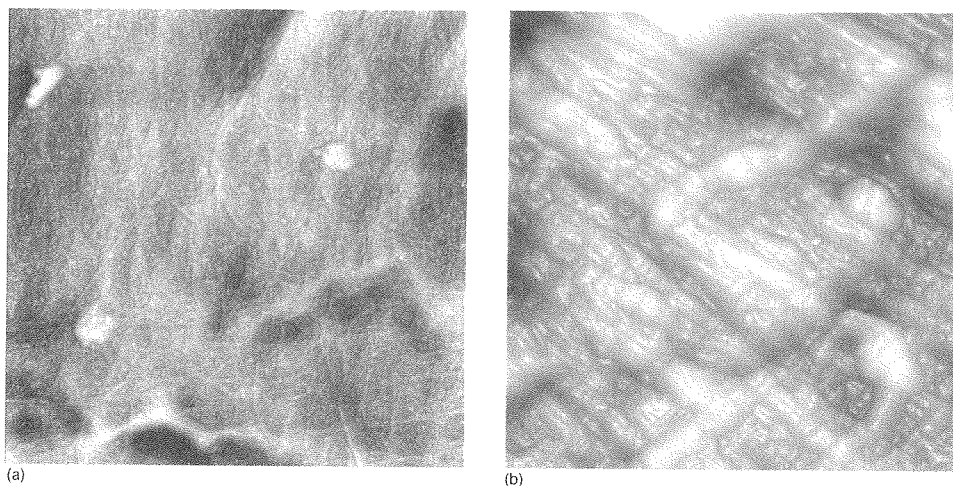


Fig. 45 Atomic force height images (5 μm scans) of loblolly pine fibers generated by (a) chemical maceration with hydrogen peroxide–acetic acid solution and (b) disk refined at a pressure of 4 bar. (Courtesy of R. Snell.)

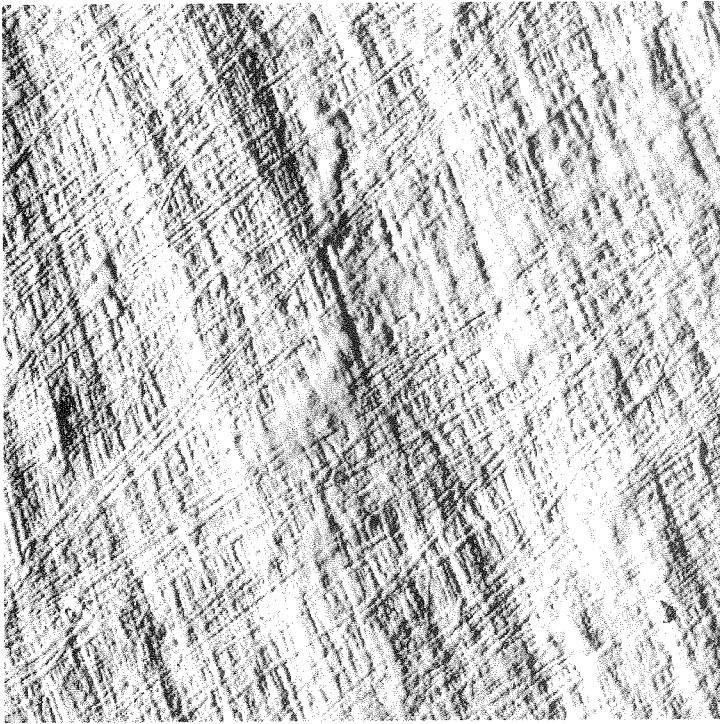


Fig. 46 Intermittent contact mode 5 μm scan of the cell wall of *Valonia ventricosa*, clearly displaying the cellulose microfibrils. (Courtesy of S. Zauscher.)

microfibrils revealed at the higher magnifications. A similar display of microfibrillar structure in a recycled wood fiber is also demonstrated in Fig. 48.

Imaging in air of cellulose microfibrils, as is the case with any hydrophilic specimen, becomes difficult at nanometer-scale resolution due to moisture present on the stylus and the specimen surface. These capillary layers of moisture coalesce as the stylus approaches the sample surface, resulting in attractive forces that distort or

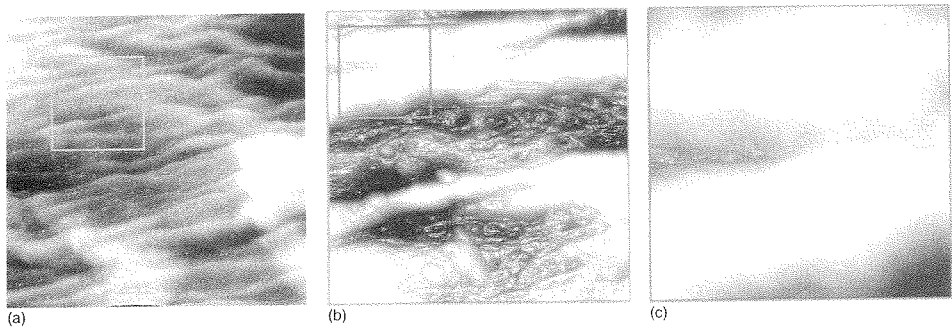


Fig. 47 Intermittent contact mode images of processed cotton fiber showing (a) a 6 μm scan with insert box magnified in (b) for 1.7 μm scan, and insert box there magnified in (c) for 530 nm scan. Longitudinal fiber axis runs from left to right.

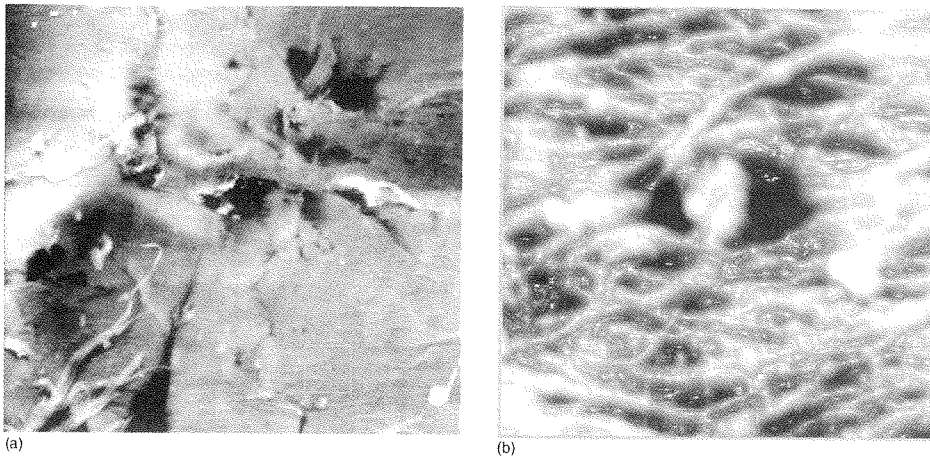


Fig. 48 Recycled (old newsprint) fiber as imaged in air operated in intermittent contact mode at (a) a 15 μm scan, with the 1.6 μm box reimaged in (b). Microfibrils, as well as contaminants, are clearly defined.

destroy image quality [334]. The problem of undesirable force interactions was circumvented by Weisenhorn et al. [350] and Hansma et al. [118]. Hansma et al [118] submersed DNA samples in liquid to acquire extremely high resolution images. Weisenhorn et al. [350] showed that immersion in liquid reduced the tip-off forces by a factor of approximately 100. Although liquid submersion produces high resolution images, the technique has several disadvantages with regard to sample adhesion, contaminants, and cantilever–liquid interactions.

Hanley et al. [114] were among the first researchers to obtain extremely high resolution of *Valonia* cellulose. The researchers were able to resolve the glucose repeating distance on the cellulose surface by imaging in air. By contrast, these images were inferior in resolution compared with recent work by Baker [11] and Baker et al. [12,13]. These recent publications relied on high magnification aqueous (water and propanol) contact mode AFM to image native *Valonia* cellulose I microcrystals (Fig. 49). The AFM images were able to resolve both the intermolecular spacing of 0.5–0.6 nm between the cellulose chains (depending on the crystal face) and the glucose subunit interval of 0.52 nm along individual chains, shown in Figs. 50a and 50b, respectively.

The high levels of magnification have also led to the physical identification of the various phases of the cellobiose unit. The AFM image shown in Fig. 51 shows cellulose chains of *Valonia*, with confirmation of the cellobiose unit achieved with Fourier transforms of the section data. Baker et al. [12] showed that the diagonal arrangement present in Fig. 51, due to the presence of a large O-6 hydroxymethyl group on the O-5–C-5 face of the glucose ring, is indicative of the I_a (triclinic) structure. The chains would have been in a more staggered arrangement if they were oriented in a I_β (monoclinic) structure [7,313]. Figure 51 shows evidence of the I_a (triclinic) structure over localized regions of the surface. Recent images have shown that this I_a phase exists over large areas of the surface and that the precise crystal face can be determined [13]. One of the most distinctive aspects of this work

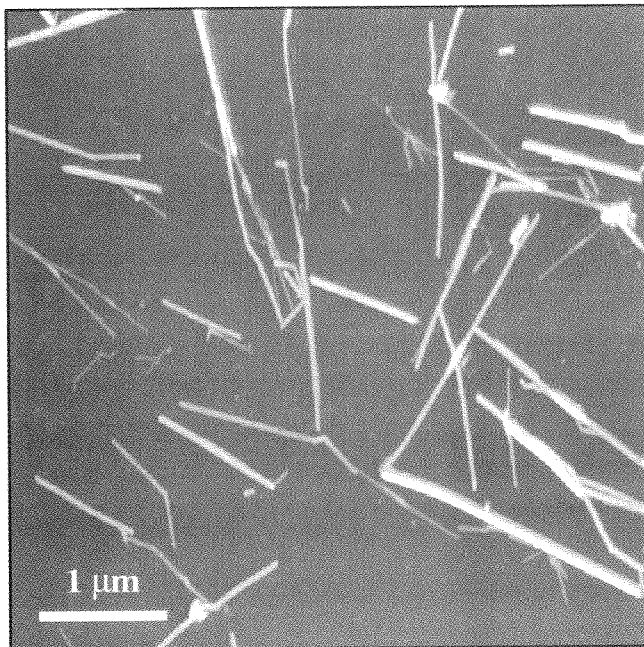


Fig. 49 A typical contact mode topographic image of microcrystals of *Valonia* cellulose immersed in propanol. The long straight microcrystals have a cross section of approximately 20×20 nm, although some are much smaller but still easily distinguished in the AFM. (From Ref. 11.)

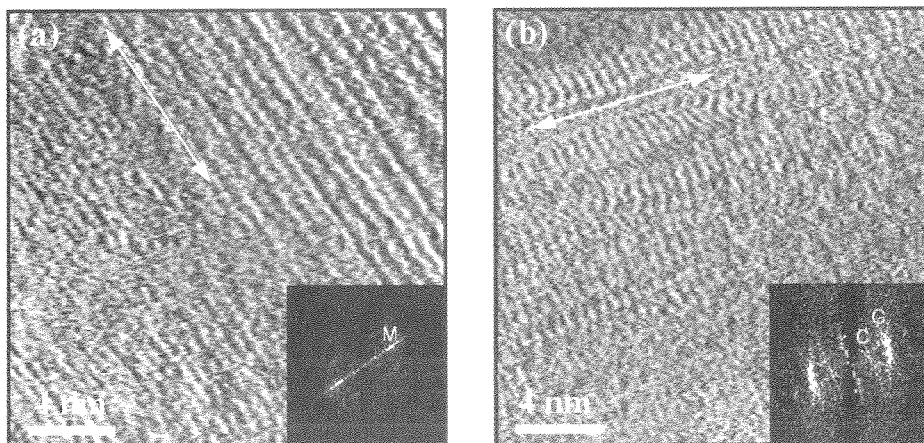


Fig. 50 (a) Contact mode deflection image showing molecules of cellulose aligned parallel to the double-headed white arrow. The spacing between the molecules is approximately 0.6 nm, and indicated by the M in the Fourier transform (insert). (b) An image showing the 0.5 nm glucose subunit interval along the chains. The Fourier transform shows both the glucose (G) and cellobiose (C) intervals of 0.52 and 1.04 nm, respectively. (From Ref. 11.)

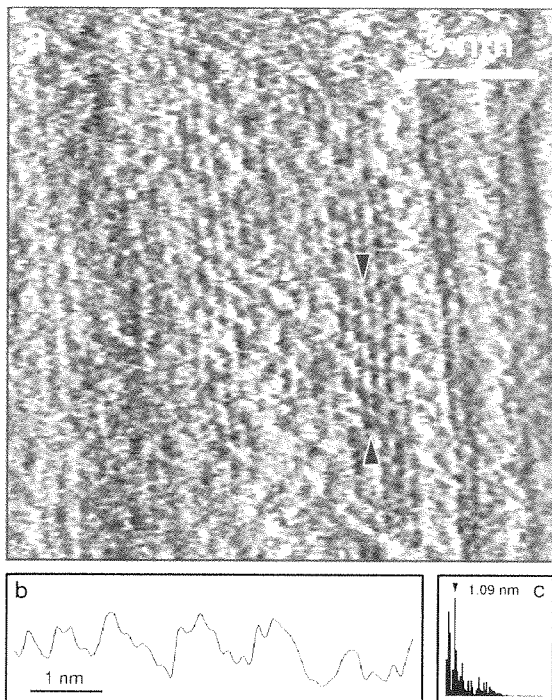


Fig. 51 (a) Contact mode deflection image of the *Valonia* cellulose surface immersed in propanol. The cellulose chains run almost vertically in the image. The line section in (b) has been taken between the two arrows in (a) and shows that the spacing between the bright spots is 1.09 nm—the cellobiose interval. This measurement is shown in the Fourier transform in (c), taken along the line profile. The features along the molecules are arranged *diagonally* to the chain direction between adjacent molecules. This is characteristic of the I_a (triclinic) phase of cellulose I and is seen most clearly in the region near the two arrows. (From Ref. 11.)

was the achievement of the highest resolution AFM imaging of a biological specimen.

High resolution AFM images of structural cellulosic fibers are more limited than those for *Valonia*. A liquid cell filled with double-distilled water was used to image the microfibrils shown in Fig. 52 [256]. The individual microfibrils are of native cotton with the cuticle removed and are of sufficient detail to show individual crystallites. Hanley and Gray [115] were the first authors to image wood fibers in a liquid cell (deionized water) showing the microfibrils of an unbleached beaten kraft pulp fiber in an approximately $1.4 \times 1.4 \mu\text{m}$ scan. A subsequent image of unbleached beaten kraft pulp by Hanley and Gray [116] is shown in Fig. 53. The scan size is approximately $250 \times 250 \text{ nm}$ and shows a marked increase in image quality.

Vertical resolution of AFMs are in fractions of angstroms. Lateral resolution, regardless of operating mode or imaging medium, is based on two factors: step size and tip radius. The step size is controlled by the user, with smaller scan sizes resulting in greater lateral resolution. The radius of commercially produced tips can vary widely, but the tips generally possess a curvature of radius of 5–50 nm. Silicon (intermittent contact) tips are at the lower end of the curvature scale, whereas silicon

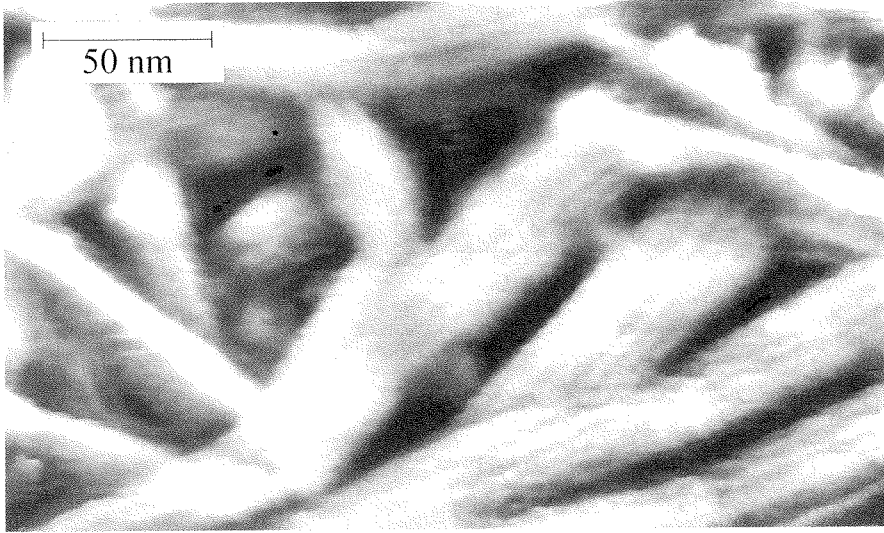


Fig. 52 Cellulose microfibrils of a cotton fiber treated with 6% NaOH at 51°C and subsequently rinsed in acetic acid and acetone. This high magnification image was produced by conducting the intermittent contact in a liquid cell filled with double-distilled water. (Courtesy of T. C. Pesacreta and B. Triplett.)

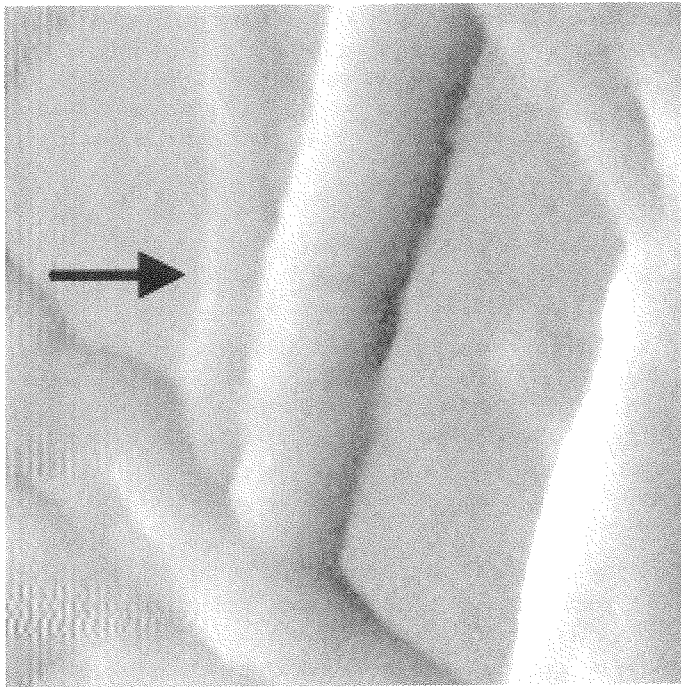


Fig. 53 AFM image of microfibrillar material produced by beating unbleached kraft fibers dried down on a glass surface. The arrow, 50 nm long, points to an element with a measured height of only 2 nm. (From Ref. 116.)

nitride (contact) tips are at the higher end. The lateral resolution of an AFM with the sharpest commercially produced tips is around 10–20 Å. Resolution limits based on tip radius have been expanded with the advent of microfabricated tips, either through adhesively attached nanotubes [58] or by carbon deposition in an SEM [162]. An example of the resolution capabilities of a commercially produced tip is shown in Fig. 54, which shows oxygen atoms imaged in intermittent contact (air) mode on the surface of freshly cleaved mica.

Surface Feature Quantification Surface and profile studies of cellulosic fibers require some degree of objectivity for valid statistical comparisons to be drawn, and this is accomplished through collection and analysis of quantifiable data. The AFM is ideally suited for this as the collected data are simply an x - y - z array of tip location. This array can then be analyzed quantitatively by using a series of algorithms that display specific morphometric details as well as overall surface topography.

Morphology Routine application of the AFM in surface morphometry has been carried out primarily in the field of polymer science to quantify features from banded polymer texture [89] to contact angles [163]. The application of morphometric algorithms to cellulosic fibers has been less forthcoming, its usefulness generally restricted to characterization of nanostructure and three-dimensional features.

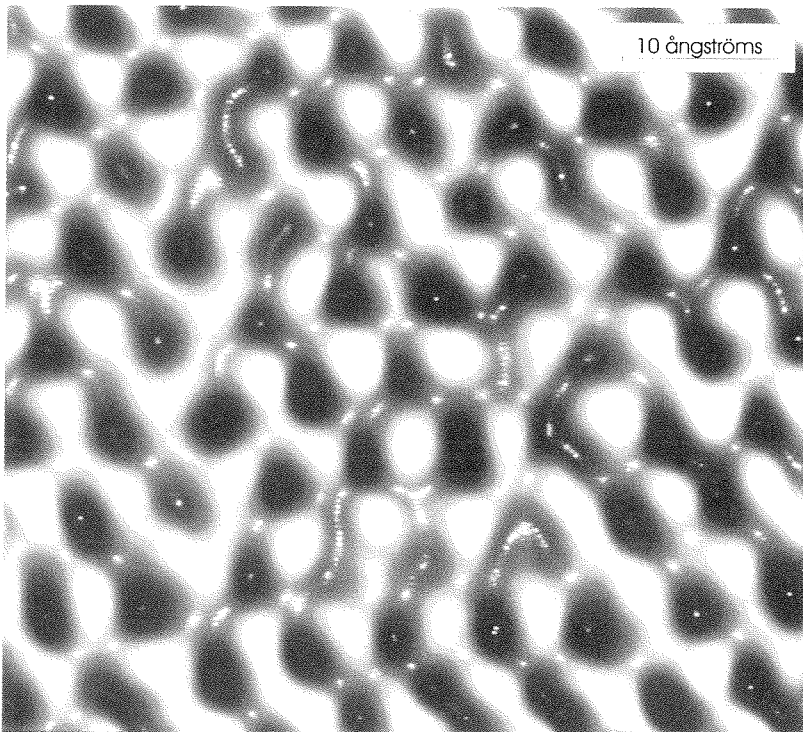


Fig. 54 AFM image (height data, intermittent contact mode) showing a 5 nm scan of an oxygen lattice on freshly cleaved mica. (Courtesy of T. C. Pesacreta.)

Nanostructure characterization is generally conducted with an algorithm referred to as a section analysis, which produces a two-dimensional profile along a user-defined digital slice. This algorithm is demonstrated in Fig. 55 for a loblolly pine fiber previously described in Fig. 44b.

Although this section analysis algorithm yields additional information regarding surface roughness, a section analysis generally depicts two-dimensional topography along with dimensions of specific features. In this case, the analysis shows that the microfibril between the vertical arrows has a diameter of 117 nm.

Another application of morphometric analysis to cellulosic fibers is the three-dimensional aspect of the fibers under investigation. Figure 56 shows AFM height images of an unbeaten, unbleached kraft pulp fiber taken during a hydration and dehydration series. The height images look identical in both the hydrated and dehydrated states even though the cell wall dimensions have changed. This change in cell wall dimensions can be seen in the section analysis (Fig. 57), which then allows us to quantitatively assess the effect of moisture on such changes.

Surface Roughness Of primary importance in the study of wood-fiber-based composites is the bond energy that is established between individual wood fibers. Fiber-fiber bond strength is generally estimated in the pulp and paper industry by several methods that evaluate the internal bond strength of paper and paperboards (Chapter 15, Vol. 1). These techniques are summarized by Koubaa and Koran [176]. The bulk of these tests measure the splitting resistance of paper or paperboard to a force applied normal to its plane [298,299]. These techniques determine bulk properties,

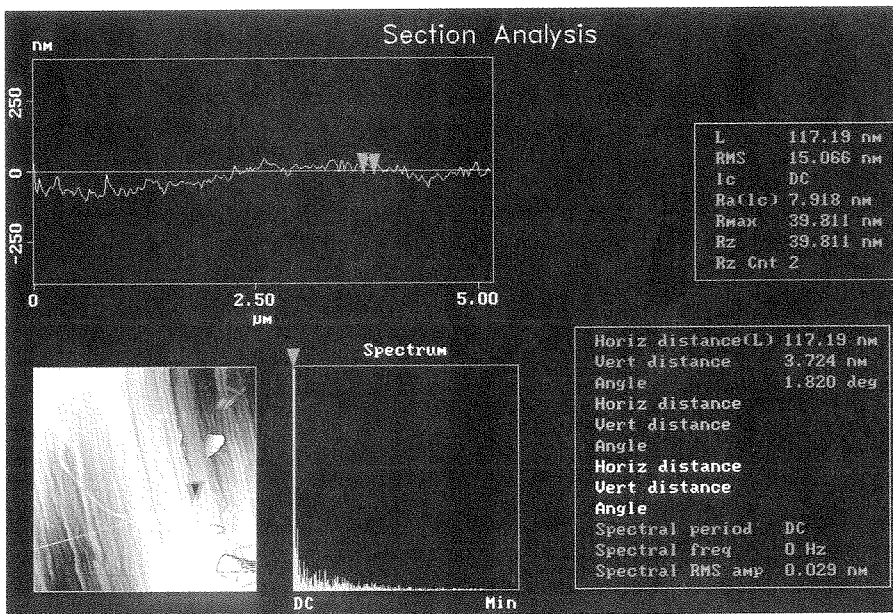


Fig. 55 Section analysis of the S2 layer of a macerated loblolly pine latewood fiber. The primary wall, S1, and a portion of the S2 layer were physically removed with a microknife and forceps. The section analysis shows a cross-sectional view (upper left) of height data from a user-defined segment (lower left) oriented perpendicular to the microfibril direction.

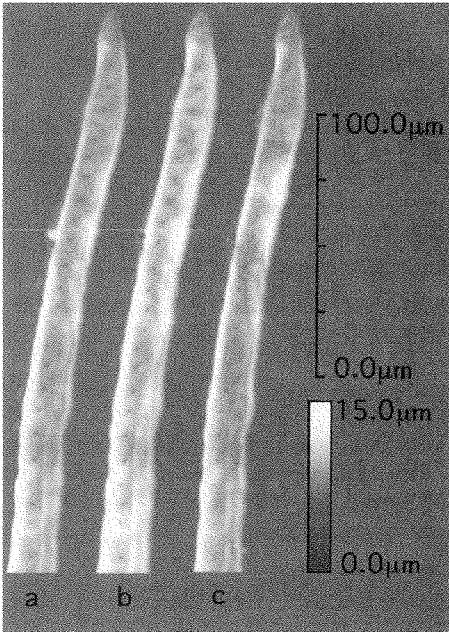


Fig. 56 AFM images of an unbeaten, unbleached kraft pulp fiber. The same fiber was imaged at ambient room conditions in air (a) after being allowed to dry down onto a glass cover slip. The fiber was then imaged in deionized water (b) in a liquid cell. The fiber was allowed to dry in ambient room conditions and imaged again (c). Each of the fiber images shown is a montage of four AFM images. The images are shown in the height mode with the x , y scale indicated by the upper bar and the height information indicated by the lower bar. (From Ref. 116.)

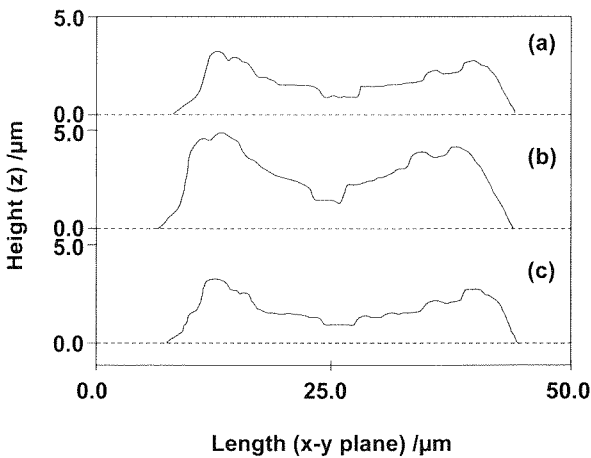


Fig. 57 Section profiles perpendicular to the same position on the fiber axis of the fiber shown in Fig. 56. Conditions for (a), (b), and (c) are the same as for Fig. 56. Note that the z scale is twice the width scale. (From Ref. 116.)

so they yield little information on individual fiber–fiber bonding energies. An analogous situation is trying to measure individual fiber mechanical properties by hand-sheet properties such as zero-span testing (Chapters 7 and 14, Vol. 1).

Bond strengths within fiber networks are a function of the “effective external surface area” [46]. Fiber surface area has been determined in a myriad of manners including pulp permeability to the flow of water or air, stock freeness, and sorption of liquid nitrogen [46]. However, none of these techniques have been able to quantify the surface roughness of individual cellulose fibers, which presents an opportunity for the AFM to provide data that will fill this void in the literature.

Currently there exist only two studies on evaluation of the surface roughness of cellulosic fibers using an AFM. Karlsson et al. [158] evaluated the surface roughness of cotton and wood fiber surfaces and found that there was a strong relationship, with favorable interphases in cellulose fiber–polymer composites. Pesacreta et al. [256] conducted a much more thorough study, focusing on the effect of cuticle removal of cotton fibers as determined by the surface roughness. Cotton fibers were evaluated in the AFM before and after removing the cuticle (Figs. 58 and 59). The surface roughness of the virgin and treated fibers were characterized on the basis of the following analyses: root-mean-square (RMS), spectral density, and fractal. RMS is the square of the deviations of height data from the central plane, an RMS algorithm being analogous to the least squares method commonly employed in statistics. Spectral density is extracted from a Fourier transform analysis and generally employs some type of graphic representation of feature distributions. The analysis reveals periodic surface features that might otherwise appear random. Pesacreta et al. [256] also employed the analysis of fractals, which relies on surface “self-similarity” over a wide range of scales of magnification [95]. Fractals are based on a numerical algorithm that evaluates the surface’s geometrical complexity as determined by an iterative approach relating fractal cell size and frequency. A more detailed explanation of fractals can be found in Mandelbrot et al. [199].

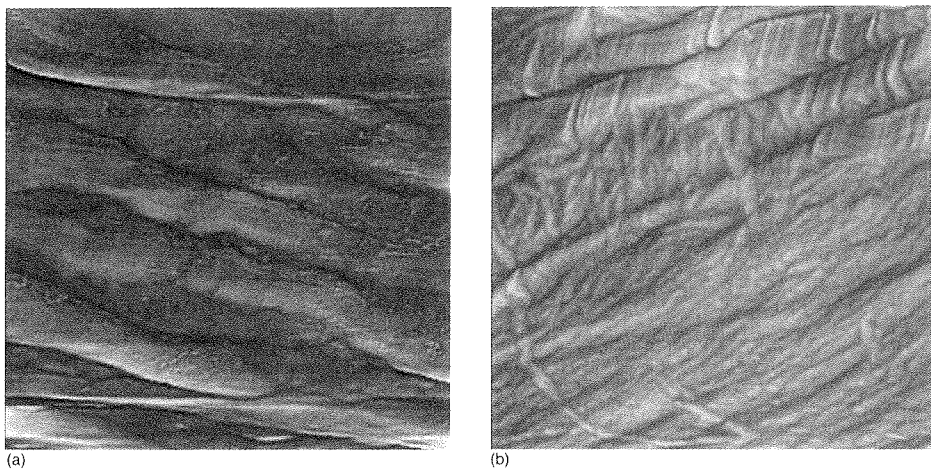
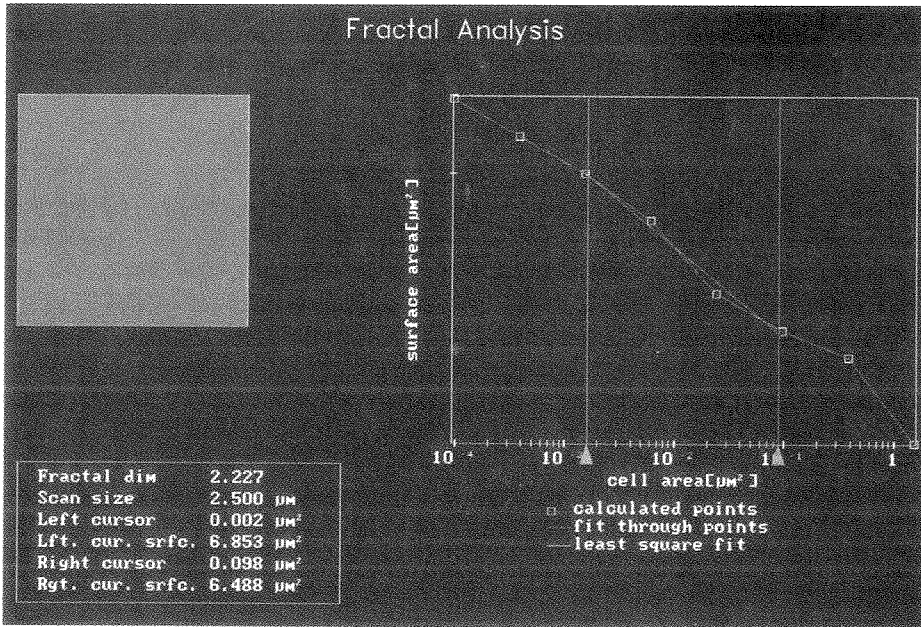
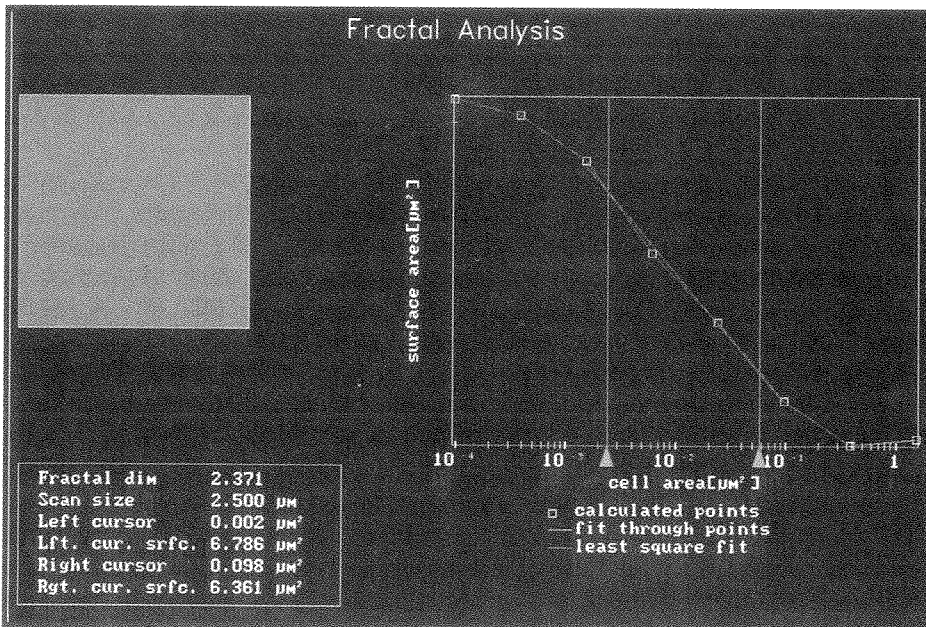


Fig. 58 AFM intermittent contact mode 2.5 μm scans of (a) untreated cotton fiber and (b) cotton fiber with the cuticle removed by an Updegraff reagent. (From Ref. 256.)



(a)



(b)

Fig. 59 A fractal analysis of the cotton fibers in Fig. 58, with (a) an untreated fiber and (b) a fiber with the cuticle removed. The primary number of importance is the fractal dimension, with the lower number expressing a "rougher" surface. (From Ref. 256.)

Pesacreta et al. [256] found that surface roughness increased as a result of removing the cuticle and that the RMS method was the least sensitive to surface roughness and fractals the most sensitive. It should be noted that this was not the first time fractals were applied to wood fiber research. A fractal analysis was conducted by Weise [349] to quantify fiber wrinkling with the CLSM.

Nanomechanical Properties Most AFMs now have the capability to monitor forces applied to the surface of specimens and, coupled with tip displacement data, are able to produce plots of force versus sample deformation. There are two general methods for ascertaining the surface moduli. One method applies displacements to the specimen surface and infers the force from the spring constant of the cantilever [127]. This is the most common method for force modulation, because no machine modifications are necessary and it allows the user to create a modulation map of the specimen surface. The operator does need the spring constant of the cantilever, either from the manufacturer or through calibration such as the technique described by Hutter and Bechhoefer [133]. A second force modulation method [146] probes the surface with known forces rather than displacements, allowing for absolute determination of contact compliance. This method eliminates erroneous readings due to secondary attractive or repulsive forces. The method indents the surface and is thus destructive, allowing only point location values for hardness and stiffness.

The second force modulation method was used in the only extensive studies of nanomechanical properties of wood fibers that have been carried out [362,363]. Wimmer and coworkers determined the stiffness and hardness values of the S2 layer and the corner middle lamella of red spruce (*Picea rubens* Sarg.). The studies showed that the modulus of elasticity of the S2 layer was approximately twice that of the corner middle lamella (Fig. 60).

As mentioned previously, the nanoindentation method of force modulation allows point location values of hardness and stiffness to be determined but does not allow for surface mapping. The reduction in accuracy of the stiffness mapping method of force modulation is compensated for by the vast number of data points and the ability to compare mechanical properties of surface features. However, the applicability of the force modulation technique in wood and fiber science is limited because of its inability to distinguish materials of similar stiffness. Figure 61 shows a surface stiffness map obtained by force modulation of a cross-sectional loblolly pine specimen of the latewood band in the 32nd growth ring. Distinctions in moduli are not realized owing to the relative similarity in stiffnesses across the cross-sectional area. Wimmer and Lucas [362] found that the S2 layer was only 2.9 times as stiff as the cell corner middle lamella. Although unable to adequately distinguish between the middle lamella and the primary/secondary walls, force modulation was able to accentuate fibrillar disruptions otherwise concealed and thus may be more useful for evaluating local disruptions.

Material Interactions and Compatibility One of the newest applications of the AFM makes use of its ability to detect subtle changes in the vertical and lateral forces that act on the cantilever tip in response to changes in chemical and physical surface composition. The most prominent and, to the pulp and paper industry, most useful of these applications are described in detail in the following paragraphs.

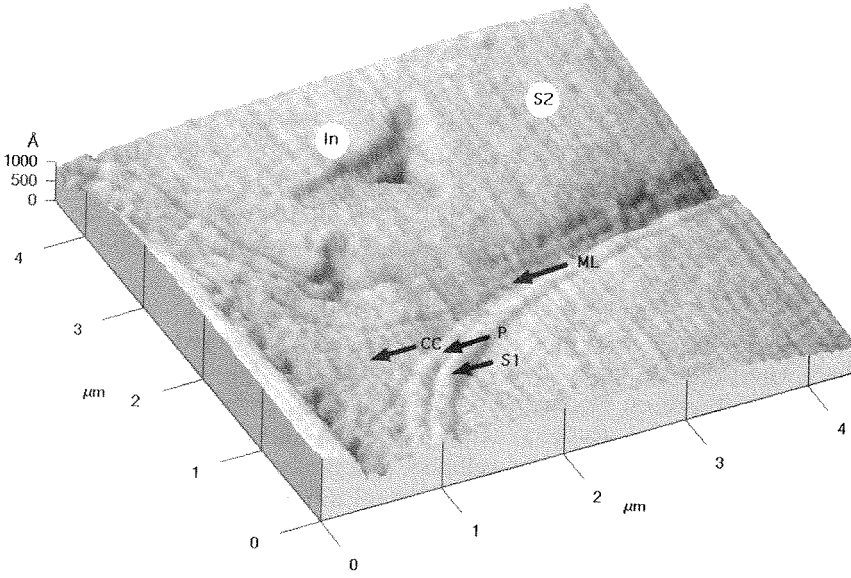


Fig. 60 Nanoindentation of spruce, where In = indentation, S1 = S1 layer of the secondary cell wall, S2 = S2 layer of the secondary cell wall, P = primary cell wall, ML = middle lamella, and CC = cell corner middle lamella. (From Ref. 362.)

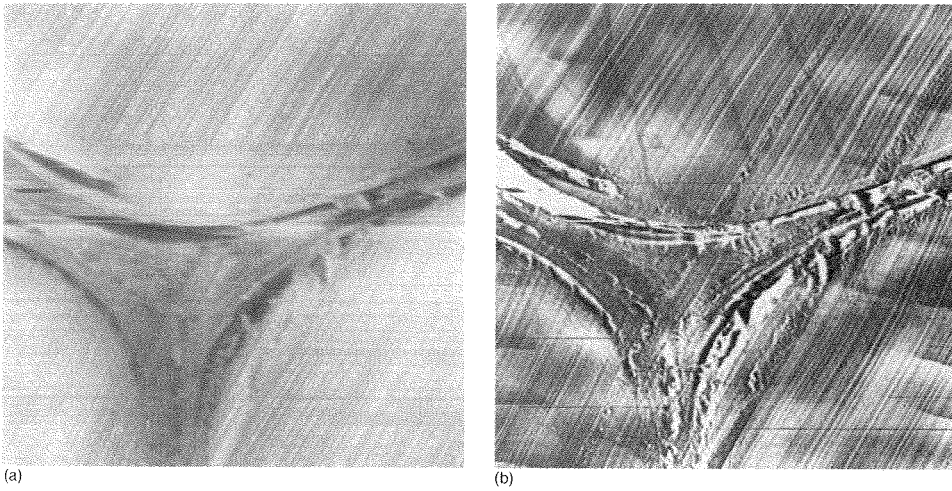


Fig. 61 Thirty-second growth ring of the latewood band of a loblolly pine specimen as shown by 17 μm scans. Diagonal lines are knife marks as a result of the hand sectioning. The cross-sectional view shows three thick-walled tracheids separated by a middle lamella, with the images displaying (a) height data and (b) force-modulation data.

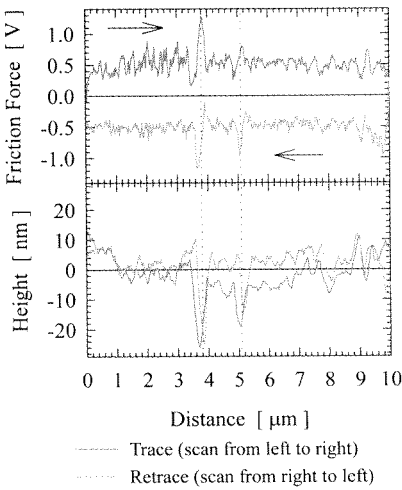


Fig. 64 Friction force and corresponding surface topography plotted as a function of sliding distance for two cellulose surfaces sliding past each other. (Courtesy of S. Zauscher.)

result when a cellulose-modified tip is scanned across the surface of a regenerated cellulose film. It is evident that the friction forces are correlated to surface topography. Frictional forces are dramatically reduced in the presence of water-soluble polymer solutions that are injected into the fluid cell of the AFM (Fig. 65). These results are directly applicable to papermaking processes in which the addition of water-soluble polymers is used to change pulp suspension rheology. It is clear that colloidal probe microscopy, applied to cellulosic systems, is a powerful tool; it may enhance through its access to nanonewton forces on nanometer length scales the understanding of friction between fibers, of particle retention on fibers, and of fiber bonding.

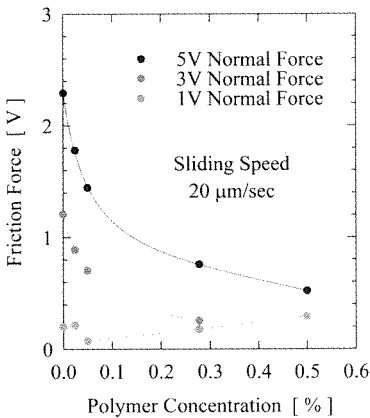


Fig. 65 Friction force between two cellulose surfaces plotted as a function of polymer concentration. (Courtesy of S. Zauscher.)

VII. CONCLUSIONS

For many of these different types of microscopy, but especially in the case of LTSEM and CLSM studies, it is biologists who have done the groundwork and so it is to their findings that one has to turn initially for information. Hence the large number of references in this chapter to papers in biological journals.

The choice of microscope is important, and the effects of preparative techniques have also to be borne in mind. Ultimately, the choice of microscopical technique depends on the material being examined and the resolution required. No single microscope is suitable for all purposes, and novel types of microscopes (i.e., CLSM, LTSEM, ESEM and AFM) do not replace the more traditional instruments, as evidenced by the fact that the established techniques continue to be used and new methods of microscopical examination are still being developed for them. Although the new microscopes open up all sorts of opportunities they should be regarded as being complementary to the older techniques.

Samples need to be examined under conditions closely related to their natural state, and optical microscopy is ideal for observing fully hydrated pulp and paper samples. Accurate evaluation of fiber morphology is not easy when fibers have undergone the dehydration processes required for electron microscopy. However, the resolution of the optical microscope is inadequate to reveal detailed structural information. The CLSM offers little improvement in resolution over the conventional optical microscope. Its main advantage lies in its unique ability to visualize cross-sectional views of samples by nondestructive optical sectioning. The LTSEM, ESEM, and AFM, on the other hand, all offer possibilities of examining the wet structure of pulp and paper at high resolution without the need for dehydration and embedding techniques but can image only surfaces.

All microscopical studies, by definition, enable examination of only very small areas of samples. They are also time-consuming. Thus speed of data collection is important because large amounts of data need to be collected for quantitative and statistical analysis. Microscopy has played a very important role in the past, and these new instruments, linked to image analysis systems, should ensure that it continues to be a necessary part of fiber and paper research in the future. In conclusion, the words of Emerton and Watts [82] of more than 40 years ago can be reiterated:

Progress in the field of fiber microscopy lies in the use of a prudent combination of the many techniques now available . . . rather than in the exclusive use of one technique.

ABBREVIATIONS

AD	air drying
AFM	atomic force microscope
BEI	backscattered electron imaging
BSE	backscattered electron
BSI	backscattered electron imaging
CFSM	confocal fluorescence scanning microscope
CLSM	confocal laser scanning microscope

CPD	critical point drying
CSM	confocal scanning microscope
CSOM	confocal scanning optical microscope
CTMP	chemithermomechanical pulp
EDS	energy-dispersive X-ray spectrometry
EDX	energy-dispersive X-ray
EDXA	energy-dispersive X-ray analysis
EM	electron microscope
ESEM	environmental scanning electron microscope
F	flatfield
FD	freeze-drying
FH	frozen hydrated
FPR, FRAP	fluorescence recovery after photobleaching
LSM	laser scanning microscope
LTSEM	low temperature scanning electron microscope
LVHRSEM	low voltage high resolution SEM
N.A.	numerical aperture
NSOM	near-field scanning optical microscopy
RBA	relative bonded area
REM	reflection electron microscope
SE	secondary electron
SEM	scanning electron microscope
SLM	scanning laser microscope
SOM	scanning optical microscope
STEM	scanning transmission electron microscope
STM	scanning tunnelling microscope
TCF	totally chlorine-free
TEM	transmission electron microscope
TMP	thermomechanical pulp
TSM, TSRLM	tandem scanning reflection light microscope
UV	ultraviolet

REFERENCES

1. Abitz, P., and Luner, P. (1989). The effect of refining on wet fiber flexibility and its relationship to sheet properties. In: *Fundamentals of Papermaking*, Vol. 1. C.F. Baker and V. W. Punton, eds. Mechanical Engineering Publications, London, pp. 67–86.
2. Alexander, S. D., Marton, R., and McGovern, S. D. (1968). Effect of beating and wet pressing on fiber and sheet properties. 1. Individual fiber properties. *Tappi* 51(6):277–283.
3. Amboss, K., Emerton, H. W., and Walls, J. (1954). A new approach to the electron microscopy of fibers. *Proc. Tech. Sect. BPBMA* 35(3):487–510.
4. Asunmaa, S. K. (1966). The fiber wall, microfibrils, and interfaces at electron microscopic resolution. *Tappi* 49(7):319–324.
5. Asunmaa, S. K., and Marteny, W. W. (1963). Morphology of refined pulps of southern pine (longleaf pine) and black ash. *Tappi* 46(10):613–622.
6. Asunmaa, S. K., and Steenberg, B. (1958). Beaten pulps and the fiber-to-fiber bond in paper. *Svensk Papperstidn.* 61(18B):685–695.

7. Atalla, R. H., and VanderHart, D. L. (1984). Native cellulose: A composite of two distinct crystalline forms. *Science* 223:283–285.
8. Attree, S. M., and Sheffield, E. (1984). Scanning electron microscopy of protoplasts isolated from gametophytes of the fern *Pteridium*. I. Preparative methods. *Micron Microsc. Acta* 15(3):181–186.
9. Bailey, I. W. (1938). Cell wall structure of higher plants. *Ind. Eng. Chem.* 30(1): 411–417.
10. Bailey, I. W., and Kerr, T. (1935). The cambium and its derivative tissues. X. Structural, optical properties and chemical composition of the so-called middle lamella. *J. Arnold Arboretum* 16:273–300.
11. Baker, A. A. (1998). High resolution atomic force microscopy of polysaccharides. Ph.D. Thesis, University of Bristol, U.K.
12. Baker, A. A., Helbert, W., Sugiyama, J., and Miles, M. J. (1997). High resolution atomic force microscopy of native *Valonia cellulose* I microcrystals. *J. Struct. Biol.* 119(2):129–138.
13. Baker, A. A., Helbert, W., Sugiyama, J., and Miles, M. J. (1998). Surface structure of native cellulose microcrystals by AFM. *Appl. Phys. A—Mat.Sci.Process.* 66(PtISS):S559–S563.
14. Batchelor, W. J., Conn, A. B., and Parker, I. H. (1997). Measuring the fibril angle of fibers using confocal microscopy. *Appita* 50(5):377–380.
15. Beckett, A., and Read, N. D. (1986). Low-temperature scanning electron microscopy. In: *Ultrastructure Techniques for Microorganisms*. H. C. Aldrich and W. J. Todd, eds. Plenum Press, New York, pp. 45–86.
16. Béland, M.-C. (1996). CLSM and AFM applied in pulp and paper research. A literature review. IOF-Tech. Rep. TR 312, Inst. Opt. Res., Stockholm, Sweden, 18 p.
17. Béland, M.-C., and Mangin, P. J. (1995). Three-dimensional evaluation of paper surfaces using confocal microscopy. In: *Surface Analysis of Paper*. T. E. Conners and S. Banerjee, eds. CRC Press, Boca Baton, FL, pp. 1–40.
18. Bergander, A., and Salmén, L. (1997). Lamellar cracks, do they appear during radial compression of wood? *Nordic Pulp Paper Res. J.* 12(4):216–219.
19. Bergh, N. O., and Thomlin, W. H. (1976). Practical aspects of paper/liquid interaction during paper coating. In: *The Fundamental Properties of Paper Related to Its Uses*, Vol. 2. F. Bolam, ed. British Paper and Board Industry Fed., London, pp. 496–510.
20. Binnig, G., Quate, C. F., and Gerber, Ch. (1986). Atomic force microscope. *Phys. Rev. Lett.* 56(9):930–933.
21. Binnig, G., and Rohrer, H. (1982). Scanning tunneling microscopy. *Helv. Phys. Acta* 55(6):726–735.
22. Binnig, G., Rohrer, H., Gerber, Ch., and Weibel, E. (1982). Surface studies by scanning tunneling microscopy. *Phys. Rev. Lett.* 49(1):57–61.
23. Blanchette, R. A., Akhtar, M., and Attridge, M. C. (1992). Using Simons stain to evaluate fiber characteristics of biomechanical pulps. *Tappi J.* 75(11):121–124.
24. Blonk, J. C. G., Don, A., Van Aalst, H., and Birmingham, J. J. (1993). Fluorescence photobleaching recovery in the confocal scanning light microscope. *J. Microsc.* 169(3):363–374.
25. Borchardt, J. K., Matalamaki, D. W., Lott, V. G., and York, G. A. (1994). Deinking of toner ink containing furnishes. Part 2. Deinking with mechanical cleaners. *Prog. Paper Recycl.* 4(1):44–56.
26. Boutelje, J., and Eriksson, I. (1984). Analysis of lignin in fragments from thermo-mechanical spruce pulp by ultraviolet microscopy. *Holzforschung* 38:249–252.
27. Bown, R. (1997). A review of the influence of pigments on papermaking and coating. In: *The Fundamentals of Papermaking Materials*, Vol. 1. C. F. Baker, ed. Pira International, Leatherhead, U.K., pp. 83–137.

28. Boyde, A. (1974). Freezing, freeze-fracturing and freeze-drying in biological specimen preparation for the SEM. In: *Scanning Electron Microscopy*. O. Johari and I. Corvin, eds. IIT Res. Inst., Chicago, pp. 1043–1046.
29. Boyde, A. (1978). Pros and cons of critical point drying and freeze drying for SEM. In: *Scanning Electron Microscopy/II*. O. Johari and I. Corvin, eds. IIT Res. Inst., Chicago, pp. 303–314.
30. Boyde, A., and Franc, F. (1981). Freeze-drying and shrinkage of glutaraldehyde fixed liver. *J. Microsc.* 122:75–86.
31. Browne, T. C., Crotogino, R. H., and Douglas, W. J. M. (1995). The effect of paper structure on behavior in a calender nip. *J. Pulp Paper Sci.* 21(10):J343–J347.
32. Buchanan, J. G., and Lindsay, R. A. (1962). Structure of paper as revealed by the scanning electron microscope. In: *Formation and Structure of Paper*. Vol. 1. F. Bolam, ed. British Paper and Board Makers' Assn., London, pp. 101–117.
33. Buchanan, J. G., and Washburn, O. V. (1962). The surface and tensile fractures of chemical fiber handsheets as observed with the scanning electron microscope. *Pulp Paper Mag. Can.* 63(10):T485–T493.
34. Buchanan, J. G., and Washburn, O. V. (1964). The surface and tensile fractures of groundwood handsheets as observed with the scanning electron microscope *Pulp Paper Mag. Can.* 65(2):T52–T60.
35. Bucher, H. (1958). Discontinuities in the microscopic structure of wood fibers. In: *Fundamentals of Papermaking Fibers*. F. Bolam, ed. British Paper and Board Makers' Assn., Kenley, England, pp. 7–34.
36. Buetow, D. E. (1968). *The Biology of Euglena*. Academic Press, New York.
37. Burgess, J., Linstead, P. J., and Harnden, J. M. (1977). The interpretation of scanning electron micrographs. *Micron* 8:181–191.
38. Butterfield, B. G., and Meylan, B. A. (1980). *Three-dimensional Structure of Wood. An Ultrastructural Approach*. Chapman and Hall, London.
39. Campbell, W. B. (1933). The cellulose-water relationship in paper-making. Forest Service Bulletin 84, Department of the Interior, Canada.
40. Carlsson, G., Lindström, T., and Söremark, C. (1978). Expression of water from cellulosic fibers under compressive loading. In: *Fiber-Water Interactions in Paper-Making*, Vol. 1. Fundamental Research Committee, ed. British Paper and Board Industry Fed., London. pp. 389–402.
41. Catling, D., and Grayson, J. (1982). *Identification of Vegetable Fibers*. Chapman and Hall, London.
42. Centonze, V., and Pawley, J. (1995). Tutorial on practical confocal microscopy and use of the confocal test specimen. In: *Handbook of Biological Confocal Microscopy*. J. B. Pawley, ed. Plenum Press, New York, pp. 549–569.
43. Chapman, J. A., and Menter J. W. (1954). A study of the shape, surface structure and frictional wear of fibers by reflection electron microscopy. *Proc. Roy. Soc. (Lond.), Ser. A* 226:400–407.
44. Christiani, C., and Bristow, A. (1995). The drying mechanisms of water-borne printing inks. Proc. 47th TAGA Conf., pp. 231–227.
45. Clark, J. d'A. (1943). The nature of hydration and fiber bonding. *Proc. Tech. Sect. BPBMA* 24:30–54.
46. Clark, J. d'A. (1978). Surface measurements. In: *Pulp Technology and Treatment for Paper*. Miller Freeman, San Francisco, pp. 533–540.
47. Clarke, B. (1972). Furnish blend optimization and evaluation. *Papermaker* 165(4):41.
48. Cogswell, C. J. (1995). Imaging immunogold labels with confocal microscopy: In: *Handbook of Biological Confocal Microscopy*. J. B. Pawley, ed. Plenum Press, New York, pp. 507–512.
49. Comer, J. J., Stetson, H. W., and Lyons, S. C. (1955). A new replica technique for making electron micrographs of surfaces of paper sheets. *Tappi* 38(10):620–624.

50. Coppick, S., and Fowler, W. F. (1939). The location of potential reducing substances in woody tissue. *Paper Trade J.* 109 (Sept. 14):TS135–TS140.
51. Core, H. A., Côté, W. A., and Day, A. C. (1979). *Wood Structure and Identification*. Syracuse Wood Sci. Ser. 6. Syracuse Univ. Press, Syracuse, NY.
52. Côté, W. A. (1967). *Wood Ultrastructure—An Atlas of Electron Micrographs*. Univ. Washington Press, Seattle.
53. Côté, W. A. (1970). The ultrastructural organization of wood and wood fibers. In: *Physics and Chemistry of Wood Pulp Fibers*. D. H. Page, ed. STAP Ser. No. 8, TAPPI, Atlanta, GA, pp. 1–18.
54. Côté, W. A. (1980). *Papermaking Fibers. A Photomicrographic Atlas*. Syracuse Univ. Press, Syracuse, NY.
55. Côté, W. A., Koran, Z., and Day, A. C. (1964). Replica techniques for electron microscopy of wood and paper. *Tappi* 47(8):477–484.
56. Cox, G. (1995). Mass storage and hard copy. In: *Handbook of Biological Confocal Microscopy*. J. B. Pawley, ed. Plenum Press, New York, pp. 535–548.
57. Crosby, C. M., and Mark, R. E. (1974). Precise S_2 angle determination in pulp fibers. *Svensk Papperstidn.* 77:636–642.
58. Dai, H., Hafner, J. H., Rinzler, A. G., Colbert, D. T., and Smalley, R. E. (1996). Nanotubes as nanoprobe in scanning probe microscopy. *Nature* 384:147–150.
59. Danilatos, G. D. (1993). Introduction to the ESEM instrument. *Microsc. Res. Techn.* 25:354–361.
60. Danilatos, G. D. (1993). Bibliography of environmental scanning electron microscopy. *Microsc. Res. Techn.* 25:529–534.
61. Davies, G. W. (1966). Optical and electron microscopy of NSSC pulps. *Appita* 19(4):95–110.
62. Davies, G. W. (1966). Optical and electron microscopy of paper made from chemical pulps. *Appita* 20(1):21–30.
63. Davies, G. W. (1968). A microscopic study of paper made from *Pinus radiata*. *Tappi* 51(10):454–461.
64. DeNee, P. B., and Abraham, J. L. (1976). Backscattered electron imaging (application of atomic number contrast). In: *Principles and Techniques of Biological Applications*, Vol. 5. M. A. Hayat, ed. Van Nostrand Reinhold, New York, pp. 144–180.
65. Dennis, D. T., and Colvin, J. R. (1964). Biosynthesis of cellulose. *Pulp Paper Mag. Can.* 65(9):T395–T399.
66. de Silveira, G., Forsberg, P., and Conners, T. (1995). Scanning electron microscopy. A tool for analysis of wood pulp fibers and paper. In: *Surface Analysis of Paper*. T. E. Conners and S. Banerjee, eds. CRC Press, Boca Raton, FL, pp. 41–71.
67. de Silveira, G., Zhang, X., Berry, R., and Wood, J. R. (1996). Location of fines in mechanical pulp handsheets using scanning electron microscopy. *J. Pulp Paper Sci.* 22(9):J315–J320.
68. Dixon, A. E., and Cogswell, C. (1995). Confocal microscopy with transmitted light. In: *Handbook of Biological Confocal Microscopy*. J. B. Pawley, ed. Plenum Press, New York, pp. 479–487.
69. Dixon, A. E., Damaskinos, S., and Atkinson, M. R. (1991). A scanning confocal microscope for transmission and reflection imaging. *Nature* 351:551.
70. Dixon, A. E., Damaskinos, S., Ribes, A., and Beesley, K. M. (1995). A new confocal scanning beam laser MACROscope using a telecentric, f-theta laser scan lens. *J. Microsc.* 178(3):261–266.
71. Dlugosz, J. (1965). The fine structure of cotton fiber as revealed by swelling during methacrylate embedding. *Polymer* 6(8):427–436.
72. Ducker, W. A., Senden, T. J., and Pashley, R. M. (1992). Measurement of forces in liquids using a force microscope. *Langmuir* 8:1831–1836.

73. Dunlop, W. F., and Robards, A. W. (1972). Some artifacts of the freeze-etching technique. *J. Ultrastruct. Res.* 40:391-400.
74. Dwivedi, A. K., and Ahmad, K. J. (1985). Scanning electron microscopy of fresh, uncoated plant parts. *Micron Microsc. Acta* 16(1):55-57.
75. Echlin, P. (1971). The examination of biological material at low temperatures. In: *Scanning Electron Microscopy*/I O. Johari and I. Corvin, eds. IIT Res. Inst., Chicago, pp. 225-232.
76. Echlin, P., Paden, R., Dronzek, B., and Wayte, R. (1970). Preparation of labile biological material for examination in SEM. In: *Scanning Electron Microscopy*. O. Johari and I. Corvin, eds. IIT Res. Inst., Chicago, p. 307.
77. Elton, N. J., Hooper, J. J., and Gane, P. A. C. (1990). Optical microscopy of paper. Methodology and applications. Proc. 24th EUCEPA Conf., Stockholm, pp. 438-458.
78. Emerton, H. W. (1957). *Fundamentals of the Beating Process*. British Paper and Board Industry Assoc., Kenley, England.
79. Emerton, H. W. (1958). The outer secondary wall. 1. Its structure. In: *Fundamentals of Papermaking Fibers*. F. Bolam, ed. British Paper and Board Makers' Assoc., Kenley, England, pp. 35-54.
80. Emerton, H. W., Page, D. H., and Hale, W. H. (1962). The structure of papers as seen in their surfaces. In: *Formation and Structure of Paper*. Vol. 1. F. Bolam, ed. British Paper and Board Makers' Assoc., London, pp. 53-99.
81. Emerton, H. W., Page, D. H., and Watts, J. (1956). The uses of solid replicas for studying fiber and paper surfaces. *Proc. Tech. Sect. BPBMA* 37(1):105-125.
82. Emerton, H. W., and Watts, J. (1953). Examination of spruce tracheids under polarized vertical illumination. *Proc. Tech. Sect. BPBMA* 34(2):269-287.
83. Enomae, T., Onabe, F., and Usuda, M. (1993). Application of new profilometry using topographic scanning electron microscope to paper surface topography. *Tappi J.* 76(1):85-90.
84. Eriksson, I., Lidbrandt, O., and Westermark, U. (1988). Lignin distribution in birch (*Betula verrucosa*) as determined by mercurization with SEM- and TEM-EDXA. *Wood Sci. Technol.* 22:251-257.
85. Eveling, D. W., and McCall, R. D. (1983). An evaluation of methods for preparing easily damaged cuticular surfaces of plants for SEM. *J. Microsc.* 129(2):113-122.
86. Fengel, D. (1970). The ultrastructural behavior of cell wall polysaccharides. In: *Physics and Chemistry of Wood Pulp Fibers*. D. H. Page, ed., STAP Ser. No. 8. TAPPI, Atlanta, GA, pp. 74-99.
87. Fergus, B. J., Procter, A. R., Scott, J. A. N., and Goring, D. A. I. (1969). The distribution of lignin in sprucewood as determined by ultraviolet microscopy. *Wood Sci. Technol.* 3(2):117-138.
88. Fernández-Morán, H. (1960). Low-temperature preparation techniques for electron microscopy of biological specimens based on rapid freezing with liquid helium II. *Ann. NY Acad. Sci.* 85:689-713.
89. Fischer, H., Miles, M. J., and Odell, J. A. (1994). Atomic force microscopy of the banded structure of lyotropic polymers. *Macromol. Rapid Commun.* 15(11):815-821.
90. Fjerdings, H., Forseth, T. F., Gregersen, Ø.W., Helle, T., Johnsen, P. O., Kure, K.-A., and Reme, P. A. (1997). Some mechanical pulp fiber characteristics, their process relationships and papermaking significance. In: *The Fundamentals of Papermaking Materials*. Vol. 1. C. F. Baker, ed. Pira Int., Leatherhead, U.K. pp. 641-662.
91. Forsberg, P., and Lepoutre, P. (1992). A new insight into the fiber-roughening phenomenon. *Nordic Pulp Paper Res. J.* 7:158-159.
92. Forsberg, P., and Lepoutre, P. (1994). ESEM examination of roughening of paper in high moisture environment. International Printing and Graphic Arts Conf., Atlanta, GA, pp. 229-336.

93. Forseth, T., and Helle, T. (1997). Effect of moistening on cross-sectional details of calendered paper containing mechanical pulp. *J. Pulp Paper Sci.* 23(3):J95–J100.
94. Frey-Wyssling, A. (1964). Ultraviolet and fluorescence optics of lignified cell walls. In: *Formation of Wood in Forest Trees*. M. H. Zimmermann, ed. Academic Press, New York, pp. 153–167.
95. Friel, J., and Pande, C. (1993). A direct determination of fractal dimension of fracture surfaces using scanning electron microscopy and stereoscopy. *Mater. Res. Soc.* 8(1):100–104.
96. Fukazawa, K., and Imagawa, H. (1983). Ultraviolet and fluorescence microscopic studies of lignin. 2nd Int. Symp. on Wood and Pulping Chemistry, Tsukuba, Japan, Vol. 1, pp. 20–23.
97. Furuta, T., Morikawa, Y., Ito, K., and Ise, N. (1994). Cellophane structure as studied by confocal laser scanning microscope. *Tappi J.* 77(8):128–131.
98. Gallay, W. (1949). Some factors in the strength of paper. *Tappi* 32(10):457–462.
99. Gane, P. A. C., and Hooper, J. J. (1989). An evaluation of the interactions between coating color and base paper by coating profile analysis. In: *Fundamentals of Papermaking*. Vol. 2. C. F. Baker, ed. Mech. Eng. Pub., London, pp. 871–893.
100. Gibbon, D. L., Simon, E. C., and Cornelius, R. C. (1989). New electron and light optical techniques for examining papermaking. *Tappi J.* 72(10):87–91.
101. Giertz, H. W. (1977). Basic wood raw material properties and their significance in mechanical pulping. Proc. Int. Mechanical Pulping Conf., Helsinki, Session 1:1–15.
102. Godjics, M. (1953). *The Genus Euglena*. Univ. Wisconsin Press, Madison, Wisconsin.
103. Goldstein, J. I., Newbury, D. E., Echlin, P., Joy, D. C., Fiori, C., and Lifshin, E. (1981). *Scanning Electron Microscopy and X-Ray Microanalysis*. Plenum Press, New York.
104. Goring, D. A. I. (1970). Microscopic patterns of lignin removal during chemical pulping. In: *Physics and Chemistry of Wood Pulp Fibers*. D. H. Page, ed. STAP Ser. No. 8. TAPPI, Atlanta, GA, pp. 107–124.
105. Graff, J. H., and Schlosser, M. A. (1942). Cross sectioning of paper. *Paper Trade J.* 114:TS87–TS91.
106. Gregersen, Ø. W., Johnsen, P. O., and Helle, T. (1995). Small-scale topographical variations of newsprint surfaces and their effects on printing ink transfer distribution. *J. Pulp Paper Sci.* 21(10):J331–J336.
107. Gregersen, Ø. W., Skinnarland, I., Johnsen, P. O., and Helle, T. (1995). Qualitative methods for the study of lignin distribution in wood and surface layers of unbleached pulp fibers and paper. *J. Pulp Paper Sci.* 21(8):J285–J287.
108. Gron, J., and Beghella, L. (1996). Cracking and roughening of coated paper surfaces. *Paperi Puu (Paper Timber)* 78(3):121–127.
109. Groom, L. H., Shaler, S. M., and Mott, L. (1995). Characterizing micro- and macro-mechanical properties of single wood fibers. Int. Paper Physics Conf., Niagara-on-the-Lake, ON, Canada, pp. 13–22.
110. Gunning, A. P., Kirby, A. R., Morris, V. J., Wells, B., and Brooker, B. E. (1995). Imaging bacterial polysaccharides by AFM. *Polym. Bull.* 34:615–619.
111. Guttman, H. N., and Styskal, R. C. (1971). Preparation of suspended cells for SEM examination of internal cellular structures. In: *Scanning Electron Microscopy I*. O. Johari and I. Corvin, eds. IIT Res. Inst., Chicago, pp. 265–271.
112. Hamad, W. Y., and Provan, J. W. (1995). Microstructural cumulative material degradation and fatigue-failure micromechanisms in wood-pulp fibers. *Cellulose* 2:159–177.
113. Hanley, S. J. (1996). Application of atomic force microscopy to cellulose, wood, kraft pulp fibers, and paper. Ph.D. Thesis, McGill Univ., Montreal, Canada.
114. Hanley, S. J., Giasson, J., Revol, J. F., and Gray, D. G. (1992). Atomic force microscopy of cellulose microfibrils: Comparison with transmission electron microscopy. *Polymer* 33(21):4639–4642.

115. Hanley, S. J., and Gray, D. G. (1994). Atomic force microscope images of black spruce wood sections and pulp fibers. *Holzforschung* 48(1):29–34.
116. Hanley, S. J., and Gray, D. G. (1999). Imaging kraft pulp fibers in air and water by atomic force microscopy. *J. Pulp Paper Sci.* 25(6):196–200.
117. Hanna, R. B. (1971). The interpretation of high resolution electron micrographs of the cellulose elementary fibril. *J. Polymer Sci., Part C* 36:409–413.
118. Hansma, H. G., Vesenska, J., Siegfist, C., Kelderman, G., Morrett, H., Sinsheimer, R. L., Elings, V., Bustamante, C., and Hansma, P. K. (1992). Reproducible imaging and dissection of plasmid DNA under liquid with the atomic force microscope. *Science* 256(5060):1180–1184.
119. Harris, T. D., Grober, R. D., Trautman, J. K., and Betzig, E. (1994). Super-resolution imaging spectroscopy. *Appl. Spectrosc.* 48(1):14A–21A.
120. Haugland, R. P. (1989). *Molecular Probes: Handbook of Fluorescent Probes and Research Chemicals*. Molecular Probes Inc., Eugene, OR.
121. Hell, S., Reiner, G., Cremer, C., and Stelzer, E. H. K. (1993). Aberrations in confocal fluorescence microscopy induced by mismatches in refractive index. *J. Microsc.* 169(3):391–405.
122. Hellowell, J. M., and Nelson, R. (1971). Scanning electron microscopy studies of paper coating structures in cross-section. *Tappi* 54(10):1647–1654.
123. Helle, T., and Johnsen, P. O. (1994). Using stereoscopic and SEM BSI for studying ink distribution details on paper and fiber surfaces. *J. Pulp Paper Sci.* 20(7):J189–J192.
124. Heyn, A. N. J. (1966). The microcrystalline structure of cellulose in cell walls of cotton, ramie and jute fibers as revealed by negative staining of sections. *J. Cell Biol.* 29:181–197.
125. Heyn, A. N. J. (1970). The elementary fibril and supermolecular structure of cellulose in softwood fiber. In: *Physics and Chemistry of Wood Pulp Fibers*. D. H. Page, ed. STAP Ser. No. 8, TAPPI, Atlanta, GA, pp. 27–43.
126. Hieta, K., Kuga, S., and Usuda, M. (1984). Electron staining of reducing ends evidences a parallel-chain structure in *Valonia* cellulose. *Biopolymers* 23:1807–1810.
127. Hoh, J. H., and Schoenenberger, C.-A. (1994). Surface morphology and mechanical properties of MDCK monolayers by atomic force microscopy. *J. Cell Sci.* 107:1105–1114.
128. Hooke, R. (1665). *Micrographia*, Dover, New York.
129. Horn, R. A., and Simmonds, F. A. (1968). Microscopical and other fiber characteristics of high-yield sodium bisulfite pulps from balsam fir. *Tappi* 51(1):67A–73.
130. Howard, R., and Sheffield, E. (1987). The wet structure of pulp and paper examined by cryo-SEM. *Paper Technol. Ind.* 27(2):425–427.
131. Howarth, P., Smith, F. H., and Fenton, F. (1975). The use of the interference microscope in a study of adhesive distribution in pigment coatings on paper. *J. Phys., Ser. E (Sci. Instrum.)* 8(12):1055–1058.
132. Howland, R., and Benatar, L. (1996). *A practical guide to scanning probe microscopy*. Parks Scientific Instruments, Sunnyvale, CA.
133. Hutter, J. L., and Bechhoefer, J. (1993). Calibration of atomic-force microscope tips. *Rev. Sci. Instrum.* 64(7):1868–1873.
134. Ivessalo-Pfäffli, M.-S. (1995). *Fiber Atlas Identification of Papermaking Fibers*. Springer, New York.
135. Ivessalo-Pfäffli, M.-S., and Laamanen, J. (1970). Application of the scanning electron microscope in pulp and paper research. *Paperi Puu (Paper Timber)* 11:163–174.
136. Isenberg, I. H. (1967). *Pulp and Paper Microscopy*. The Institute of Paper Chemistry, Appleton, WI.
137. Iwasaki, T., Lindberg, B., and Meier, H. (1962). The effect of ultrasonic treatment on individual wood fibers. *Svensk Papperstidn.* 65(20):795–816.

138. Jackson, L. S., Heitmann, J. A., and Joyce, T. W. (1993). Enzymatic modifications of secondary fiber. *Tappi* 76(3):147–154.
139. Jackson, L. S., Heitmann, J. A., and Joyce, T. W. (1994). Visualization of enzymes binding to secondary fiber silver-enhanced colloidal gold. *Prog. Paper Recycling* 3(2):32–41.
140. James, C. J., Rees, A. J., and Plummer, M. K. (1996). Applications of the scanning electron microscope to the study of Australian newsprint mills papers: Product evolution/development. Proc. 50th Appita Annual General Conf., Auckland, Vol. 1, pp. 341–345.
141. Jang, H. F. (1998). Measurement of fibril angle in wood fibers with polarization confocal microscopy. *J. Pulp Paper Sci.* 24(7):224–230.
142. Jang, H. F., Amiri, R., Seth, R. S., and Karnis, A. (1996). Fiber characterization using confocal microscopy. Collapse behavior of mechanical pulp fibers. *Tappi* 79(4):203–210.
143. Jang, H. F., Howard, R. C., and Seth, R. S. (1995). Fiber characterization using confocal microscopy. The effects of recycling. *Tappi J.* 78(12):131–137.
144. Jang, H. F., Robertson, A. G., and Seth, R. S. (1992). Measuring fiber coarseness and wall thickness distributions with confocal microscopy. 78th Annual Meeting, Technical Section, CPPA, Montreal, pp. B189–192.
145. Jang, H. F., Robertson, A. G., and Seth, R. S. (1992). Transverse dimensions of wood pulp fibers by confocal laser scanning microscopy and image analysis. *J. Mater. Sci.* 27:6391–6406.
146. Jarvis, S. P., Oral, A., Weihs, T. P., and Pethica, J. B. (1993). A novel force microscope and point contact probe. *Rev. Sci. Instrum.* 64(12):3515–3520.
147. Jayme, G. (1963). Production and characteristics of spruce sulfate pulps with biological properties. *Tappi* 46(7):415–420.
148. Jayme, G., and Hunger, G. (1956). Hornification and cellulose fiber structure seen in the electron microscope. *Monatsh. Chem.* 87(1):8–23 (in German).
149. Jayme, G., and Hunger, G. (1958). The rearrangement of microfibrils in dried cellulose and the implication of this structure alteration on pulp properties. In: *Fundamentals of Papermaking Fibers*. F. Bolam, ed. British Paper and Board Makers' Assoc., Kenley, England, pp. 263–271.
150. Jayme, G., and Hunger, G. (1962). Electron microscope 2- and 3-dimensional classification of fiber bonding. In: *Formation and Structure of Paper*. Vol. 1. F. Bolam, ed. British Paper and Board Makers' Assn., London, pp. 135–170.
151. Jenkins, L. M., and Donald, A. M. (1997). Use of the environmental scanning microscope for the observation of the swelling behavior of cellulosic fibers. *Scanning* 19:92–97.
152. Jensen, W. A. (1962). *Botanical Histochemistry*. Freeman, San Francisco.
153. Jones, D., McHardy, W. J., and Tait, J. M. (1984). LTSEM of biological specimens. *Trans. Br. Mycol. Soc.* 82(1):164–170.
154. Jordan, B. D., and O'Neill, M. A. (1994). The birefringence of softwood mechanical pulp fines. *J. Pulp Paper Sci.* 20(6):J172–J174.
155. Jordan, B. D., and Page, D. H. (1981). Application of image analysis to pulp fiber characterization. In: *The Role of Fundamental Research in Paper Making*, Vol. 2. J. Brander, ed. Mech. Eng. Pub., London, pp. 745–776.
156. Kallmes, O. (1960). Distribution of the constituents across the wall of unbleached spruce sulfite fibers. *Tappi* 43(2):143–153.
157. Kallmes, O., and Eckbert, C. (1964). The structure of paper. VIII. The application of the relative bonded area concept to paper evaluation. *Tappi* 47(9):540–548.
158. Karlsson, J. O., Andersson, N., Berntsson, P., Chihani, T., and Gatenholm, P. (1998). Swelling behavior of stimuli-responsive cellulose fibers. *Polymer* 39(16):3589–3595.

159. Kasten, F. H. (1990). The origins of modern fluorescence microscopy and fluorescent probes. In: *Cell Structure and Function by Microspectrofluorometry*. E. Kohen and J. G. Hirschberg, eds. Academic Press, New York, pp. 3–50.
160. Kellenberger, E., Carlemalm, E., and Villiger, W. (1985). Physics of the preparation and observation of specimens that involve cyroprocedures. In: *The Science of Biological Specimen Preparation for Microscopy and Microanalysis*. J.-P. Revel, T. Barnard, and G. H. Haggis, eds. SEM Inc., AMF O'Hare (Chicago), pp. 1–20.
161. Keller, H. E. (1995). Objective lenses for confocal microscopy. In: *Handbook of Biological Confocal Microscopy*. J. B. Pawley, ed. Plenum Press, New York, pp. 111–125.
162. Keller, D. J., and Chou, C. C. (1992). Imaging steep, high structures by scanning force microscopy with electron-beam deposited tips. *Surf. Sci.* 268(1–3):333–339.
163. Kerle, T., Cohen, S. R., and Klein, J. (1997). Dihedral angle at solid/liquid-polymer interfaces determined by atomic force microscopy. *Langmuir* 13:6360–6362.
164. Kibblewhite, R. P. (1973). Structural modifications to pulp fibers: Definitions and roles in papermaking. *Tappi* 60(10):141–143.
165. Kibblewhite, R. P. (1989). Effects of pulp drying and refining on softwood fiber wall structural organizations. In: *Fundamentals of Papermaking*, Vol. 1. C. F. Baker and V. W. Punton, eds. Mech. Eng. Pub., London, pp. 121–152.
166. Kibblewhite, R. P., and Bailey, D. G. (1988). Measurement of fiber cross-section dimensions using image processing. *Appita* 41(4):297–303.
167. Kibblewhite, R. P., Bawden, A. D., and Hughes, C. (1991). Hardwood market kraft fiber and pulp qualities. *Appita* 44(5):325–332.
168. Kibblewhite, R. P., and Brookes, D. (1977). Dimensions and collapse behavior of kraft and bisulfite fibers in wet pulps and 'in situ' in handsheets. *Appita* 31(2):111–118.
169. Kibblewhite, R. P., and Shelbourne, C. J. A. (1997). Genetic selection of trees with designer fibers for different paper and pulp grades. In: *The Fundamentals of Papermaking Materials*, Vol. 1. C. F. Baker, ed. Pira International, Leatherhead, U.K., pp. 641–662.
170. Kirby, A. R., Gunning, A. P., and Morris, V. J. (1995). Atomic force microscopy in food research: A new technique comes of age. *Trends Food Sci. Technol.* 6: 359–365.
171. Kistler, J., and Kellenberger, E. (1977). Collapse phenomena in freeze-drying. *J. Ultrastruct. Res.* 59:70–75.
172. Klofta, J. L., and Miller, M. L. (1994). Effects of deinking on the recycle potential of papermaking fibers. *Pulp Paper Mag. Can.* 95(8):41–44.
173. Klungness, J., Caulfield, D., Sachs, I., Sykes, M., and Shilts, R. (1994). Fiber-loading: A progress report. Tappi Proc. 1994 Recycling Symp., Boston, MA, pp. 283–290.
174. Knebel, W. (1991). Dual-channel applications with the confocal laser scanning microscope CLSM of Leica Lasertechnik GmbH. *Sci. Tech. Info.* 10(2):46–52.
175. Knebel, W., and Schnepf, E. (1991). Confocal laser scanning microscopy of fluorescently stained wood cells: A new method for three-dimensional imaging of xylem elements. *Trees* 5(1):1–4.
176. Koubaa, A., and Koran, Z. (1995). Measure of the internal bond strength of paper/board. *Tappi J.* 78(3):103–111.
177. Kučera, L., and Bariska, M. (1982). On the fracture morphology in wood. Part 1: A SEM-study of deformation in wood of spruce and aspen under ultimate axial compression load. *Wood Sci. Technol.* 16:241–259.
178. Kunnas, L., Lehtinen, J., Paulapuro, H., and Kiviranta, A. (1993). The effect of Condebelt drying on the structure of fiber bonds. *Tappi* 76(4):95–104.
179. Laamanen, J., Ora, M., and Eklund, H. (1986). Influence of post refining on the properties of TMP fibers. International Paper Physics Conf., Adirondack, NY.

180. Lackner, R., Srebotnik, E., and Messner, K. (1992). Localization of extracellular ligninases of *Phanerochaete chrysosporium*. In: *Ligno-Cellulosics: Science, Technology, Development and Use*. J. F. Kennedy, G. O. Phillips, and P. A. Williams, eds. Ellis Horwood, London, pp. 41–44.
181. Lammi, T., and Heikkurinen, A. (1997). Changes in fiber wall structure during defibration. In: *The Fundamentals of Papermaking Materials*, Vol. 1, C. F. Baker, ed. Pira International, Leatherhead, U.K., pp. 641–662.
182. Lange, J., Månson, J.-A. E., and Hult, A. (1994). Defects in solvent-free organic coatings studied by atomic force microscopy, scanning acoustic microscopy, and confocal laser microscopy. *J. Coatings Technol.* 66(838):19–26.
183. Lange, P. W. (1958). The distribution of the chemical constituents throughout the cell wall. In: *Fundamentals of Papermaking Fibers*. F. Bolam, ed. British Paper and Board Makers' Assoc., Kenley, England, pp. 7–34.
184. Leney, L. (1981). A technique for measuring fibril angle using polarized light. *Wood Fiber* 13(1):13–16.
185. Leopold, B., and McIntosh, D. C. (1961). Chemical composition and physical properties of wood fibers. III. Tensile strength of individual fibers from alkali extracted loblolly pine holocellulose. *Tappi* 44(3):235–240.
186. Lepoutre, P., and de Silveira, G. (1991). Examination of cross-sections of blade- and roll-coated LWC paper. *J. Pulp Paper Sci.* 17(5):J184–J186.
187. Lichtman, J. W. (1994). Confocal microscopy. *Sci. Am.* 271(2):30–35.
188. Lindsay, J. (1993). Relative flow porosity in paper. In: *Products of Papermaking*, Vol. 2. C. F. Baker, ed. Pira International, Leatherhead, U.K., pp. 935–968.
189. Løvhaugen, O. (1995). Possible effects of fluorescence bleaching/saturation on the definition of the paper surface in CLSM measurements. *Zool. Stud.* 34(Suppl. 1):230–231.
190. Løvhaugen, O. (1995). Average pore volume measurement using confocal laser scanning microscopy. Image Analysis for Pulp and Paper Research and Production. 3rd European Res. Symp., STFI, Stockholm.
191. Løvhaugen, O., Berli, E. L., and Bjerke, F. (1996). Pore volumes and their relations to standard surface parameters and print quality. Proc. Int. Printing and Graphic Arts Conf., pp. 111–114.
192. Luong, C. H., and Lindem, P. E. (1995). A method to determine heat conduction in paper during calendering. Int. Paper Physics Conf., Niagara-on-the-Lake, ON, Canada, pp. P1–P3.
193. Luukko, K. (1994). Characterization of chemical pulp fines. M.Sc. Thesis, Laboratory of Paper Technology, Helsinki University of Technology, Espoo, Finland (in Finnish).
194. Luukko, K., Kemppainen-Kajola, P., and Paulapuro, H. (1997). Characterization of mechanical pulp fines by image analysis. *Appita* 50(5):387–392.
195. MacGregor, M. A. (1992). The technical challenge of making better paper: Preparing for the 21st century. Proc. TAPPI Engineering Conf., Boston, MA, pp. 39–54.
196. MacGregor, M. A. (1996). Measuring water-induced roughening of LWC paper and its effect on printed gloss. Tappi Proc. 1996 Process and Product Quality Conf., Cincinnati, OH, pp. 129–137.
197. MacGregor, M. A., Johansson, P. R., and Béland, M.-C. (1994). Measurement of small-scale gloss variation in printed paper. Int. Printing and Graphic Arts Conf., Atlanta, GA, pp.33–43.
198. Maganov, S. N. (1993). Surface characterization of materials at ambient conditions by scanning tunneling microscopy (STM) and atomic force microscopy (AFM). *Appl. Spectrosc. Rev.* 28(1&2):1–121.
199. Mandelbrot, B. B., Passoja, D. E., and Pullay, A. J. (1984). Fractal character of fracture surfaces of metals. *Nature* 308(5961):721–722.

200. Mangin, P. J., and Béland, M.-C. (1993). Three-dimensional evaluation of paper surfaces using confocal microscopy: Applications to research and development. IARIGAI 22nd Int. Res. Conf., Munich, Germany.
201. Mangin, P. J., Béland, M.-C., and Cormier, L. M. (1994). Paper surface compressibility and printing. Proc. 1994 Int. Printing and Graphic Arts Conf., Halifax, NS, pp. 19–31.
202. Mardon, J., Monahan, R. E., Carter, R. A., and Wilder, J. E. (1966). Dynamic consolidation of paper during calendering. In: *Consolidation of the Paper Web*, Vol. 1. F. Bolam, ed. British Paper and Board Makers' Assoc., London, pp. 576–634.
203. Martínez-Nistal, A., Alonso, M., González-Río, F., Sampedro, A., and Astorga, R. (1998). 3D reconstruction of wood fibers using confocal microscopy. *Microsc. Anal.* 63:19–20.
204. Marton, R., and Crosby, C. M. (1969). Distribution of phenolic resins in laminating papers. *Tappi* 52(4):681–688.
205. Maxwell, M. H. (1978). Two rapid and simple methods used for the removal of resins from 1.0 μm thick epoxy sections. *J. Microsc.* 112(2):253–255.
206. McCool, M. A., and Taylor, C. J. (1983). Image analysis techniques in recycled fiber. *Tappi* 66(8):69–71.
207. McIntosh, D. C. (1967). The effect of refining on the structure of the fiber wall. *Tappi* 50(10):482–488.
208. McIntosh, D. C., and Leopold, B. (1962). Bonding strength of individual fibers. In: *Formation and Structure of Paper*, Vol. 1, F. Bolam, ed., British Paper and Board Makers' Assoc., London, pp. 171–193.
209. McKenzie, A. W., and Higgins, H. G. (1964). Conformability and surface texture of cellulose fibers in relation to paper strength. *Paper Technol.* 5(2):155–158.
210. Miller, K. R., Prescott, C. S., Jacobs, T. L., and Lassignal, N. L. (1983). Artifacts associated with quick-freezing and freeze-drying. *J. Ultrastruct. Res.* 82:123–133.
211. Minsky, M. (1988). Memoir on inventing the confocal scanning microscope. *Scanning* 10(4):128–138.
212. Mislankar, A., Darabie, A., and Reeve, D. W. (1997). Detection of ortho-quinones in wood using confocal scanning laser microscopy. *J. Pulp Paper Sci.* 23(2):J73–J76.
213. Mohlin, U.-B. (1975). Cellulose fiber bonding: Part 5. Conformability of pulp fibers. *Svensk Papperstidn.* 78(11):412–416.
214. Mora, F., Ruel, K., Comtat, J., and Joseleau, J.-P. (1986). Aspect of native and re-deposited xylans at the surface of cellulose microfibrils. *Holzforschung* 40:85–91.
215. Morris, V. J. (1994). Biological applications of scanning probe microscopes. *Prog. Biophys. Mol. Biol.* 61:131–185.
216. Moss, P. A. (1990). A study of the frozen hydrated structure of pulp. Ph.D. Thesis, Department of Paper Science, University of Manchester Institute of Science and Technology, Manchester, U.K.
217. Moss, P. A., Kropholler, H. W., and Sheffield, E. (1989). LTSEM: Great potential for pulp evaluation. *Paper Technol.* 30(9):12–14.
218. Moss, P. A., Nyblom, I., Sneek, A., and Hyvärinen, H.-K. (1999). The location and quantification of lignin in kraft pulps using a confocal laser scanning microscope (CLSM) and image analysis. In: *Microscopy as a Tool in Pulp and Paper Research and Development*, STFI Proceedings, Stockholm, pp. 221–227.
219. Moss, P. A., and Retulainen, E. (1997). The effect of fines on fiber bonding; cross-sectional dimensions of TMP fibers at potential bonding sites. *J. Pulp Paper Sci.* 23(8):J382–J388.
220. Moss, P. A., Retulainen, E., Paulapuro, H., and Aaltonen, P. (1993). Taking a new look at pulp and paper. Applications of confocal laser scanning microscopy (CLSM) to pulp and paper research. *Paperi Puu (Paper Timber)* 75(1/2):74–79.

221. Mott, L., Shaler, S. M., Liang, B.-H., and Groom, L. H. (1995). The tensile testing of individual wood fibers using environmental scanning electron microscopy and video image analysis. *Tappi J.* 78(5):43-148.
222. Naito, T., Nishi, K., and Kawano, Y. (1995). Delamination resistance of paper. International Paper Physics Conf., Niagara-on-the-Lake, ON, Canada, pp. 125-130.
223. Nanko, H., Ansano, S., and Ohsawa, J. (1991). Shrinking behavior of pulp fibers during drying. Proc. Int. Paper Physics Conf., Kona, HI, Book 2, pp. 365-373.
224. Nanko, H., and Ohsawa, J. (1989). Mechanisms of bond formation. In: *Fundamentals of Papermaking*, Vol. 1. C. F. Baker and V. W. Punton, eds. Mech. Eng. Pub., London, pp. 783-830.
225. Nanko, H., Ohsawa, J., and Okagawa, A. (1989). How to see interfiber bonding in paper sheets. *J. Pulp Paper Sci.* 15(1):J17-J22.
226. Nanko, H., and Tada, Y. (1995). Mechanisms of hygroexpansion of paper. Int. Paper Physics Conf., Niagara-on-the-Lake, ON, Canada, pp.159-171.
227. Nanko, H., and Wu, J. (1995). Mechanisms of paper shrinkage during drying. Int. Paper Physics. Conf., Niagara-on-the-Lake, ON, Canada, pp. 103-113.
228. Nissan, A. H. (1951). Particle size analysis from sedimentation curves. *Disc. Faraday Soc.* 11:15-27.
229. Nissan, A. H., and Sternstein, S. S. (1964). Cellulose-fiber bonding. *Tappi* 47(1):1-6.
230. Nordman, L. S., and Qvikström, B. (1970). Variability in the mechanical properties of fibers within a growth period. In: *Physics and Chemistry of Wood Pulp Fibers*. D. H. Page, ed. STAP Ser. No. 8. TAPPI, Atlanta, GA, pp. 177-200.
231. O'Brien, T. P., and McCully, M. E. (1981). *The Study of Plant Structure: Principles and Selected Methods*. Termacarphi Pty. Ltd., Melbourne.
232. Page, D. H. (1960). Fiber-to-fiber bonds. Part I. A method for their direct observation. *Paper Technol. Ind.* 1(5):519-530.
233. Page, D. H. (1967). The collapse behavior of pulp fibers. *Tappi* 50(9):449-455.
234. Page, D. H. (1969). A method of determining the fibrillar angle of wood fibers using polarized light. *J. Microsc.* 90(2):137-143.
235. Page, D. H. (1969). A theory for the tensile strength of paper. *Tappi* 52(4):674-681.
236. Page, D. H. (1989). The beating of chemical pulps: The action and the effects. In: *Fundamentals of Papermaking*. Vol. 1. C. F. Baker and V. W. Punton, eds. Mech. Eng. Pub., London, pp. 1-38.
237. Page, D. H., and De Grâce, J. H. (1967). The delamination of fiber walls by beating and refining. *Tappi* 50(10):489-495.
238. Page, D. H., El-Hosseiny, F. E., Winkler, K., and Lancaster, A. P. S. (1977). Elastic modulus of single wood pulp fibers. *Tappi* 60(4):114-117.
239. Page, D. H., and Emerton, H. W. (1959). The microscopic examination of fibers, paper, board and wood. Part I. Improved methods for the study of surfaces. *Svensk Papperstidn.* 62(9):318-332.
240. Page, D. H., and Sargent, J. W. (1962). The fine structure of fiber bonding. In: *Formation and Structure of Paper*, Vol. 1. F. Bolam, ed. British Paper and Board Makers' Assoc., London, pp. 193-200.
241. Page, D. H., Sargent, J. W., and Nelson, R. (1966). Structure of paper in cross-section. In: *Consolidation of the Paper Web*, Vol. 1. F. Bolam, ed. British Paper and Board Makers' Assoc., London, pp. 313-352.
242. Page, D. H., and Tydeman, P. A. (1960). Fiber-to-fiber bonds. Part 2. A preliminary study of their properties in paper sheets. *Paper Technol. Ind.* 1(5):519-530.
243. Page, D. H., and Tydeman, P. A. (1966). Physical processes occurring during the drying phase. In: *Consolidation of the Paper Web*, Vol. 1. F. Bolam, ed. British Paper and Board Makers' Assoc., London, pp. 371-396.

244. Page, D. H., Tydeman, P. A., and Hunt, M. (1962). A study of fiber-to-fiber bonding by direct observation. In: *Formation and Structure of Paper*, Vol. 1. F. Bolam, ed. British Paper and Board Makers' Assoc., London, pp. 171–193.
245. Page, D. H., Tydeman, P. A., and Hunt, M. (1962). The behavior of fiber-to-fiber bonds in sheets under dynamic conditions. In: *Formation and Structure of Paper*, Vol. 1. F. Bolam, ed. British Paper and Board Makers' Assoc., London, pp. 249–263.
246. Panshin, A. J., and de Zeeuw, C. (1960). *Textbook of Wood Technology*. McGraw-Hill, New York.
247. Parham, R. A. (1973). X-ray/SEM analysis of materials: Principles and applications to paper. *Paperi Puu (Paper Timber)* 55(12):959–972.
248. Parham, R. A. (1974). Electron microscopy of pulp and paper. *Wood Sci.* 6(3):245–255.
249. Parham, R. A. (1975). Critical-point drying for fiber microscopy. *Tappi* 58(3):138–140.
250. Parham, R. A., and Gray, R. L. (1982). *The Practical Identification of Wood Pulp Fibers*. TAPPI, Atlanta, GA.
251. Parsons, E., Dole, B., Hall, D. J., and Thomas, W. D. E. (1974). A comparative survey of the techniques for preparing plant surfaces for the scanning electron microscope. *J. Microsc.* 101(1):59–75.
252. Patnaik, S. S., Bunning, T. J., Adams, W. W., Wang, J., and Labes, M. M. (1995). Atomic force microscopy and high-resolution scanning microscopy study of the banded surface morphology of hydroxypropyl cellulose thin films. *Macromolecules* 28(1):393–395.
253. Pawley, J. B., ed. (1995). *Handbook of Biological Confocal Microscopy*. Plenum Press, New York.
254. Pelton, R., Jordan, B., and Allen, L. (1985). Particle size distribution of fines in mechanical pulps and some aspects of their retention in papermaking. *Tappi J.* 68(2):91–94.
255. Pereira, D. E. D., and da Silva, E. C., Jr. (1995). Improvement of atomic force microscopy (AFM) as an analytical instrument for residual lignin characterization. Proc. 8th Int. Symp. on Wood and Pulping Chemistry, Helsinki, Finland, Vol. 1, pp. 467–474.
256. Pesacreta, T. C., Carlson, L. C., and Triplett, B. (1997). Atomic force microscopy of cotton fiber cell wall surfaces in air and water: Quantitative and qualitative aspects. *Planta* 202:435–442.
257. Peterson, R. A., and Williams, C. L. (1992). Determining paper-coating thickness with electron microscopy and image analysis. *Tappi J.* 75(10):122–126.
258. Pye, I. T., Washburn, O. V., and Buchanan, J. G. (1966). Structural changes in paper on pressing and drying. In: *Consolidation of the Paper Web*, Vol. 1. F. Bolam, ed. British Paper and Board Makers' Assoc., London, pp. 353–367.
259. Quackenbush, D. W. (1958). A photomicrographic technique for observing the contours of textured surfaces. *Tappi* 41(12):772–775.
260. Quackenbush, D. W. (1971). Faults in paper coatings and their relationship to base sheet structure. *Tappi* 54(1):47–52.
261. Quackenbush, D. W. (1988). Case studies in the use of the optical microscope in the analysis of coated paper. *Tappi J.* 71(5):70–75.
262. Radmacher, M., Tillmann, R. W., Fritz, M., and Gaub, H. E. (1992). From molecules to cells: Imaging soft samples with the atomic force microscope. *Science* 257:1900–1905.
263. Rånby, B. G. (1952). The fine structure of cellulose fibrils. In: *Fundamentals of Papermaking Fibers*. F. Bolam, ed. British Paper and Board Makers' Assoc., Kenley, England, pp. 7–34.
264. Read, N. D., and Beckett, A. (1983). Effects of hydration on the surface morphology of urediospores. *J. Microsc.* 132(2):179–184.
265. Retulainen, E., and Ebeling, K. (1985). Effect of paper on the load-elongation behavior of fiber-to-fiber bonds. In: *Papermaking Raw Materials*, Vol. 1. V. Punton, ed. Mech. Eng. Pub., London, pp. 229–263.

266. Retulainen, E., Moss, P., and Nieminen, K. (1993). Effects of fines on the properties of fiber networks. In: *Products of Papermaking*, Vol. 2, C. F. Baker, ed. Pira Int., Leatherhead, U.K., pp. 727–769.
267. Retulainen, E., Moss, P., and Nieminen, K. (1997). Effect of calendaring and wetting on paper properties. *J. Pulp Paper Sci.* 23(1):J34–J39.
268. Revol, J. F. (1982). On the cross-sectional shape of cellulose crystallites in *Valonia ventricosa*. *Carbohydr. Polym.* 2:123–134.
269. Revol, J. F. (1985). Change of the D-spacing in cellulose crystals during lattice imaging. *J. Mater. Sci. Lett.* 4(11):1347–1349.
270. Rezanowich, A. (1968). Some applications of the scanning electron microscope at the Pulp and Paper Research Institute of Canada. In: *Scanning Electron Microscopy*. O. Johari and I. Corvin, eds. IIT Res. Inst., Chicago, pp. 13–27.
271. Rials, T. G., and Glasser, W. G. (1989). Multiphase materials with lignin. VI. Effect of cellulose derivative structure on blend morphology with lignin. *Wood Fiber Sci.* 21(1):80–90.
272. Robards, A. W., and Sleytr, U. B. (1985). *Low Temperature Methods in Biological Electron Microscopy*. Elsevier, New York.
273. Robertson, A. A., and Mason, S. G. (1962). The role of fiber collapse in papermaking. In: *Formation and Structure of Paper*, Vol. 2. F. Bolam, ed. British Paper and Board Makers' Assoc., London, pp. 639–647.
274. Robertson, L. R. (1993). The use of phase-contrast microscopy to assess and differentiate the microbial population of a paper mill. *Tappi J.* 76(3):83–87.
275. Robertson, L. R., and Taylor, N. R. (1993). Biofilms and dispersants: A less toxic approach to deposit control. Tappi Proc. 1993 Papermakers Conf., Atlanta, GA, pp. 631–638.
276. Rollins, M. L., Cannizzaro, A. M., and Goynes, W. R. (1972). Electron microscopy of cellulose and cellulose derivatives. In: *Instrumental Analysis of Cotton Cellulose and Modified Cotton Cellulose*. R. T. O'Connor, ed. Marcel Dekker, New York, pp. 171–271.
277. Rollins, M. L., and deGruy, I. V. (1972). Light microscopy in the study of cellulose. In: *Instrumental Analysis of Cotton Cellulose and Modified Cotton Cellulose*. R. T. O'Connor, ed. Marcel Dekker, New York, pp. 93–169.
278. Rosowski, J. R., and Gilder, W. V. (1977). Comparative effects of metal coating by sputtering and by vacuum evaporation on delicate features of Euglenoid flagellates. In: *Scanning Electron Microscopy*/I. O. Johari and I. Corvin, eds. IIT Res. Inst., Chicago, pp. 471–480.
279. Ruel, K., and Joseleau, J.-P. (1984). Use of enzyme-gold complexes for the ultrastructural localization of hemicelluloses in the plant cell wall. *Histochemistry* 81:573–580.
280. Ruska, E. (1933). Formation of pictures of surfaces irradiated by electrons in the electron microscope. *Z. Physik* 83:492–497 (in German).
281. Sachs, I. B. (1985). Preserving and recovering pulp fibrils subsequent to drying. *Paper Tech. Ind.* 20(1):38–41.
282. Sachs, I. B. (1986). Retaining raised fibrils and microfibrils on fiber surfaces. *Tappi J.* 69(11):124–127.
283. Saka, S., and Thomas, R. J. (1982). Evaluation of the quantitative assay of lignin distribution by TEM-EDXA technique. *Wood Sci. Technol.* 16:1–18.
284. Saka, S., Thomas, R. J., and Gratzl, J. S. (1978). Lignin distribution determination by energy dispersive analysis of X rays. *Tappi* 61(1):73–76.
285. Saka, S., Whiting, P., Fukazawa, K., and Goring, D. A. I. (1982). Comparative studies on lignin distribution by UV microscopy and bromination combined with EDXA. *Wood Sci. Technol.* 16:269–277.
286. Scallan, A. M. (1974). The structure of the cell wall of wood: A consequence of anisotropic inter-microfibrillar bonding? *Wood Sci.* 6(3):266–271.

287. Scallan, A. M. (1978). The accommodation of water within pulp fibers. In: *Fiber-Water Interactions in Paper-Making*, Vol. 1. Fundamental Research Committee, ed. British Paper and Board Industry Fed., London, pp. 9-29.
288. Scott, J. A. N., Procter, A. R., Fergus, B. J., and Goring, D. A. I. (1969). The application of ultraviolet microscopy to the distribution of lignin in wood. Description and validity of the technique. *Wood Sci. Technol.* 3(1):73-92.
289. Sears, G. R., and Kregel, E. A. (1942). Application of the electron microscope to problems of the pulp, paper and paperboard industry. *Paper Trade J.* 114(19th March):TS139-TS145.
290. Seth, R. S., Jang, H. F., Chan, B. K., and Wu, C. B. (1997). Transverse dimensions of wood pulp fibres and their implications for end use. In: *The Fundamentals of Papermaking Materials*, Vol. 1. C. F. Baker, ed. Pira Int., Leatherhead, U.K., pp. 473-503.
291. Settlemeyer, L. A. (1992). Topography and the corresponding effect on gloss as detailed with the scanning electron microscope. Proc. TAPPI Int. Printing and Graphic Arts Conf., Pittsburgh, PA, pp. 41-47.
292. Sheehan, J. G., and Whalen-Shaw, M. (1990). High-magnification cryogenic scanning electron microscopy (cryo-SEMs) of wet coating microstructures. *Tappi J.* 73(5):171-178.
293. Shijun, K. (1983). Ultrastructure of bagasse and distribution of hemicellulose across its cell wall. *Cellulose Chem. Technol.* 17:507-514.
294. Shotton, D. M. (1989). Confocal scanning optical microscopy and its applications for biological specimens. *J. Cell Sci.* 94:175-206.
295. Siegel, B. M. (1949). The structure of cellulose in the electron microscope range. *Tappi* 32(3):109-116.
296. Simons, F. L. (1950). A stain for use in the microscopy of beaten fibers. *Tappi* 33(7):312-314.
297. Skowronski, J. (1990). Surface roughening of pre-calendered base sheets during coating. *J. Pulp Paper Sci.* 16(3):J102-J110.
298. Skowronski, J. (1991). Fiber-to-fiber bonds in paper. Part II: Measurement of the breaking energy of fiber-to-fiber bonds. *J. Pulp Paper Sci.* 17(6):J217-J222.
299. Skowronski, J., and Bichard, W. (1987). Fiber-to-fiber bonds in paper. Part I. Measurement of bond strength and specific bond strength. *J. Pulp Paper Sci.* 13(5):J165-J169.
300. Sloane, C. M. (1993). A preliminary study of the effect of recycling on the bonding potential of unbleached radiata pine and Scandinavian spruce kraft pines. Proc. 47th Appita Annual General Conf., Rotorua, New Zealand, pp. 533-540.
301. Smith, K. C. A. (1959). Scanning electron microscopy in pulp and paper research. *Pulp Paper Mag. Can.* 60(12):T366-T371.
302. Söremark, C., Johansson, G., and Kiviranta, A. (1994). Characterization and elimination of fiber orientation streaks. TAPPI Engineering Conf., San Francisco, Book 1, pp. 97-104.
303. Srebotnik, E., and Messner, K. (1991). Immunoelectron microscopical study of the porosity of brown-rot degraded pine wood. *Holzforschung* 45(2):95-101.
304. Srebotnik, E., and Messner, K. (1992). The use of immunoelectron microscopy to study the diffusion of proteins in wood and pulp. In: *Ligno-Cellulosics: Science, Technology, Development and Use*. J. F. Kennedy, G. O. Phillips, and P. A. Williams, eds. Ellis Horwood, London, pp. 775-778.
305. Steadman, R. K. (1982). The apparent density of paper. Ph.D. Thesis, Department of Paper Science, University of Manchester Institute of Science and Technology, Manchester, U.K.
306. Steadman, R., and Luner, P. (1985). The effect of wet fiber flexibility on sheet apparent density. In: *Papermaking Raw Materials*, Vol. 1. V. Punton, ed. Mech. Eng. Pub., London, pp. 311-337.

307. Stelzer, E. H. K., and Bacallao, R. (1988). Confocal fluorescence microscopy of epithelial cells. *SPIE 1028*:167–168.
308. Stone, J. E., and Scallan, A. M. (1965). A study of the cell wall structure by N₂ adsorption. *Pulp Paper Mag. Can.* 66(8):T407–T414.
309. Stone, J. E., and Scallan, A. M. (1967). The effect of component removal upon the porous structure of the cell wall of wood. II. Swelling in water and the fiber saturation point. *Tappi* 50(10):496–501.
310. Strachan, J. (1932). Further notes on the hydration of cellulose in papermaking. *Proc. Tech. Sect. PMA. GB and Ireland* 13:61–81.
311. Stratton, R. A., and Colson, N. L. (1993). Fiber wall damage during bond failure. *Nordic Pulp Paper Res. J.* 2:245–249.
312. Sugiyama, J., Harada, H., Fujiyoshi, Y., and Uyeda, N. (1984). High resolution observations of cellulose microfibrils. *Mokuzai Gakkaishi* 30(1):98–99.
313. Sugiyama, J., Vuong, R., and Chanzy, H. (1991). Electron diffraction study on the two crystalline phases occurring in native cellulose from an algal cell wall. *Macromolecules* 24(14):4168–4175.
314. Suleman, A. U. M. (1996). Atomic force microscope studies of cellulosic fibers. M.Sc. Thesis, Dept. of Paper Science, Univ. Manchester Institute of Science and Technology, Manchester, U.K.
315. Sundin, J., Sundström, L., and Hartler, N. (1996). Determination of collapse and coarseness of fibers in paper sheets from cross-sectional dimensions using confocal microscopy and image analysis. *Nordic Pulp Paper Res. J.* 1:56–57.
316. Suominen, I., Suihko, M.-L., and Salkinoja-Salonen, M. (1997). Microscopic study of migration of microbes in food packaging paper and board. *J. Ind. Microbiol. Biotechnol.* 19:104–113.
317. Szikla, Z., and Paulapuro, H. (1988). Changes in z-direction density distribution of paper in wet pressing. *J. Pulp Paper Sci.* 15(1):J11–J17.
318. Tam Doo, P. A., and Kerekes, R. J. (1981). A method to measure wet fiber flexibility. *Tappi* 64(3):113–116.
319. TAPPI T 205 (1995). Forming handsheets for physical tests of pulp.
320. TAPPI T 234 (1984). Coarseness of pulp fibers.
321. TAPPI T 246 (1989). Foreign particulate matter in pulp by transmitted light.
322. TAPPI T 259 (1993). Species identification of nonwood plant fibers.
323. TAPPI T 263 (1993). Identification of wood and fibers from conifers.
324. TAPPI T 267 (1985). Compression wood identification.
325. TAPPI T 401 (1993). Fiber analysis of paper and paperboard.
326. TAPPI T 421 (1991). Qualitative (including optical microscopic) analysis of mineral filler and mineral coating of paper.
327. Teder, A. (1964). The properties of spruce pulps as related to paper structures observed with the scanning electron microscope. *Svensk Papperstidn.* 67(17):670–685.
328. Teder, A. (1964). The effect of drying, heat-treatment and beating on the papermaking properties of birch pulps. *Svensk Papperstidn.* 66(22):911–923.
329. Terasaki, M., and Dailey, M. E. (1995). Confocal microscopy of living cells. In: *Handbook of Biological Confocal Microscopy*. J. B. Pawley, ed. Plenum Press, New York, pp. 327–344.
330. Thayer, W. S., and Thomas, C. E. (1971). Analysis of the glue lines in corrugated board. *Tappi* 54(11):1853–1858.
331. The Second Report of the Pulp Evaluation Committee to the Technical Section of the Paper Makers' Association, 1936, London.
332. Thode, E. F., and Ingmanson, W. L. (1959). Factors contributing to the strength of a sheet of paper. I. External specific surface and swollen specific volume. *Tappi* 42(1):74–83.

333. Thomason, J. L., and Knoester, A. (1990). Application of confocal scanning optical microscopy to the study of fiber-reinforced polymer composites. *J. Mater. Sci. Lett.* 9:258–262.
334. Thundat, T., Allison, D. P., Warmack, R. J., and Ferrel, T. L. (1992). Imaging isolated strands of DNA-molecules by atomic force microscopy. *Ultramicroscopy* 42(B):1101–1106.
335. Ting, T. H. D., Chiu, W. K., and Johnston, R. E. (1997). Network changes in paper under compression in the z-direction: The effect of loading rate and fiber wall thickness. *Appita* 50(3):223–229.
336. Tripp, V. W., and Giuffria, R. (1954). Concentric cellulose layers in cotton fiber cell wall. *Textile Res. J.* 24:757–758.
337. Tsien, R. Y., and Bacsikai, B. J. (1995). Video-rate confocal microscopy. In: *Handbook of Biological Confocal Microscopy*. J. B. Pawley, ed. Plenum Press, New York, pp. 459–477.
338. Vaughan, D., ed. (1983). *Energy-Dispersive Xray Microanalysis: An Introduction*. Kevex Corp., Foster City, CA.
339. Verbelen, J.-P., and Stickens, D. (1995). In vivo determination of fibril orientation in plant cell walls with polarization CLSM. *J. Microsc.* 177(1):1–6.
340. Visser, T. D., and Oud, J. L. (1994). Volume measurements in three-dimensional microscopy. *Scanning* 16(4):198–200.
341. Wågberg, P., and Johansson, P.-Å. (1993). Surface profilometry: A comparison between optical and mechanical sensing on printing papers. *Tappi J.* 76(12): 115–121.
342. Walbaum, H. H. (1972). Pigment dispersion property evaluation by scanning electron microscopy. *Tappi* 55(7):1108–1114.
343. Wardrop, A. B. (1962). The path of penetration of pulping media into wood. In: *Formation and Structure of Paper*, Vol. 2. F. Bolam, ed. British Paper and Board Makers' Assoc., London, pp. 621–637.
344. Wardrop, A. B., and Preston, R. D. (1951). The submicroscopic organization of the cell wall in conifer tracheids and wood fibers. *J. Exp. Bot.* 2:20–30.
345. Washburn, O. V., and Buchanan, J. G. (1964). Changes in wet structure on pressing and drying. *Pulp Paper Mag. Can.* 65(9):T400–T408.
346. Watts, J., and Emerton, H. W. (1954). The interpretation of electron micrographs. *Proc. Tech. Sect. BPBMA* 35(2):303–318.
347. Webb, R. H. (1995). Bibliography of confocal microscopes. In: *Handbook of Biological Confocal Microscopy*. J. B. Pawley, ed. Plenum Press, New York, pp. 571–577.
348. Weidner, J. P. (1939). The influence of humidity on changes in diameter and length of sulfite fibers. *Paper Trade J.* 108:T1–T10.
349. Weise, U. W. H. (1995). Monitoring of fiber wrinkling in drying: An approach by fractal analysis. Proc. Third Eur. Res. Symp., Image Analysis in Pulp and Paper Research and Production, Stockholm, Sweden.
350. Weisenhorn, A., Schmitt, F., Knoll, W., and Hansma, P. (1992). Streptavidin binding observed with an atomic force microscope. *Ultramicroscopy* 42(B):1125–1132.
351. Westermarck, U., Lidbrandt, O., and Eriksson, I. (1988). Lignin distribution in spruce (*Picea abies*) determined by mercurization with SEM-EDXA technique. *Wood Sci. Technol.* 22:243–250.
352. White, N. S. (1995). Visualization systems for multidimensional CLSM images. In: *Handbook of Biological Confocal Microscopy*. J. B. Pawley, ed. Plenum Press, New York, pp. 211–254.
353. Wickramasinghe, H. K. (1989). Scanned-probe microscopes. *Sci. Am.* 261(4):74–81.
354. Wilke, V. (1985). Optical scanning microscopy: The laser scan microscope. *Scanning* 7(2):88–96.

355. Wilkins, M. J., Davies, M. C., Jackson, D. E., Mitchell, J. R., Roberts, C. J., Stokke, B. T., and Tendler, S. J. B. (1993). Comparison of scanning tunnelling microscopy and transmission electron microscopy image data of a microbial polysaccharide. *Ultramicroscopy* 48:197–201.
356. Williams, G. J., and Drummond, J. G. (1994). Preparation of large sections for the microscopical study of paper structure. Proc. TAPPI Papermakers Conf., pp. 517–523.
357. Williams, G. J., Drummond, J. G., and Cisneros, H. A. (1994). A microscopical approach for examining fiber and paper structures. *J. Pulp Paper Sci.* 20(4):J110–J113.
358. Williams, R. C., and Wykoff, R. W. G. (1944). The thickness of electron microscopic objects. *J. Appl. Phys.* 15:712–716.
359. Williams, R. C., and Wykoff, R. W. G. (1946). Applications of metallic shadow-casting to microscopy. *J. Appl. Phys.* 17:23–33.
360. Wilson, T., ed. (1990). *Confocal Microscopy*. Academic Press, New York.
361. Wilson, T., and Sheppard, C. (1984). *Theory and Practice of Scanning Optical Microscopy*. Academic Press, New York.
362. Wimmer, R., and Lucas, B. N. (1997). Comparing mechanical properties of secondary wall and cell corner middle lamella in spruce wood. *IAWA J.* 18(1):77–88.
363. Wimmer, R., Lucas, B. N., Tsui, T. Y., and Oliver, W. C. (1997). Longitudinal hardness and Young's modulus of spruce tracheid secondary walls using nanoindentation technique. *Wood Sci. Technol.* 31(2):131–141.
364. Wolken, J. J. (1961). *Euglena*. Rutgers, The State University, New Brunswick, NJ.
365. Xu, L., Filonenko, Y., Li, M., and Parker, I. (1997). Measurement of wall thickness of fully collapsed fibers by confocal microscopy and image analysis. Proc. 51st Appita Annual General Conf.
366. Xu, L., Osborne, C., and Parker, I. (1995). Determination of fiber 3D orientation in paper using confocal microscopy and image analysis. Dicta-95, Brisbane, pp. 515–520.
367. Xu, L., Parker, I., and Osborne, C. (1996). Technique for determining the fiber distribution in the z direction using confocal microscopy and image analysis. Proc. 50th Appita Annual General Conf., Auckland, Vol. 2, pp. 603–607.
368. Yang, C.-F., Eusufzai, A. R. K., Sankar, R., Mark, R. E., and Perkins, R. W. (1978). Measurements of geometrical parameters of fiber networks. Part I. Bonded surfaces, aspect ratios, fiber moments of inertia, bonding state probabilities. *Svensk Papperstidn.* 81(13):426–433.
369. Ye, C., and Sundström, O. (1997). Determination of S2-fibril angle and fiber-wall thickness by microscopic transmission ellipsometry. *Tappi* 80(6):181–190.
370. Ylikoski, J. (1992). Characterization of fiber surface properties and fibrillation by confocal laser scanning microscopy. M.Sc. Thesis, Helsinki Univ. Technology, Espoo, Finland (in Finnish).
371. Young, J. Z., and Roberts, F. (1951). A flying-spot microscope. *Nature* 167:231.
372. Young, R., Ward, J., and Scire, F. (1971). Observations of metal-vacuum-metal tunneling, field emission, and the transition region. *Phys. Rev. Lett.* 27(14):922–924.

